

CARBON FIBER-REINFORCED PREPREGS AND COMPOSITES OF ONE-COMPONENT EPOXY RESINS CONTAINING THERMAL LATENT CURING AGENTS

by
CUMA ALI UCAR

**Submitted to the Graduate School of Engineering and Natural Sciences
in partial fulfillment of the requirements for the degree of
Doctor of Philosophy**

**SABANCI UNIVERSITY
JUNE 2025**

© CUMA ALI UCAR 2025

All Rights Reserved

To myself...

ABSTRACT

CARBON FIBER-REINFORCED PREPREGS AND COMPOSITES OF ONE-COMPONENT EPOXY RESINS CONTAINING THERMAL LATENT CURING AGENTS

Cuma Ali UCAR

Doctor of Philosophy, 2025

Materials Science and Nano Engineering

Thesis Advisor: Asst. Prof. Dr. Bekir DIZMAN

Keywords: Thermal Latent Curing Agents, Epoxy Resin, Thermoset Prepregs, Curing Kinetics, Cure Rheology

Carbon fiber-reinforced composites are increasingly replacing metals in sectors such as aerospace and defense due to their key advantages, including low density, high specific strength, and superior corrosion resistance. High-performance, state-of-the-art composites are typically fabricated using thermoset prepeggs. However, the susceptibility of these prepeggs to premature curing at ambient temperatures limits their shelf life and necessitates cold storage, leading to increased energy consumption, reduced storage flexibility, and higher processing costs. To overcome these limitations, prepeggs formulated with thermal latent curing agents (TLCs) are designed to remain stable at ambient temperatures and initiate curing only upon exposure to elevated temperatures, thereby addressing issues related to premature reactivity, storage stability, energy consumption, and processing reliability.

This thesis focuses on the design, synthesis, and application of thermal latent curing agents (TLCs) in one-component epoxy resins (OCERs) to enhance the processing of carbon fiber-reinforced prepeggs and the mechanical performance of the resulting composites. This research encompasses molecular-level advancements in TLCs and prepeggs and their translation into composite manufacturing through four interconnected studies.

The first study investigated the formulation and cure behavior of an OCER incorporating the newly developed small-molecule TLC, phenylurea propyl imidazole (PUPI), in combination with diglycidyl ether of bisphenol A (DGEBA). This OCER demonstrated high conversions at moderate temperatures while maintaining ambient temperature stability for up to three days. Moreover, PUPI synergistically accelerated cure kinetics in the presence of

dicyandiamide (DICY), significantly lowering the onset and peak curing temperatures as confirmed by DSC analysis.

The second study involved the synthesis of a novel sulfonyl urea-based TLC, PTSU-EDA, from p-toluenesulfonyl isocyanate and ethylenediamine, and its incorporation into DGEBA to formulate an OCER. This OCER demonstrated superior thermal latency compared to imidazole-based formulations and reduced cure temperatures relative to OCERs with conventional urea accelerators. However, the cured network's low cross-link density highlighted the need for further structural optimization or stoichiometric adjustment.

To overcome limitations of small-molecule TLCs, the third study focused on the synthesis of poly(2-phenyl-2-oxazoline)-Im (PPhOZ-Im), a polymeric TLC featuring a relatively hydrophobic polyoxazoline backbone and a terminal imidazole group. PPhOZ-Im was incorporated into DGEBA either alone as a curing agent or combined with dicyandiamide (DICY) as an accelerator to formulate OCERs, which were subsequently used to prepare prepgs and composites. Incorporation of PPhOZ-Im into OCERs significantly enhanced composite mechanical properties, increasing tensile strength by 31.3% and compressive strength by 4.5% relative to controls.

Building on these material developments, the fourth study investigated the relationship between prepreg processability—specifically drapeability and tackiness—and the interlaminar shear strength (ILSS) of cured composites. Prepgs with varied degrees of cure (DoC) were produced using off-stoichiometric curing ratios and cured under identical conditions. Results demonstrated a strong relationship between prepreg drapeability and composite ILSS, highlighting the importance of carefully controlling processing conditions when optimizing prepreg formulations with TLCs and dual-cure systems.

These studies collectively establish a robust framework for designing ambient temperature-stable, more efficient OCERs tailored for high-performance composite applications. Further optimization—including predictive modeling of prepreg behavior and the development of tailored TLC architectures—can broaden the applicability of these resins. Moreover, integrating in-line characterization tools may enable precise fine-tuning of prepreg and composite properties, ultimately improving manufacturing efficiency and reducing costs.

ÖZET

TERMAL GECİKTİRİCİ KÜRLEME AJANLAR İÇEREN TEK BİLEŞENLİ EPOKSİ REÇİNELERİN KARBON LİF TAKVİYELİ PREPREG VE KOMPOZİTLERİ

Cuma Ali UÇAR

Doktora Tezi, 2025

Malzeme Bilimi ve Nano Mühendisliği

Tez Danışmanı: Asst. Prof. Dr. Bekir DIZMAN

Anahtar Kelimeler: Termal Geciktirici Kürleme Ajanları, Epoksi Reçine, Termoset Prepregler, Kür Kinetiği, Kür Reolojisi

Karbon elyaf takviyeli kompozitler, düşük yoğunluk, yüksek özgürlük mukavemet ve üstün korozyon direnci gibi temel avantajları nedeniyle havacılık ve savunma gibi sektörlerde metallerin yerini giderek daha fazla almaktadır. Yüksek performanslı, son teknoloji kompozitler tipik olarak termoset pre pregler kullanılarak üretilir. Ancak, bu pre preglerin oda sıcaklığında erken kürlenmeye yatkın olması, raf ömrünü sınırlar ve soğuk depolama gerektirir; bu da enerji tüketimini artırmakta, depolama esnekliğini azaltmakta ve işlem maliyetlerini yükseltmektedir. Bu sınırlamaları aşmak için, termal geciktirici kürleme ajanları (TLC'ler) içeren pre pregler, ortam sıcaklığında stabil kalacak ve yalnızca yüksek sıcaklıklara maruz kalınca kürleşmeyi başlatacak şekilde tasarlanır; böylece erken reaksiyon, depolama stabilitesi, enerji tüketimi ve işlem güvenilirliğiyle ilgili sorunlar giderilir.

Bu tez, karbon elyaf takviyeli pre preglerin prosesini iyileştirmek ve oluşan kompozitlerin mekanik performansını artırmak amacıyla, termal geciktirici kürleme ajanlarının tek bileşenli epoksi reçinelerde (OCER'ler) tasarımı, sentezi ve uygulamasına odaklanmaktadır. Bu çalışma, TLC'ler ve pre preglerde moleküler düzeydeki gelişmeleri ve bunların kompozit üretimine aktarımını içeren birbirine bağlı dört çalışmadan oluşmaktadır.

Birinci çalışmada, yeni geliştirilmiş küçük molekül TLC olan fenilüre propil imidazol (PUPI) ile bisfenol A diglisidil eter (DGEBA) kombinasyonunu içeren bir OCER formülasyonu ve bu formülasyonun kür davranışını incelenmiştir. Bu OCER, oda sıcaklığında üç güne kadar stabil kalırken, orta sıcaklıklarda yüksek dönüşüm sağlamıştır. Ayrıca, PUPI,

disyenandiamid (DICY) varlığında kür kinetiğini sinerjik olarak hızlandırarak, DSC analizleriyle doğrulanın başlangıç ve pik kürleme sıcaklıklarını anlamlı şekilde düşürmüştür.

İkinci çalışma, p-toluenesülfonil izosianat ve etilen diaminden sentezlenen yeni bir sülfonil üre bazlı TLC olan PTSU-EDA'nın sentezini ve bunun DGEBA'ya eklenmesiyle elde edilen OCER formülasyonunun hazırlanmasını kapsamaktadır. Bu OCER, imidazol bazlı formülasyonlara göre üstün termal geciktiricilik ve geleneksel üre hızlandırıcılar içeren OCER'lere kıyasla daha düşük kür sıcaklıkları göstermiştir. Ancak, kürlenmiş ağ yapısının düşük çapraz bağ yoğunluğu, yapısal optimizasyon veya stokiyometrik ayar gerekliliğini ortaya koymuştur.

Küçük moleküllü TLC'lerin sınırlamalarını aşmak için üçüncü çalışma, nispeten hidrofobik bir polioksazolin omurgası ve terminal imidazol grubu içeren polimerik bir TLC olan poli(2-fenil-2-oksazolin)-Im (PPhOZ-Im) sentezine odaklanmıştır. PPhOZ-Im, DGEBA'ya ya tek başına kür ajanı olarak ya da disyenandiamid (DICY) ile birlikte hızlandırıcı olarak eklenmiş ve OCER'ler formüle edilmiştir. Bu OCER'ler daha sonra prepreg ve kompozit üretiminde kullanılmıştır. PPhOZ-Im'nin OCER'lere eklenmesi, kontrol örneklerine kıyasla çekme dayanımında %31,3 ve basma dayanımında %4,5 artışla mekanik özelliklerin anlamlı ölçüde iyileşmesini sağlamıştır.

Bu malzeme gelişmelerinin üzerine inşa edilen dördüncü çalışma, prepreg işlenebilirliği-ozellikle yayılabilirlik (drapeability) ve yapışkanlık-ile kürlenmiş kompozitlerin tabakalararası kayma dayanımı (ILSS) arasındaki ilişkiyi incelemiştir. Farklı kürlenme derecelerine (DoC) sahip prepregler, stokiyometrik olmayan kür oranları kullanılarak hazırlanmış ve aynı koşullar altında kürlenmişdir. Sonuçlar, prepreg yayılabilirliği ile kompozit ILSS arasında güçlü bir ilişki olduğunu göstererek, TLC'ler ve çift-kürleme ajanına sahip sistemler kullanılarak prepreg formülasyonlarının optimize edilmesinde işlem koşullarının dikkatlice kontrol edilmesinin önemini vurgulamıştır.

Bu çalışmalar, yüksek performanslı kompozit uygulamaları için oda sıcaklığında stabil, daha verimli OCER'lerin tasarlanması için sağlam bir temel oluşturmuştur. Daha ileri optimizasyonlar - prepreg davranışının öngörülmesi ve özelleştirilmiş TLC mimarilerinin geliştirilmesi dahil - bu reçinelerin uygulama alanını genişletebilir. Ayrıca, entegre hat içi karakterizasyon araçları, prepreg ve kompozit özelliklerinin hassas bir şekilde ayarlanması sağlayarak üretim verimliliğini artırabilir ve maliyetleri düşürebilir.

ACKNOWLEDGMENTS

First and foremost, I would like to express my utmost thanks and gratitude to my advisor, Asst. Prof. Dr. Bekir Dizman, whose patience with me and belief in my skills has convinced me to pursue my goals further where the journey to this point had many doubts in it. His expertise, approach to difficulties in research and life have contributed to adaptation of my work immensely. I carry full of joy and content that he has been my supervisor, and I feel fortunate to work with him.

I would like to further thank my thesis proposal and progress committee Hatice Sinem Sas Cayci and Yusuf Menceloglu for their guidance, valuable support and insights for my work as well as my life.

I would like to thank my group members, Ceren Özsaltık, Negar Amirhaghian, Aylin Yıldırım, Mariam Omar, Büşra Amanvermez, Mehmet Sinan Tübcil, Ece Ateşpare Şahin and Ashik Abedin. Their support in the most critical situations that I encountered during this journey has led me to continue further.

I would like to thank Prof. Dr. Mehmet Yıldız and Asst. Prof. Serkan Ünal for their initiative in believing me to employ as an engineer first and then a Ph.D. student in the university. I have learned a lot from them.

Special thanks go to the Sabancı University Integrated Manufacturing Technologies Research and Application Center (SU-IMC) staff members, especially to Mehmet Olcaz, and engineers. Additionally, I acknowledge the financial support of The Scientific and Technological Research Council of Turkey (TÜBİTAK) (Grant Number: 121Z597 & 118Z898).

I would like to thank to my family; my mother, Naciye Uyan, my father Abdulkadir Uçar, my sister EYLÜL Şarman and my wife Ragibe Yeşil Uçar for their unwavering support throughout this hard path. I would like to thank my business partner Ertan Acar for believing in my skills and vision and for not giving up.

Table of Contents

LIST OF FIGURES	xiii
LIST OF TABLES.....	xvi
LIST OF SYMBOLS AND ABBREVIATIONS	xviii
CHAPTER 1	1
1. INTRODUCTION AND STATE OF THE ART	1
LITERATURE SURVEY	8
CURING KINETICS OF EPOXY RESINS	9
PREPREG MANUFACTURING, LATENT CURING AGENTS	14
STABILITY OF EPOXY PREPREGS	20
MECHANICAL PROPERTIES OF EPOXY COMPOSITES	22
APPROACH	23
CHAPTER 2	31
2. Synthesis and characterization of 1-(3-aminopropyl)imidazole-phenyl isocyanate adduct and its application as a thermal latent curing agent for diglycidylether bisphenol A resin31	
2.1. Introduction.....	31
2.2. Experimental.....	34
2.2.1. Materials	34
2.2.2. Instruments.....	34
2.3. Methods	35
2.3.1. Synthesis of phenyl urea propyl imidazole (PUPI)	35
2.3.2. Preparation of the OCER	35
2.4. Results.....	36
2.4.1. ^1H NMR Analysis of PUPI	36
2.4.2. FTIR Analysis of PUPI.....	37
2.4.3. TGA Analysis of PUPI	38
2.4.4. DSC Analysis of PUPI.....	38
2.4.4.1. Dynamic DSC Analysis of the OCER formulated with PUPI.....	39
2.4.4.2. Isothermal DSC Results of the OCER formulated with PUPI.....	40

2.4.4.3. Dynamic DSC Results of the OCER formulated with 5% PUPI after Isothermal Curing	40
2.4.5. Optical Microscopy Images of the OCER	42
2.4.6. Rheology Results	45
2.4.6.1. Storage and Loss Moduli of PUPI:DGEBA	45
2.4.6.2. Viscosity Profile of the OCER formulated with 5% PUPI.....	46
2.4.7. Room Temperature Stability Tests	50
2.4.8. PUPI as catalyst for DICY	50
2.5. Conclusion	53
CHAPTER 3	54
3. Para-toluene sulfonyl isocyanate-ethylene diamine adduct as a thermal latent curing agent for epoxy resins	54
3.1. Introduction.....	54
3.2. Experimental.....	56
3.2.1. Materials	56
3.2.2. Synthesis of PTSU-EDA	56
3.2.3. Preparation of the OCER	57
3.2.4. Preparation of DMA samples	57
3.2.5. Preparation of optical microscopy samples	58
3.3. Methods/Characterization.....	58
3.4. Results and Discussion	59
3.4.1. NMR Analysis	59
3.4.2. FTIR analysis	61
3.4.3. TGA analysis	62
3.4.4. DSC analysis.....	64
3.4.4.1. DSC thermogram of the TLC	64
3.4.4.2. DSC thermogram of the OCER	64
3.4.4.3. DSC thermograms of PTSI-DGEBA vs. PTSU-EDA-DGEBA mixtures.....	66
3.4.4.4. Isothermal DSC thermograms of the OCER.....	67
3.4.5. Rheology results of the OCER.....	69
3.4.6. Optical Microscopy Analysis of the OCER.....	71

3.4.7. DMA analysis	73
3.5. Conclusions.....	75
CHAPTER 4	77
4. Ambient-Temperature-Stable Epoxy Prepregs with Tunable Processability and Curing Behavior: Correlating Prepreg Structure with Composite Performance	77
4.1. Introduction.....	77
4.2. Experimental.....	80
4.2.1. Materials	80
4.2.2. Resin preparation	80
4.2.3. Prepreg manufacturing.....	81
4.2.4. Composite manufacturing.....	81
4.3. Methods/Characterization.....	82
4.4. Results and discussion	84
4.4.1. Characterization of Prepreg	84
4.4.1.1. DSC results	84
4.4.1.2. Rheology results	87
4.4.1.3. Drapability and tackiness results	88
4.4.2. Mechanical testing	92
4.4.2.1. ILSS Results	92
4.5. Conclusions.....	93
CHAPTER 5	95
5. Mechanical properties of epoxy composites cured with dicyandiamide and polyphenyloxazolineimidazole as an accelerator for dicyandiamide	95
5.1. Introduction.....	95
5.2. Composite Manufacturing	97
5.3. Mechanical Test Results	98
5.4. Conclusions.....	102
CHAPTER 6	104
6. CONCLUSIONS	104
7. REFERENCES	107
APPENDIX A	120

APPENDIX B	121
------------------	-----

LIST OF FIGURES

Figure 1. Chemical structure of DGEBA epoxy resin	4
Figure 2. A two reactant reaction kinetics scheme	10
Figure 3. Ketene formation through reversible bonds	13
Figure 4. Isocyanate formation through reversible bonds	14
Figure 5. Representation of prepreg tack in ATL (Budelmann et al., 2020)	16
Figure 6. Methods of encapsulation (Lowry et al., 2008).....	17
Figure 7. Diamine (left) reactions with isocyanates (right) (Stoutland et al., 1959)	19
Figure 8. Phenyl isocyanate (left) and amino propyl imidazole (phenyl urea propyl imidazole) reaction scheme	19
Figure 9. Polymers and molecules as TLCs for thesis studies.....	24
Figure 10. Epoxy-Imidazole reaction scheme (Chain growth polymerization).....	25
Figure 11. Epoxy-amine reaction (Step growth polymerization)	25
Figure 12. Tackiness measurement setup	27
Figure 13. Drapeability measurement setup (Pouladvand et al., 2020a)	27
Figure 14. Prepreg lay-up scheme (CRIPPS et al., 2000).....	29
Figure 15. Synthesis of PUPI.....	35
Figure 16. ^1H NMR spectrum of PUPI (in CDCl_3).....	36
Figure 17. FTIR spectra of (a) 1-(3-aminopropyl)imidazole, (b) phenyl isocyanate, and (c) PUPI.....	37
Figure 18. TGA profile of PUPI	38
Figure 19. DSC thermogram of PUPI.....	39
Figure 20. Dynamic DSC thermogram of the OCER formulated with PUPI.....	39
Figure 21. Isothermal curing profile of the OCER formulated with 5% PUPI.....	40
Figure 22. Dynamic DSC tests performed after isothermal curing to obtain residual curing data.....	41
Figure 23. Optical microscopy images (25x) of the OCER (5% PUPI in DGEBA) (A: 25°C, B: 80°C 2 min, C: 60°C 6 hours)	42
Figure 24. Optical microscopy images of the OCER (5% PUPI in DGEBA) at 60°C at different magnifications a: 25x, b:50x, c:100x, d:200x (left to right: 1, 2, 3, 4, 5 h)	45

Figure 25. Storage and loss moduli in temperature sweep rheology test of the OCER formulated with 5% PUPI.....	46
Figure 26. Complex viscosity profile of the OCER at isothermal rheology tests.....	47
Figure 27. Estimation of process times (upper data and graphs) and shelf-life times (lower data and graphs) at lower temperatures (shown in blue color) using rheology and isothermal DSC data obtained at higher temperatures (shown in green color)	49
Figure 28. Complex viscosity results at room temperature storage.....	50
Figure 29. Dynamic DSC results of the OCERs formulated with 1% PUPI + DICY (blue), 5% PUPI + DICY (red), and 10% PUPI + DICY (green)	51
Figure 30. Synthesis of PTSU-EDA	57
Figure 31. NMR spectrum of PTSU-EDA in DMSO-d6.....	60
Figure 32. FTIR spectra of PTSI, EDA and PTSU-EDA	62
Figure 33. FTIR spectrum comparisons of DGEBA, PTSU-EDA, uncured and cured mixture	62
Figure 34. a) TGA thermogram of PTSU-EDA, b) DSC thermogram of PTSU-EDA	63
Figure 35. a) Dynamic DSC curing profile of PTSU-EDA-DGEBA mixture (OCER), b) Dynamic DSC curing profiles of PTSI-DGEBA (red line) and PTSU-EDA-DGEBA (black line) mixtures	66
Figure 36. a) Isothermal DSC thermograms of the OCER and b) dynamic leftover curing profile of PTSU-EDA and DGEBA after isothermal curing	68
Figure 37. Complex viscosity profile of the OCER.....	70
Figure 38. Storage and loss modulus of the OCER	71
Figure 39. Optical microscopy images of unground PTSU-EDA (a), ground PTSU-EDA (b), and the OCER after mixing at 40°C for 10 mins (c) under 200x magnification.	72
Figure 40. Optical microscope images of the OCER at different mixing durations (5, 10, 15 min).....	73
Figure 41. The DMA results of the cured OCER	74
Figure 42. Prepreg T _g for different DoC prepgs	84
Figure 43. T _g vs degree of cure (DoC).....	85
Figure 44. Viscosity of resin mixtures at room temperature and flexural rigidity (inverse drapability) values of prepgs	88

Figure 45. Drapability vs viscosity behavior above 10 % and bleeding of resin for 10 % cured prepreg	88
Figure 46. ILSS vs Drapability values for varying DoC (10-15-20-25%)	90
Figure 47. Tackiness vs Drapability values for varying DoC (10-15-20-25%).....	90
Figure 48. ILSS values with varying DoC.....	93
Figure 49. Thermal latent curing POZ based polymers with imidazole group covalently attached	96
Figure 50. Stages of hand lay-up and vacuum bagging during composite manufacturing..	97
Figure 51. DICY + Epoxy compressive strength.....	98
Figure 52. DICY + Epoxy tensile strength	99
Figure 53. DICY+Epoxy+PPhOZ-Im compressive strength	99
Figure 54. DICY+Epoxy+PPhOZ-Im tensile strength	100
Figure 55. Compression Test Specimens of the Produced Composites a&b) DICY + DGEBA, c&d) PPhOZ-Im+DICY+DGEBA	102
Figure 56. Tensile Test Specimens of the Produced Composites a) DICY+DGEBA, b) PPhOZ-Im+DICY+DGEBA	102

LIST OF TABLES

Table 1. Polymer matrix composite manufacturing processes (Advani et al., 2003)	2
Table 2. Curing studies of different OCERs	25
Table 3. Mechanical test dimensions	30
Table 4. Isothermal and dynamic DSC curing analysis of PUPI-DGEBA	42
Table 5. Enthalpy, limit and peak temperature values of DICY:PUPI cured DGEBA formulations	51
Table 6. Enthalpy values for isothermal and dynamic DSC curing of PTSI-DGEBA mixture and OCER	69
Table 7. Curing agent and TLC ratios.....	83
Table 8. Properties of the B-staged prepreg and mechanical properties of the cured composites	85
Table 9. ILSS and void content results	87
Table 10. Drapability, tackiness and ILSS results	93
Table 11. Tensile and compression test standards and dimensions	100
Table 12. Compression modulus and strength results of DICY+Epoxy and DICY+Phenyl oxazoline-imidazole+Epoxy	100

Equation 1. Equation for the reaction kinetics near T_g	10
Equation 2. Flexural rigiditiy of fabrics	28
Equation 3. Conversion calculation using enthalpy values	47
Equation 4. Arrhenius equation for the 1st order reaction in natural logarithmic form.....	47

LIST OF SYMBOLS AND ABBREVIATIONS

a Degree of conversion (from isothermal DSC)

k Reaction rate constant

t Time (s, h, or days depending on context)

T Temperature (K or °C)

ΔH_t Partial enthalpy (at time t)

ΔH_{total} Total enthalpy (full cure)

[A]₀ Initial concentration of reactant

[A]_t Concentration of reactant at time t

ln Natural logarithm

G Flexural rigidity

C Bending length

O Overhang length

μJ/m Microjoules per meter (unit for flexural rigidity)

Pa·s Pascal-seconds (unit of viscosity)

°C Degrees Celsius

1/T Inverse temperature, used in Arrhenius plots

MMC Metal Matrix Composites

CMC Ceramic-Matrix Composites

PMC Polymer-Matrix Composites

FRPC Fiber Reinforced Plastic Composites

OCER One-Component Epoxy Resin

TLC Thermal Latent Curing Agent

PUPI Phenyl Urea Propyl Imidazole

DGEBA Diglycidyl Ether of Bisphenol A

DGEBF Diglycidyl Ether of Bisphenol F

DICY Dicyandiamide

PTSI Para-Toluene Sulfonyl Isocyanate

EDA Ethylenediamine

PTSU-EDA Para-Toluene Sulfonyl Isocyanate-Ethylene Diamine Adduct

PPhOZ-Im Poly(2-phenyl-2-oxazoline)-Imidazole

DMA Dynamic Mechanical Analysis

DSC Differential Scanning Calorimetry

TGA Thermogravimetric Analysis

FTIR Fourier Transform Infrared Spectroscopy

NMR Nuclear Magnetic Resonance

T_g Glass Transition Temperature

ILSS Interlaminar Shear Strength

DoC Degree of Cure

GSM Grams Per Square Meter

RPM Revolutions Per Minute

COV Coefficient of Variation

UTM Universal Testing Machine

SC4-21 Spindle Code for Viscometer

ASTM American Society for Testing and Materials

mPa·s Millipascal-Second (Viscosity Unit)

phr Parts per Hundred Resin

VBO Vacuum bag only

CHAPTER 1

1. INTRODUCTION AND STATE OF THE ART

Composites are obtained by mixing two or more relatively homogeneous materials. They have superior properties compared to their individual constituents (Advani et al., 2003). The desirable properties of the constituents can be tailored to yield a product suppressing the undesired properties of the constituents. Composites can be classified based on the reinforcement type and matrix type. Based on the reinforcement type, they are classified as fiber-reinforced composites, particulate-reinforced composites, and structural composites. Among these, the fiber-reinforced composites are the most common. Based on the matrix type, composites are classified into metal-matrix composites (MMCs), ceramic-matrix composites (CMCs), and polymer-matrix composites (PMCs). Within this group, PMCs are the most used composites, which are classified into two main classes considering the polymer matrix type used: thermoplastic or thermoset PMCs. PMCs are commonly reinforced with fibers. Fiber-reinforced polymer-matrix composites (FRPCs) are used in many applications due to their high strength-to-weight ratio. Fibers withstand the loads a composite comes

across due to their stiff nature whereas polymer matrices bind fibers together and provide area and load distribution to the fibers. There are several manufacturing methods for FRPCs, which differ regarding the type of polymer matrix. The monomers of thermoset polymers are less viscous compared to thermoplastic polymers and therefore can be transferred using pumps into the fabric and crosslinked in situ. Resin transfer molding, hand lay-up, and vacuum infusion are the manufacturing methods that can be applied to fiber-reinforced thermoset polymer composites (Advani et al., 2003). Fiber-reinforced thermoplastic polymer composites can be manufactured through methods such as injection molding and extrusion where the reinforcement materials are short fibers. Thermoplastic polymers can also be used with continuous fibers, but they need to be manufactured as preprints or tapes, which are the precursor materials for composites. In **Table 1**, FRPC manufacturing processes are listed.

Table 1. Polymer matrix composite manufacturing processes (Advani et al., 2003)

Process	Matrix type	Reinforcement type	Products
Injection molding	Thermoplastic	Short fiber	Small complex shape parts, high volume
Extrusion	Thermoplastic	Short fiber	Tubes, T- sections, any cross-sectionally long part
Compression molding	Thermoplastic	Long discontinuous/continuous fibers	Large net shape parts
Wet & Tape Layup	Thermoset	Unidirectional continuous fiber/ preprints	Small low curvature parts
Liquid molding (RTM, Vacuum infusion)	Thermoset	Random, woven, knitted fabric preforms in any form	Near-net shape parts
Pultrusion	Thermoplastic Thermoset	Uni-directional tape or fabric rovings	Continuous crosssection parts
Autoclave	Thermoplastic Thermoset	Unidirectional continuous fiber/ preprints	Part size limited by autoclave size
Filament winding	Thermoset	Preprints or fiber rovings	Parts with hollow cores

Prepregs are obtained by combining either a thermoset resin or a thermoplastic resin with fibers or fabric. They are used to manufacture structural, high-quality composites in aerospace, defense, marine, and railway applications as their laminate design and resin content can be controlled (Hassan, 2021). However, composite parts obtained from prepgs show several defects such as uneven thickness distribution, water spot, whitewash, fiber wrinkling, interlaminar defects, and non-uniform resin distribution (Hassan, 2021) (Cem Özturk, 2019). There are mainly two prepreg manufacturing methods: solvent-based and hot melt prepreg manufacturing (Rusnáková et al., 2018). In the solvent-based manufacturing method, fibers are simply dipped into a solvent bath, the excess resin is removed, and the prepreg is dried out. Although the dilution of the resin with a solvent eases the penetration of the resin into the fibers, the use of solvents carries a potential health risk due to the potential carcinogenic effects of the solvents and a safety risk due to their flammability and explosivity. On the other hand, hot melt prepreg manufacturing method involves either resins with high viscosities or resins that are in solid form at room temperature, which are applied onto the fabrics as coatings or films. Thus, unlike solvent-based prepgs, hot melt prepgs do not propose a health and safety risk during manufacturing. The fibers are coated from top and bottom and heated through the conveyor belt to ensure impregnation. The issues with solvent dipping are namely solvent vapor formation, residual solvent content in the prepreg, and risk of sedimentation (Rusnáková et al., 2018). For hot melt prepgs, impregnation of the fabric is the major issue as the viscosity of the resin is high. Moreover, depending on the resin content there is a risk of generating exotherms during manufacturing depending on the resin content (Rusnáková et al., 2018). Furthermore, the use of anhydride and boron-based curing agents also propose health risks for hot melt processing (Cem Özturk, 2019). The use of latent curing agents strives to eliminate these problems, but they are also prone to whitening due to the absorption of humidity and CO₂ (Cem Özturk, 2019).

In 1936, first epoxy resin synthesis was reported by Pierre Castan and Sylvan Greenlee (M R et al., 2022; Parameswaranpillai et al., 2021). Epichlorohydrin was reacted with bisphenol A to produce diglycidyl ether of bisphenol A (DGEBA) **Figure 1**, which is one of the most used commercial epoxy resin. Diglycidyl ether of bisphenol F (DGEBF) is a slightly chemically altered version of DGEBA. Bisphenol F is the product of phenol and

formaldehyde whereas bisphenol A is the product of phenol with acetone (Parameswaranpillai et al., 2021). Another epoxy resin is the phenolic novolac epoxy, which is the product of epichlorohydrin and phenol novolac (Parameswaranpillai et al., 2021).

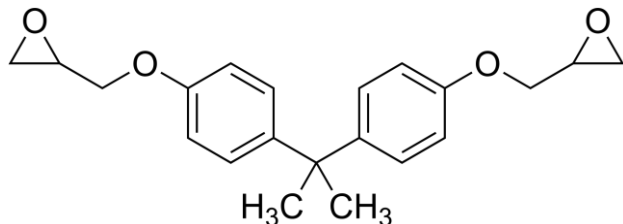


Figure 1. Chemical structure of DGEBA epoxy resin

Epoxy resins can be cured with different curing agents (Parameswaranpillai et al., 2021). There are three main types of curing agents for epoxy resins: active hydrogen-containing curing agents, cationic or anionic initiators, and thermal latent curing agents (Parameswaranpillai et al., 2021). Hydrogen-containing curing agents are the most widely used curing agents, which involve aliphatic and aromatic amines. Aliphatic amines can cure epoxy resins at room temperature whereas aromatic amines need higher temperatures to start curing process (Parameswaranpillai et al., 2021). Amines can be classified into primary, secondary, and tertiary amines. Primary and secondary amines react with epoxy resin via a step-growth polymerization whereas tertiary amines are used as catalysts for the homopolymerization of epoxy resin (Parameswaranpillai et al., 2021). Anionic polymerization is generally initiated through tertiary amines and especially with imidazoles (Vidil et al., 2016). Moreover, tertiary amines are used for anionic alternating copolymerization of epoxides with cyclic anhydrides as well as they catalyze the epoxy-hardener step growth polymerizations with hardeners such as carboxylic acids and thiols (Dušek, 1986; Ooi et al., 2000; Vidil et al., 2016). Hydroxyl groups are formed through epoxide chain opening, which interact with the oxygens of the unreacted epoxy groups. This provides the basis of a nucleophilic attack of the amino groups on the epoxy polymers and through this autocatalytic process the reaction is catalyzed (Bashir, 2023). Lewis acids are used for cationic polymerization of epoxy resins (Vidil et al., 2016). Metal halides and triflates are common examples that initiate cationic polymerization of epoxy resins. The metal halides react with few epoxy groups to form metal halides and alkoxide groups on each binding site of the metal halide. This reaction occurs at room temperature but rapidly stops

where it needs further activation at elevated temperatures at a very slow rate (Vidil et al., 2016). Thus, except BF_3 , the Lewis acid initiators are not used for commercial applications (Vidil et al., 2016). For epoxy-based preangs, curing at low temperatures is not desired since several plies of preangs need to be stacked before the preangs are gelled. To prevent the curing of the epoxy resin at low temperatures, one-component epoxy resins (OCERs) with thermal latent curing agents (TLCs) have been developed over the years using different methods.

The latent curing agents are designed to provide flexibility in terms of fine-tuning the desired curing temperature as well as ensuring that the manufactured composite preangs are stable at room temperature. The room temperature stability will enable the preangs to be stored at ambient temperatures saving high transportation and storage costs compared to the conventional preangs, which are normally transported and stored in the cold chain to prevent crosslinking reactions. In addition, the control over the reactions can be increased using multiple latent curing agents regarding the reaction initiation point (Pouladvand et al., 2020a)(Yao et al., 2017a). However, latent curing agents such as DICY (dicyandiamide) absorb humidity and CO_2 , which cause white spots to occur resulting in visual problems on the cured part (Cem Özturk, 2019). Still, the activation of latent curing agents at desired temperatures through different stimuli such as light irradiation and heat is a promising area of application and research. The control over the degree of cure of the preangs enables them to meet certain tackiness and drape properties, which are quite beneficial for layup processes for complex parts.

Encapsulation of latent curing agents in epoxy resins is a widely used method to cure epoxy resin at desired temperatures and in a controlled manner (X. Yang et al., 2020a). Several encapsulation methods such as interfacial polymerization, spray drying, in-situ polymerization, and solvent evaporation have been applied up to date (X. Yang et al., 2020a). Depending on the latent curing agent used, the encapsulation method can be altered. Polymers such as polyethyleneglycol (PEG), polyvinylpyrrolidone, polyvinylacetate, polymethylmethacrylate (PMMA) and nanoparticles such as graphene nanoplatelets (GNP) (Jee et al., 2020) are used as encapsulation agents. However, there are several challenges in

encapsulation method, some of which are the synthesis of the capsule materials, formation of the capsules, intensity of the amphiphilic nature of the capsules, the homogeneity of the capsule polymers with regards to their molecular weights (narrow polydispersity index), etc. These challenges affect the capsule's performance on capsule formation and the size of the formed capsules, stability of capsules in the mixture over a broad range of conditions up to desired release conditions. For instance, if the capsules are broken down prior to their desired release conditions then they are not useful due to early release of the curing agent that will cause complications in the released environment. Furthermore, the narrow distribution of the size of the capsules ensures that the entrapped number of molecules in a capsule is the same in each capsule. This contributes to the control over the molecules that are desired to be trapped. Yuan reported in his study that most of the epoxy curing agents that are amine based are amphoteric and cannot form capsules in acidic conditions with poly (urea-formaldehyde) (Yuan et al., 2008). A new class of polymer that has been recently used by our group as encapsulating agent is polyoxazolines(Atespare et al., 2024, 2025; Behroozi Kohlan et al., 2023; Kohlan et al., 2022; Salamatgharamaleki et al., 2025; Viegas et al., 2011). Polyoxazolines are a class of polymers that can be designed, controlled, and manufactured with high quality. They have low polydispersity and they are nonionic, stable, and highly soluble both in water and organic solvents (Viegas et al., 2011). Polyoxazolines can form capsules due to their tunable hydrophilicity/ hydrophobicity parts which can easily be modified depending on their end groups. Furthermore, polyoxazolines can be easily synthesized depending on the desired properties such as hydrophilicity, amphiphilicity, temperature responsiveness, and biocompatibility (Dworak et al., 2014; Oleszko-Torbus et al., 2020; Viegas et al., 2011). These properties enable polyoxazolines to be considered a strong candidate for encapsulation applications such as latent curing agents.

Covalent attachment and reversible bonding of curing agents are other methods of creating latent curing agents. These systems can be classified into covalent and dynamic covalent interactions according to their type of interactions with the matrix polymers (Z. P. Zhang et al., 2014). Dynamic covalent interactions are Diels-Alder, alkoxyamine, urea bonds etc. (Z. P. Zhang et al., 2014). These systems offer more stability compared to physical capsules as the covalent and reversible bonds release upon stimulation such as heat, pH, and light and they remain stable at room temperature (Z. P. Zhang et al., 2018). Furthermore, these systems

eliminate the use of solvents and provide a more environmentally friendly processing on the contrary of physical encapsulation systems where a solvent is used to form the capsules. Moreover, reversible bond systems such as substituted ureas can be produced in bulk and with ease due to their simplicity of hindered urea chemistry (Ying et al., 2014). The reversibility of the bonds in the reversible systems can be characterized through spectroscopic measurement methods such as FTIR with respect to temperature. This enables the reaction kinetics of the system to be tracked in a controlled fashion when performance over temperature of these systems is put under consideration. In encapsulation methods, optical measurement methods provide information on the system through the observation of capsules within the matrix, which then does not provide any information on reaction kinetics of the system. Reversible bond systems might also prove to be beneficial for prepreg manufacturing where a degree of cure between 5-30% (Banks et al., 2004a) is needed for prepgs, which requires control over reaction kinetics of the epoxy resin.

Polyoxazolines can also be further functionalized with curing agents/catalysts such as imidazole where they can be used as reversible covalent bond utilized curing agents. Polyoxazolines can be retarded with these curing agents and these systems can provide more stability at room temperature and be released upon stimuli. Moreover, molecules such as ureas are reported to be used as reversible covalent attachments and be used for several applications as they bear high bond strength and more control on reversibility (Ying et al., 2014).

This thesis focuses on the incorporation of small molecule- and polymer-based thermal latent curing agents into epoxy resins to obtain OCERs, manufacturing prepgs with these OCERs, investigating curing properties of both resins and prepgs, and determination of the properties of prepgs and mechanical properties of the cured laminates. The OCERs will be prepared using substituted ureas through the reactions of aromatic isocyanates and amines and POZ polymers terminated with imidazole end groups mixed with DGEBA epoxy resin. These TLCs were mixed with epoxy resin through a homogenizer at certain ratios and durations and they were characterized for their cure characteristics and morphology. Moreover, different properties such as resin melt viscosity, stability, dynamic

thermomechanical behavior (DMA) of the OCERs and tackiness and drapeability of the preprints and mechanical properties (tensile, compression, interlaminar shear strength) of the cured composites were investigated. The curing properties of the resins were studied with dynamic and isothermal DSC methods. For each system, the reaction enthalpy, the curing temperature and T_g were measured and recorded. The prepreg manufacturing conditions were set through a certain temperature and duration, which were determined with respect to DSC profile of the used curing agent using off-stoichiometric ratios. The preprints' drapeability and tackiness values were measured to link the effect of them on ILSS with respect to the changes in degree of cure. For instance, the loss of tackiness is an undesired property as it makes the layup of the preprints more difficult and can decrease the interlaminar shear strength (ILSS) (Amare et al., 2022). Moreover, the loss of drapeability causes wrinkles and voids on the corners of the 3D complex shapes of the parts and loss of dimensions and shapes of the cured parts and thus mechanical properties. Therefore, the tracking of these properties is crucial for the prepreg manufacturers to suggest suitable shelf life under certain conditions as well as for manufacturing preprints with optimum properties. Finally, the preprints were cured to investigate the effect of the thermal latent curing agents on the mechanical properties of the cured composites regarding their tensile, compressive, and ILSS properties. The T_g values of the cured composites were measured and tracked through DMA and DSC to observe the effect of different polymers on the T_g of the composite.

LITERATURE SURVEY

Epoxy resins are one of the most used thermoset resins in composites due to their excellent physical, chemical, and mechanical properties (Kudo et al., 2015; Mozaffari & Beheshty, 2018; Wei et al., 2020; X. Yang et al., 2020b; Yao et al., 2017b; Yen et al., 2016; S. Zhang et al., 2017). Various curing agents are used for curing epoxy resins such as amines, anhydrides, imidazoles, polyamides, polysulfides, phenol formaldehyde, and polybenzoxazines (Kudo et al., 2015; Mozaffari & Beheshty, 2018; Wei et al., 2020; X. Yang et al., 2020b; Yao et al., 2017b; Yen et al., 2016; S. Zhang et al., 2017). These curing agents have different curing mechanisms. Primary and secondary amines polymerize epoxy resins through step-growth polymerization, but tertiary amines undergo chain-growth

polymerization of the epoxy (Ham et al., 2010). The curing agents react with epoxy resins at different temperatures. For instance, imidazoles are reported to react with epoxy resin at room temperature (Kudo et al., 2015; Yen et al., 2016; S. Zhang et al., 2017) whereas DICY can only be activated at temperatures around 170 °C. The activation of the curing agents is related to their solubility in the resin as well as their reactivity with the epoxy group at a certain temperature. This also influences the cured epoxy properties such as its glass transition temperature (T_g) and mechanical strength (Michel & Ferrier, 2020).

CURING KINETICS OF EPOXY RESINS

Epoxy resins can be cured with different types of curing agents but mainly with the curing agents under the classes of amines, anhydrides, and alkali curing agents (Jin et al., 2015). Amine curing agents are further classified into three sub-groups: aliphatic, cycloaliphatic, and aromatic amines. Amine-type curing agents react with the epoxy group through nucleophilic addition (Jin et al., 2015). Triethylenetetraamine (TETA), diethylenetriamine (DETA), and ethylenediamine are aliphatic amine curing agents that react rapidly with epoxy resin at room temperature as they are not sterically hindered. Isophoronediamine (IDA) and piperidine are examples of cycloaliphatic amines that provide intermediate cured resin properties between aliphatic and aromatic amines. Diamino diphenylmethane (DDM) and diamino diphenyl sulfone (DDS) are the two most common aromatic amine curing agents that are used in curing epoxy resins. Imidazoles and tertiary amines are examples of alkali curing agents that are mostly used along with other curing agents such as mercaptans, anhydrides, polyamides, and amidoamines (Jin et al., 2015). Anhydride curing agents are reported to have a very long pot life and are generally used with amines.

Epoxy curing stages have been identified by Dusek as extensive branching, transformation of soluble part, gel point, gel formation, and formation of a dense network (Dušek, 1986). Dusek has also proposed that regarding the mass law action the curing kinetics is controlled by the chemical kinetics and not by diffusion. However, Fujimoto and Turi stated that the activation energy, E_a , and the change in the reaction kinetics from chemical to diffusion control takes place as the curing advances (Edith A. Turi, 1981; Oishi & Fujimoto, 1992).

Dusek investigated the homogeneity or inhomogeneity of the epoxy curing through several characterization methods such as small angle x-ray scattering (SAXS), small angle neutron scattering (SANS), and static light scattering (SLS). The studies were performed to compare the properties of the electron densities before and after epoxy curing. Although some methods indicate that before gelation no inhomogeneity occurs, during gelation and curing some inhomogeneities are present as Dusek reported (Dušek, 1986). The claims are valid only for epoxy-amine systems which can only cross-link through a single alternating reaction. Thus, partly compatible systems, cyclization through polyetherification (homopolymerization of epoxy), and simultaneously and consecutively occurring reactions should be further studied for inhomogeneity or homogeneity, which later would be linked to kinetic studies. In the reaction scheme below, one can simply see the reaction of reactants A and B with intermediate AB and the final product -AB-.

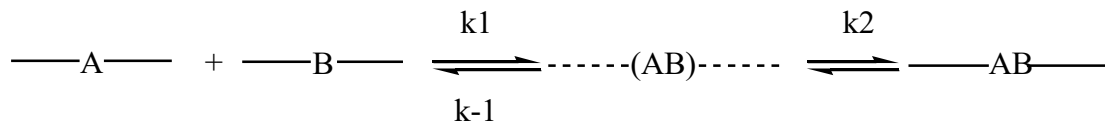


Figure 2. A two reactant reaction kinetics scheme

If k_1 & $k_{-1} \gg k_2$, then diffusion plays no role in the kinetics of the reaction. Diffusion control can be effective at temperatures over T_g , but the extent of it to the overall network formation has not been identified fully (Dušek, 1986). Dusek stated that near T_g , the following equation can hold with regards to free volume theory:

$$\ln k \propto (T - T_g) / (T - T_g) + c^g$$

Equation 1. Equation for the reaction kinetics near T_g

This equation indicates that k approaches zero when $T_g - T = c^g$ where c^g is a constant about 50 K but experimental data shows that k approaches zero around 25-30 K of difference, which means that the reaction at those temperatures is controlled by diffusion kinetics (Dušek, 1986). T_g also is determined by a huge increase in rigidity in DMA and a simultaneous decrease in the rate constant of the autocatalytic epoxy-amine reaction. Reaction rates at different temperatures influence kinetics through diffusion control due to

T_g but there is not any evidence that they influence the network formation (Dušek, 1986). Dusek and Ilavsky also studied epoxy curing statistically to find out the dominating mechanisms in curing and they found out that the substitution effect of the amine has little effect on the conversion (Dušek et al., 1975). They also found that a greater effect is caused by the change in the ratio of the amine and epoxide functionalities.

Choe and Kim studied the curing properties of polyamide for epoxy resin, and they stated that polyamide hinders epoxy curing as shown by a low conversion at the end of the reaction (Choe & Kim, 2002). Polyamide and epoxy seem completely miscible up to 120°C and therefore it has been proposed that polyamide may trap some epoxy in its matrix, causing epoxy to be left uncured. Zhou and his friends studied the curing of epoxy resin with imidazole using two kinetic methods and they observed that activation energy increases throughout the reaction from 34.3 to 63.84 kJ/mol. (Zhou et al., 2005). They, along with other researchers, reported that epoxy reacts with imidazole to form an adduct first and then the formed adduct polymerizes epoxy through etherification (Ham et al., 2010; Ooi et al., 2000; Zhou et al., 2005). Vidil et al. stated that the cross-linking depends on the nucleophilicity of the amine group considering the reactants are DGEBA and an amine crosslinker (Vidil et al., 2016). Moreover, Heise et al. stated that imidazole cures epoxy through anionic polymerization as well as forms the adducts with epoxy in 1:1 and 1:2 ratios (Heise & Martin, 1989).

Ignatenko et al. tried to accelerate the epoxy curing using several different curing agents and found out that the autocatalytic effect of the reaction is due to the OH groups that are formed after the epoxy group reaction with amidoamine (Ignatenko et al., 2020). Cook et al. observed two peaks, which they related to the adduct formation and etherification (Ooi et al., 2000). Moreover, they concluded that only 1-MI (methyl imidazole) displayed a single peak whereas the other curing agents 2-MI and 1-PhI (phenyl imidazole) displayed two peaks. Bernath investigated a commercial epoxy system that is used for resin transfer molding (RTM) systems where the curing temperature is far below the glass transition temperature (Bernath et al., 2016). He used a DGEBA epoxy resin with a mixture of amine curing agents, which included isophorone diamine and 2-piperazynyl 1-ethylamine. He concluded that the

huge difference between the curing temperature and T_g meant that vitrification occurred prematurely, and this caused the cross-linking to be very slow due to the bulk polymer. This is reported to have caused problems like warpage in composite parts due to the internal residual stresses left in the material after curing and cooling (O'Brien & Mather, 2001). Vidil stated that mechanical and optical properties are also influenced by curing kinetics (Vidil et al., 2016). Ying et. al stated that to obtain reversible bond structures, both forward and backward reaction constants should be large (k_1 & k_{-1}) (Ying et al., 2014). Moreover, the second criterion that should be met is that the reaction should favor polymer formation (large $K_{eq}=k_1/k_{-1}$). They concluded that molecules such as 1,1- diisopropyl urea (DIPU) and 1,1-diethyl urea (DEU) showed large K_{eq} values in the range of 10^7 (Ying et al., 2014). Moreover, they added that amide bonds are stable at mild conditions due to the conjugation of nitrogen atom's lone electrons with carbonyl's π electrons but can be weakened with bulky substituents to yield ketenes without the requirement of extreme conditions (Ying et al., 2014). The addition of the bulky substituent is believed to be disturbing the co-planarity of the amide bond and weakens the amide-carbonyl interaction. However, the formed ketene structure, **Figure 3**, is not stable to be used as a reversible bond. A functional group that satisfies these conditions is isocyanate. It is reasonably stable at mild conditions and can react readily with amines to yield polyureas and polyurethaneureas (Ying et al., 2014). Isocyanate formation through urea bond breakage is shown in **Figure 4**. The release of isocyanates, amine and imidazole are expected to cure and catalyze the epoxy curing reaction. The adduct formation through the combination of imidazole with epoxy catalyzes etherification which can be simultaneously cross-linked with the amines and isocyanates to yield cross-linked networks.

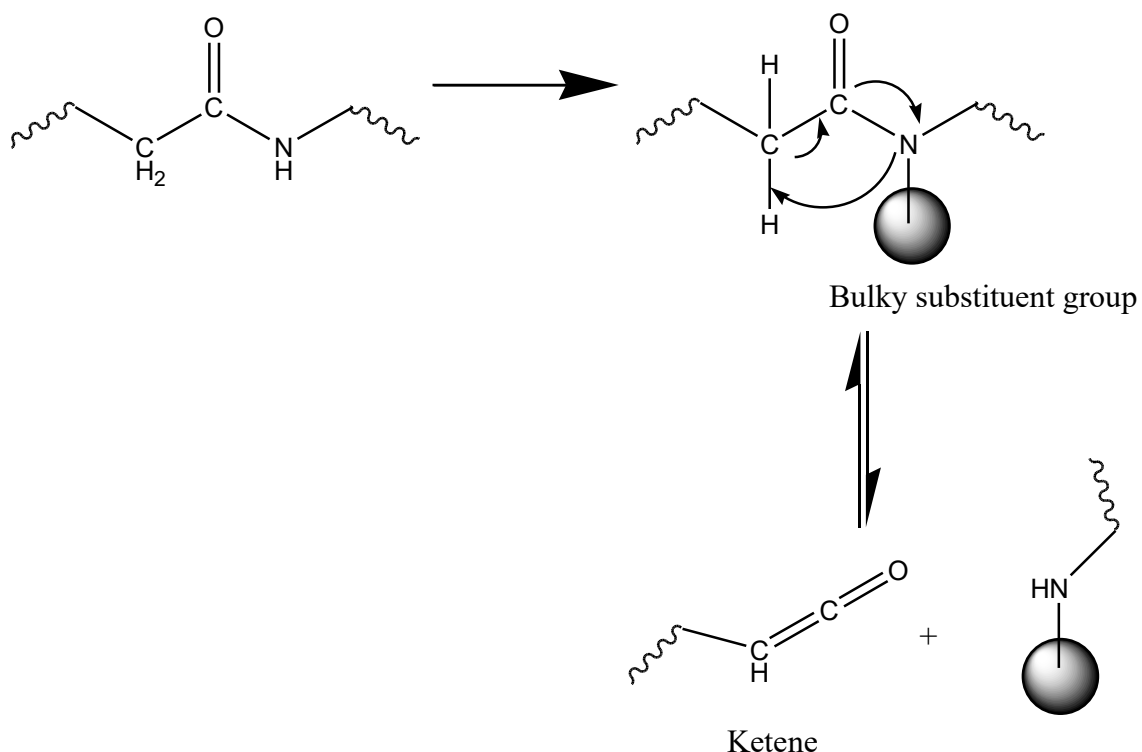


Figure 3. Ketene formation through reversible bonds

Liu and et. al investigated the properties of dynamic imine bonds to be used as a functional agent in epoxy resin composites which should incorporate properties such as self-healing, reprocessable, degradable and thermadapt shape memory (Liu et al., 2023). They reported that imine bonds can be attacked under acidic conditions to yield the starting materials as well as the imine materials that bear easy reprocessing show weaker thermodynamic properties. Pannone and Macosko studied the kinetics of isocyanate and amine reactions for RIM (reaction injection molding) systems and they concluded that reaction heats for aliphatic amines were higher than aromatic amines for an adiabatic temperature rise system that they constructed (Pannone & Macosko, 1987).

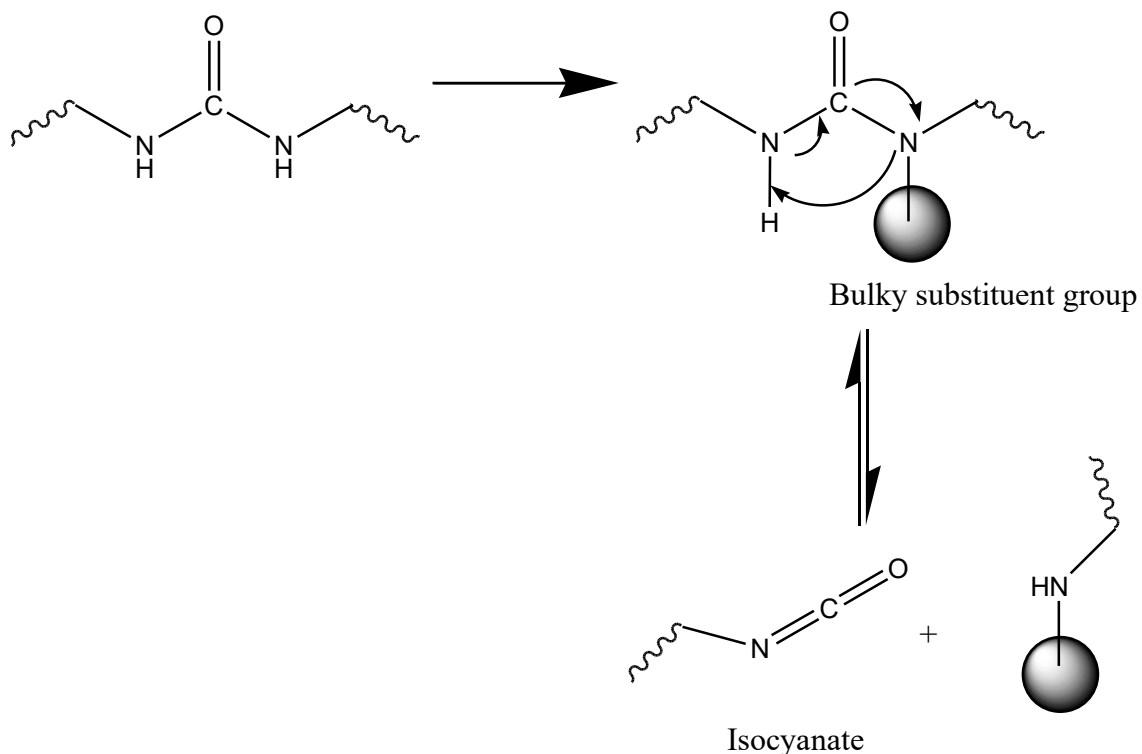


Figure 4. Isocyanate formation through reversible bonds

PREPREG MANUFACTURING, LATENT CURING AGENTS

Prepreg materials are semi-finished products. They are stored at low temperatures to prevent a complete reaction of the thermoset polymers. They provide the highest quality composite products as they provide several advantages such as optimum resin/fiber ratio, low void content, and, certain thickness to be manufactured in the high quality manufacturing systems such as autoclave, press, and oven (Ahn & Seferis, 1993; Cem Özturk, 2019; Hassan, 2021; Rusnáková et al., 2018; R.-M. Wang et al., 2011). For the hot melt prepgs, it is reported that the heat transfer from the resin to the fabric is crucial in the final quality of the prepreg (Ahn & Seferis, 1993). The main problem for the solvent dip prepgs is reported to be the residual solvent present in the prepgs (Deng et al., 2022; Grunenfelder et al., 2017). For B-staged prepgs, the degree of cure is proposed to be between 5-30% to obtain the optimum prepg properties (Banks et al., 2004a; Cem Özturk, 2019). However, a relationship between the degree of cure, stability, and tackiness remains open for research.

Drapeability and tackiness measurements are often overlooked in research but both properties remain quite important for the manufacturers as they influence the quality of the composite end product. The prepreg manufacturers have developed in-house built methods to measure these properties and thus the developed methods are not shared within the academy and industry. ASTM has also announced that it is developing a tackiness measurement standard, ASTM WK70428, which has not been concluded up to now. Especially in manufacturing methods such as automated fiber placement (AFP) and automated tape lay-up (ATL), (see **Figure 5**), the tackiness of the tapes is an important parameter for the quality of the manufactured composite. Tapes are slitted from prepgs and thus it holds an important topic for the prepreg manufacturers. Drapeability is modeled through different fabric orientations and is considered more of a textile property (Han & Chang, 2021) whereas tackiness is directly related to the resin properties that are used in prepreg manufacturing. The manufacturers prefer prepgs with an optimum tackiness because a low tackiness provides difficulty in adhering the subsequent plies and possible movement of the prepreg causing the ply angels to mismatch to each other whereas a high tackiness is not desired as wrong placements are harder to correct due to the strong bonding.

Dubelmann suggested that tackiness is like pressure-sensitive adhesives (PSA) as tackiness is the intrinsic stickiness in the absence of any crosslinking reaction or solvent evaporation (Budelmann et al., 2020). However, the presence of fibers, B-staging, and induced defects in the prepreg during manufacturing makes the tackiness a complex problem to solve for the prepgs compared to PSAs. Moreover, the tackiness of the prepreg can cause problems in both AFP and ATL machines during conveying, cutting, and removal of the tape from the backing material before adhering to the substrate. Dubois studied tackiness experimentally and suggested that tackiness and debonding energy were different when the test parameters were changed (Dubois & Beakou, 2009). For the analysis, he selected humidity and aging time as environmental factors, and probe temperature, contact force, contact time, and debonding rate as the test parameters. Bashir found out that tackiness was not lost until %60 of conversion for epoxy-amine systems (Bashir, 2023).

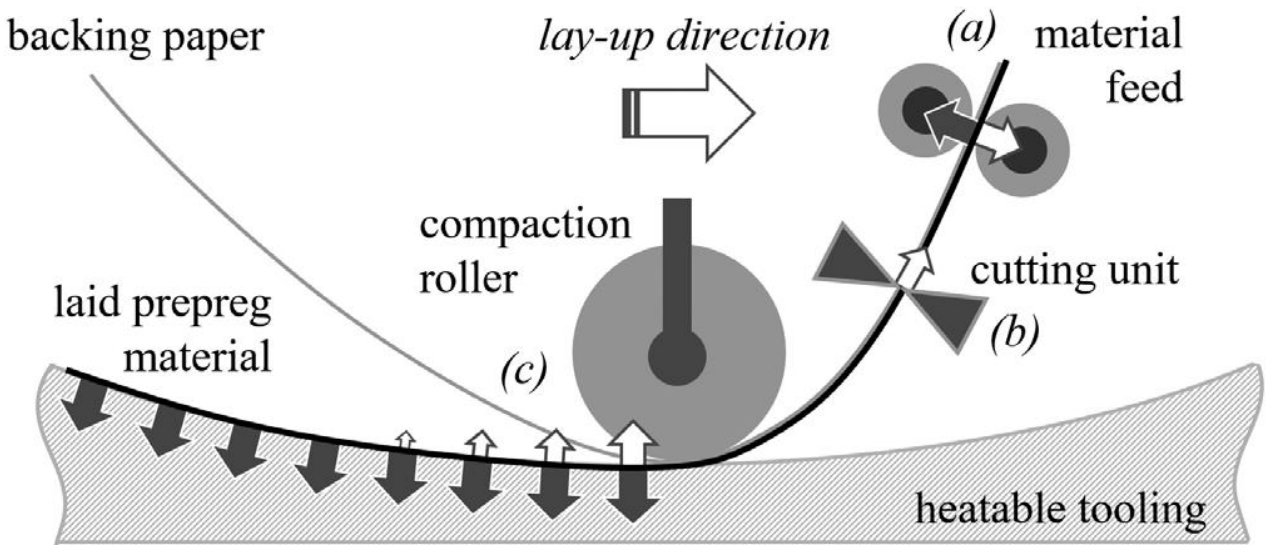


Figure 5. Representation of prepreg tack in ATL (Budelmann et al., 2020)

Banks et al. proposed that 30% of curing at B-staging provided high drape, good tackiness, low residual stress, and a good level of handling (Banks et al., 2004a). However, they used a different approach for measuring tackiness, which is the ASTM D 3167, the floating roller peel test. In this test, the prepgs are placed onto an aluminum tool, which is mostly used for composite manufacturing, and a force of 10 kN is applied for the adhesion for one minute. Then, the prepreg is detached from the plate with a debonding rate of 100 mm/min.

LATENT CURING AGENTS

Latent curing agents are highly sought systems in the composites industry due to their ability to be stored at room temperature, have controllable and tunable reaction kinetics, and be stimulated through various sources such as light, heat, or pressure (Mozaffari & Beheshty, 2018; Rahmathullah et al., 2009; X. Yang et al., 2020b, 2020a; S. Zhang et al., 2017). Encapsulation is a method in which the reactive curing agents are trapped inside an encapsulating polymer physically either in core-shell structures or in matrix structures (Lowry et al., 2008). In **Figure 6**, the reactive agents are called core materials, which are shielded by the encapsulating polymers forming shell layers, thus providing latency. The solubility difference of the shell polymer's end groups with the solvent that it is prepared in forms the shell structure whereas there are also groups of the shell polymer that are compatible with the curing agent and thus surround the curing agent, thus preventing its

reaction with the resin matrix when it is incorporated into it later. To form the capsules, mainly solvents are used, and both the shell polymer and core curing agent are used through combinations of mixing speed, temperature, and duration. Studies suggest that the use of a solvent-free dry coating process (DCP) to form the capsules eliminates the health risks associated with the solvents (Jee et al., 2020). The performance of the latent curing agents can be tracked through the viscosity increase of the resin matrix, changes in drapeability and tackiness, and the degree of cure (conversion), α .

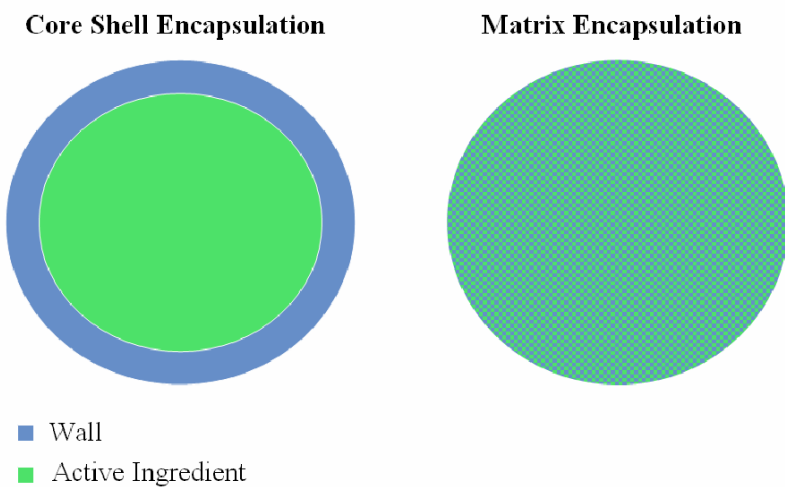


Figure 6. Methods of encapsulation (Lowry et al., 2008)

Polymers such as polyethyleneglycol (PEG), polyvinylpyrrolidone, polyvinylacetate, polymethylmethacrylate (PMMA), nanoparticles such as graphene nanoplatelets (GNP) [10] are used as encapsulation agents. The capsules that are prepared using these polymers are prepared through interfacial and *in situ* polymerization. Both processes are difficult to control as they depend on many parameters (Zhao et al., 2019). Polymer capsules can be prepared by solvent evaporation method which offers good control on the parameters such as evaporation temperature of the solvent and they have been reported to be useful encapsulating latent curing agents for epoxy systems (Dworak et al., 2014). Polyoxazolines can form capsules due to their tunable hydrophilic/ hydrophobic parts which can easily be modified. Moreover, polyoxazolines are reported to have easy control over their synthesis for tuning the desired properties such as hydrophilicity, amphiphilicity, temperature responsiveness, and biocompatibility [16]– [18]. These properties enable polyoxazolines to be considered a

strong candidate for covalent attachment of the curing agents and catalysts to POZ chain and release them upon temperature stimuli. The capability of the substituents in the oxazoline chain determine the hydrophilicity or hydrophobicity of polyoxazolines (Dworak et al., 2014). This enables polyoxazolines to be synthesized in a controlled manner and with tailored properties. Thus, polyoxazolines may present the opportunity to trap curing agents in epoxy resins and later release them upon activation at desired curing temperatures.

Isocyanates and diamines react to yield substituted ureas (Stoutland et al., 1959). The use of these substituted ureas as latent curing agents/accelerators are also reported in the industrial works and patents by Kretow and Maurice in different studies (Robert P. Kretow, 1996; Schiller Arthur Maurice et al., 2010). However, all these studies stated that substituted ureas are mainly used together with DICY (dicyandiamide) to accelerate DICY's reaction with epoxy at lower temperatures and therefore save energy and time. Therefore, there are not so many studies on the curing properties of substituted ureas and it is an open area for research. Stoutland et. al researched the reactions of diamines with isocyanates and proposed the reaction scheme as in **Figure 7**. Depending on the nature of the aryl or alkyl group attached to the isocyanate, the reactivity of the molecule changes (Stoutland et al., 1959). In this work, substituted ureas which are the reactions of isocyanates and amines will be used to observe the effectiveness of these molecules. In **Figure 8**, reaction between phenyl isocyanate and amino propyl imidazole has been shown to yield phenyl urea propyl imidazole.

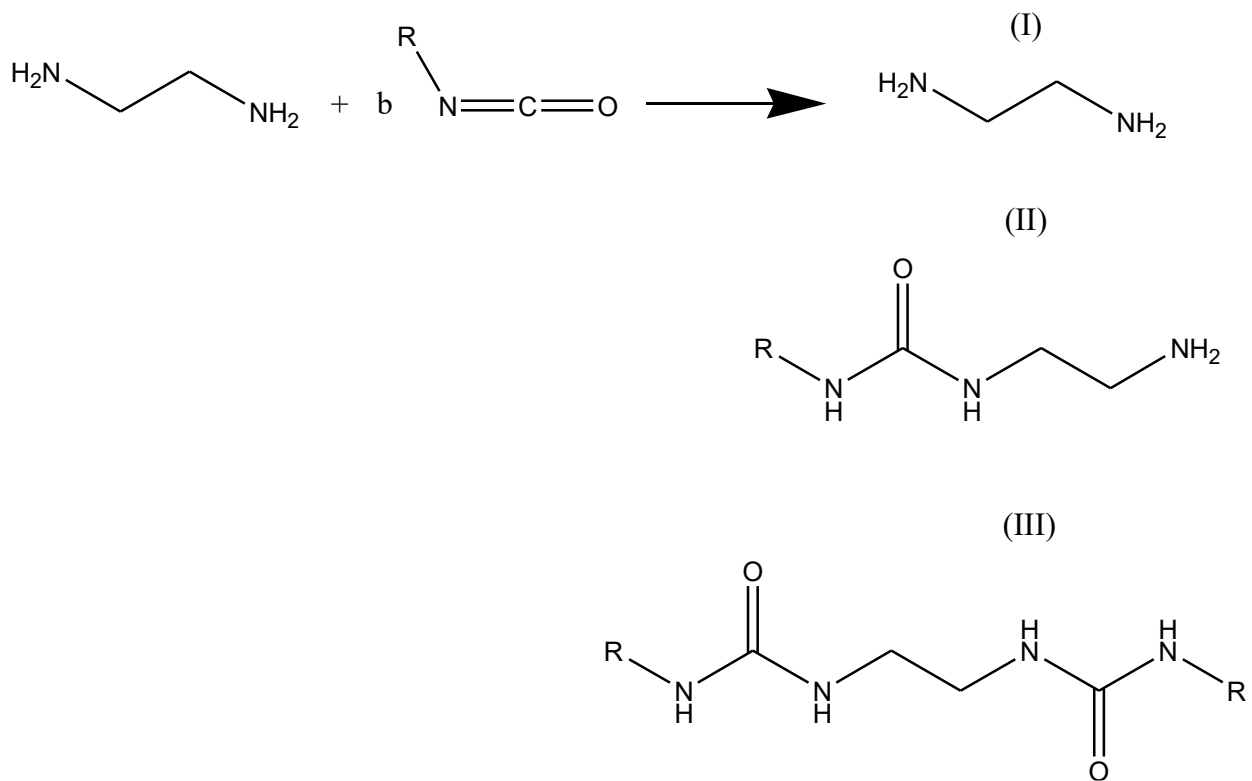


Figure 7. Diamine (left) reactions with isocyanates (right) (Stoutland et al., 1959)

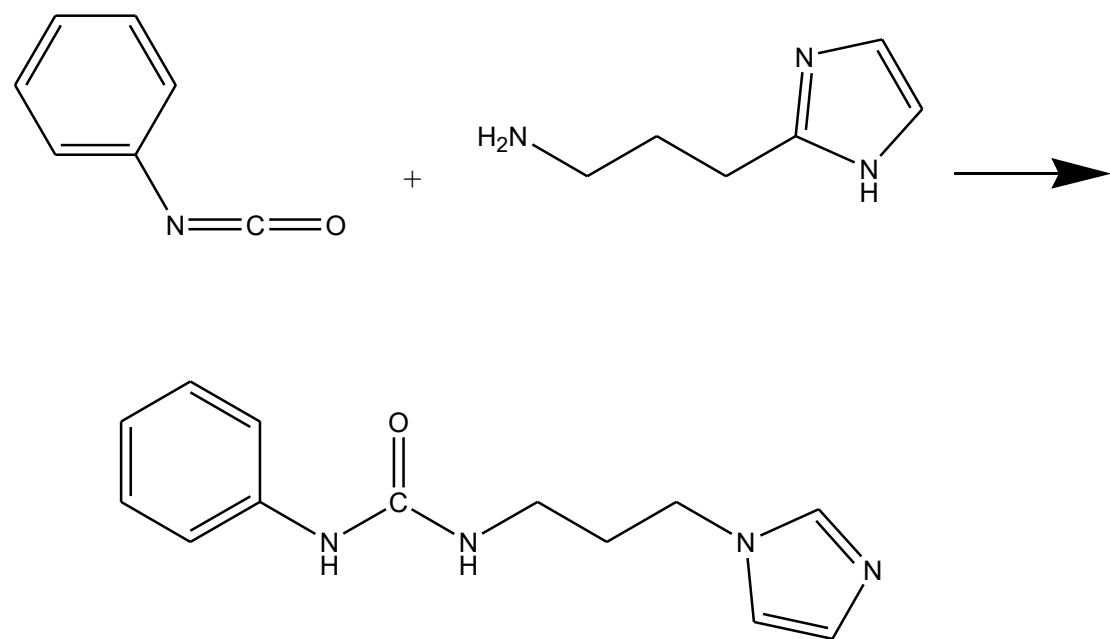


Figure 8. Phenyl isocyanate (left) and amino propyl imidazole (phenyl urea propyl imidazole) reaction scheme

STABILITY OF EPOXY PREPREGS

The solubility of the latent curing agents in epoxy is also an important aspect regarding the stability of the prepgs. A room-temperature insoluble agent will not react with the epoxy resin yielding stability at room temperature. Shi stated that the latent curing agents are insoluble powders in epoxy resin at room temperature but are also mostly difficult to mix in epoxy resin after heating (Shi et al., 2019a). There are several methods to measure the stability of prepgs over time. After a prepg reaches its shelf life it cannot be used further as it will crosslink to a certain degree and the prepg would lose its drapeability which cannot be stacked to form a laminate. Thus, faults like delamination, uncured regions, watersports, and/or whitening spots (Cem Özturk, 2019) can be observed for these materials.

Stability studies are critical in measuring the degree of cure over the time and temperature that prepgs are exposed to but also quite important to understand the chemical changes occurring in the reaction of the epoxy resin with regards to the factors such as humidity, time, and temperature. Cole et al. found that a high moisture level exposure causes an increase in tackiness, but it also changes the viscosity profile during curing and this yields in void formation, which ends up in having inferior mechanical performance (Cole et al., 1989). They used several techniques such as DSC, FTIR, reverse phase liquid chromatography (RPLC), and high-performance size exclusion chromatography (HPSEC). They tracked the epoxide content through FTIR, which decreased by 0.34% per day for 66 days at room temperature and 50% relative humidity for an epoxy system consisting of %70 tetraglycidyl diamino diphenyl methane (TDDM), 8% bisphenol A novolac type epoxy, and 22% curing agent diamino diphenyl sulfone (DDS). They also reported a decrease of 0.26% per day in the heat of the reaction, which was measured by DSC. Cole also stated that although they did not measure any change to resin flow using conventional methods, they observed a higher resin content in the cured laminates after aging, which can be interpreted as resin could not flow as much as the unaged prepg. Jones et al. used photoacoustic spectroscopy to track aging influences on epoxy content and interlaminar shear strength (ILSS). They reported a low change in the IR spectra intensity of epoxy peaks during aging under low humidity aging for

60 days coupled with a low decrease in ILSS value changes. They used desiccants to provide low humidity levels but did not measure or report humidity levels as their main aim was to link photoacoustic spectroscopy with aging and mechanical properties and they concluded that a healthy correlation can be made over 60 days of data (Jones et al., 2008). Luis developed a characterization methodology to track aging and it included six methods namely: tackiness, drape, and solubility as well as mechanical tests such as Tensile, DMA, ILSS, and compression after impact (CAI) tests to quantify the stability of the prepgs comprehensively (Luís, 2014). He stated that he used processability tests as an indication of deterioration and after a certain degree of deterioration, he proceeded to the mechanical tests, which saves time and budget. DMA showed the highest variation value of %80 regarding the secondary relaxation energy, which can be interpreted as the molecular transformation occurring within the prepreg when it is exposed to aging conditions. Pouladvand studied the effects of dual curing using two curing agents. He used the first curing agent, diethylene triamine (DETA), for initial curing (B-staging) and the second curing agent DICY to complete the curing at elevated temperatures (Pouladvand et al., 2020a). He used DSC and FTIR to track changes where he associated the peak at 916 cm^{-1} in FTIR with the epoxide group and tracked the intensity change of the peak after certain aging intervals. They concluded the study stating only a %7 increase in the degree of cure was measured after 21 days of room temperature storage. Simmons et al. from Hexcel company acquired a room temperature stable prepreg patent in 2004, stating that the manufactured epoxy prepreg is stable at room temperature between 3 to 6 months (Simmons et al., 2004). They stated that the epoxy prepreg needs to be crystallized between -5 to 10°C for two days to achieve complete crystallization Sijbesma et al. investigated the reversibility of hydrogen bonding using 2-ureido 4-pyrimidone dimers and found that high directionality of the assemblies prevented network formation and gelation (Sijbesma et al., 1997). They added that this directionality prevents microphase separation through crystallization in the bulk polymer. This leads to the prevention of unspecified aggregation which enables the control over network formation and architecture (Sijbesma et al., 1997). This property is desired for hot melts with a tunable temperature dependent rheology which would be quite suitable for prepreg manufacturing.

MECHANICAL PROPERTIES OF EPOXY COMPOSITES

Epoxy resins are brittle in nature and therefore they are generally reinforced with additives such as nanoclays, carbon nanotubes (CNT), graphene, or thermoplastics such as polysulfone (PS), poly aryletherketone (PAEK) or polyetherimide (PEI) (Shi et al., 2019a). High temperature curing of epoxy resins can cause internal stresses left in the resin after curing due to high shrinkage and difference in thermal expansion coefficients of the resin and the mold that is used to cure (Pouladvand et al., 2020a). Beside these points, the chemistry of the curing agent, temperature, and duration of the cure also have crucial roles in the curing and thereafter on mechanical properties.

Shie et al. investigated the properties of modified imidazole with α , β -unsaturated diester and found that modified imidazole improved epoxy's impact strength (Shi et al., 2019a). The group reported an increase in the impact strength of cured DGEBA epoxy from 1.4 kJ/m^2 to 5.2 kJ/m^2 compared to neat epoxy when they used 2-phenyl imidazole with diethyl fumarate (PZDF) as a curing agent. Vacche et al. studied DGEBA with DICY (dicyandiamide) latent curing agent with three different accelerators, two being urea derivatives and one polyamine. He found that the tensile properties of the epoxy that was cured with polyamine showed a slightly better strength and strain at break compared to urea ones. However, for flexural strength, the urea-cured ones displayed a better performance compared to the polyamine cured. All three formulations yielded similar and comparable results with a commercial DGEBA epoxy system (Dalle Vacche et al., 2016). Zhang et al. developed a sizing agent for high-modulus carbon fibers with a latent curing agent embedded in them. They observed an increase of %8.6 in interlaminar shear strength (ILSS) compared to an unmodified sizing agent used in carbon fibers (X. Zhang, 2011). Zhang stated that this is due to the better wettability of the fibers with the use of a latent curing agent. Interfacial performance between the fiber and epoxy resin was improved using a latent curing agent, which was used as sizing of the carbon fiber. Zhang et al. investigated the mechanical properties of epoxy resin that is cured with a bio-based maleopimamic acid (RAM) and imidazole-type salt as a latent curing agent and compared it to a system that is cured with a petroleum-based methyl hexahydrophthalic anhydride (MHHPA). They concluded that an increase of %44, %40 and

70°C were observed for bending strength, modulus, and T_g (X. Zhang et al., 2017). Palmieri showed in his work on latent epoxy systems that the fracture toughness values yielded similar values to the conventional 2K epoxy systems (Palmieri et al., 2022). He used the offset epoxy technique, which uses excess resin to unbalance the stoichiometric ratio to partially cure the initial part with a resin-rich layer and then cure the excess with a joint part assembly, which has a hardener-rich layer further. Xing et al. developed a butyl glycidyl ether modified 2-ethyl 4-methyl imidazole with polyetherimide (PEI) as a shell material and investigated its encapsulation properties. They stressed an important point in the release of the curing agents at elevated temperatures. During the curing of the epoxy resin, they observed difficulties in the release and diffusion of the curing agent from the capsule into the epoxy resin, which caused inferior mechanical properties due to the insufficient degree of curing (Xing et al., 2015).

APPROACH

1. CURING STUDIES

EXPECTED/PROPOSED OUTPUTS: Development of processes for the incorporation of the TLCs into the epoxy resin to obtain OCERs, cure cycles for different TLCs

Materials that were studied in this thesis are: PPhOZ 1K-Im (**OCER 3**), Phenyl urea aminopropyl imidazole (PU-API, **OCER 4**), and p-Toluenesulfonyl urea-ethylenediamine (pTSU-EDA, **OCER 8**). Their molecular structures are shown in **Figure 9**.

The TLCs prepared here can be classified into two main categories: Polyoxazoline-imidazole based TLCs (covalent attachment of imidazole to polyoxazoline end group) (**OCER 3**), and small molecule TLCs with reversible urea bonds and imidazole (**OCER 4**, **OCER 8**). The first group contains polyoxazoline terminated with imidazole. Since imidazole curing agent is covalently attached to a large molecule in this case, its reactivity is lowered. Additionally, the first adduct formation step of the imidazole is already completed thus it can react only at higher temperatures. The variation of the type of polyoxazoline was utilized here to change

the hydrophobicity/hydrophilicity of the polymer and its miscibility/solubility in epoxy resin, which will affect its curing temperature. In the second group, small molecules with urea and sulfonylurea groups were used. The small molecules are more advantageous than large molecules in terms of the amounts being used. The epoxy equivalent weight corresponding to their molecular weight is much less than the polymer counterparts as polymers are at least 1,000 g/mol whereas the molecular weight of small molecules are between 250-350 g/mol.

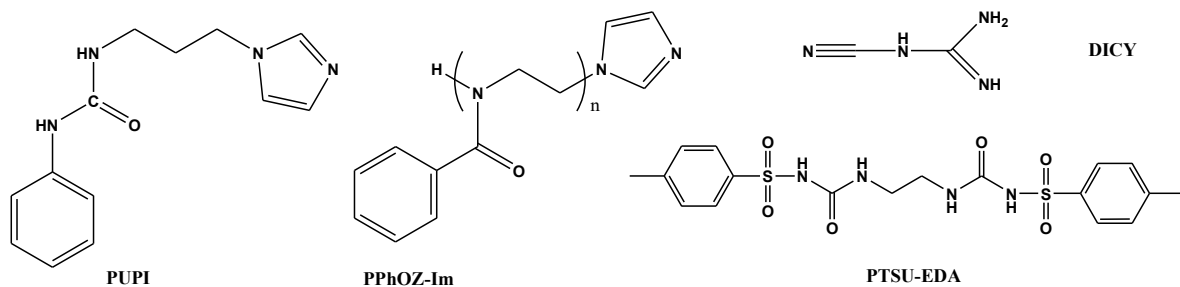


Figure 9. Polymers and molecules as TLCs for thesis studies

Cure kinetics studies were performed for OCERs and prepgs containing OCERs with TLCs by dynamic and isothermal DSC analyses. Dynamic DSC tests were performed at varying heating rates and the conversion and activation energy data obtained were used in model-free kinetics (MFK) to estimate the isothermal DSC cure conditions. Based on the MFK estimations, the isothermal DSC tests will be carried out. The data generated in dynamic and isothermal DSC studies will be used to come up with the cure cycles for the prepgs. The curing mechanism of the epoxy resins changes depending on the curing agents used. For instance, the curing proceeds through a chain growth polymerization (**Figure 10**) with imidazole whereas primary amines cure epoxy via a step-growth polymerization (**Figure 11**).

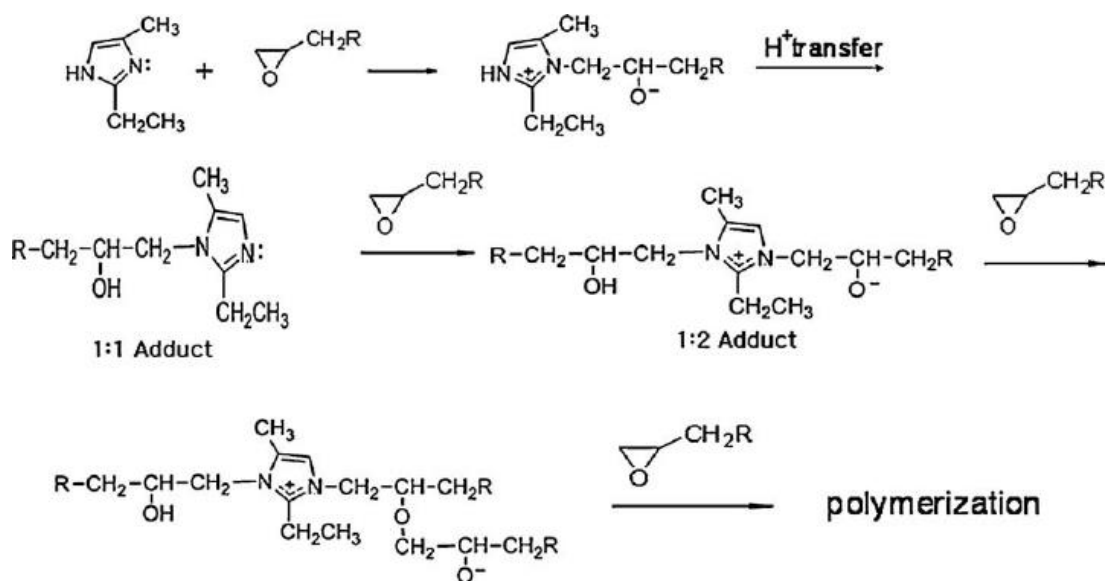


Figure 10. Epoxy-Imidazole reaction scheme (Chain growth polymerization)

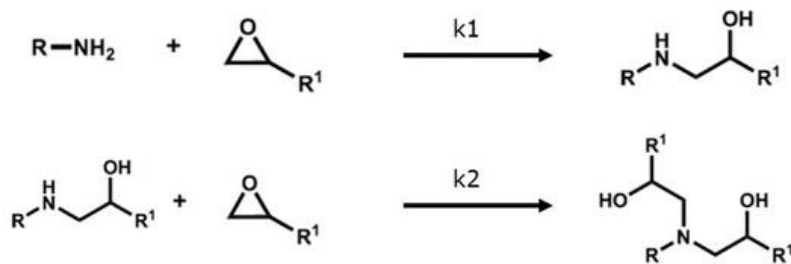


Figure 11. Epoxy-amine reaction (Step growth polymerization)

Table 2. Curing studies of different OCERs

OCER	TLC	TLC% in DGEBA	Optical microscope	DSC	
				Dynamic	Isothermal
OCER 3	PPhOZ 1K-Im	5	X	3	3
		10	X	3	3
OCER 4	Phenyl urea aminopropyl imidazole (PU-API)	5	X	3	3
		10	X	3	3
OCER 8	p-toluenesulfonyl urea- ethylenediamine (pTSU-EDA)	33	X	3	3

Im: Imidazole

2. PREPREG MANUFACTURING

EXPECTED/PROPOSED OUTPUTS: Lab scale prepreg manufacturing method, methods for tackiness and drapeability measurements

The prepared TLCs were incorporated into the epoxy resin through a mechanical mixer at a certain rpm to disperse the TLCs. After the dispersion of the TLCs, the resin will be poured onto the fabric (carbon/glass) and coated manually and a compaction force was applied to the resin through the rollers for further penetration into the fabric, or by hand lay-up. During the hand lay-up process, the resin was poured on top of the fabric and distributed through plastic scrapers manually with the minimum damage is done to the fabric to prevent the integrity of the woven structure of the fabric.

Manufactured prepgs were non-reactive up to certain temperatures. For lay-up processes, a certain degree of cure is needed for the drapeability and tackiness of the semi-/prepgs. Furthermore, the viscosity drop at elevated temperatures will cause the resin to penetrate the fibers and wet them easier for hot melt resins. The viscosity drop would also initiate the movement of voids inside the resin and therefore remove them from the resin. For this thesis, a DGEBA epoxy resin, which is liquid at room temperature, will be used for manufacturing prepgs and composites.



Figure 12. Tackiness measurement setup

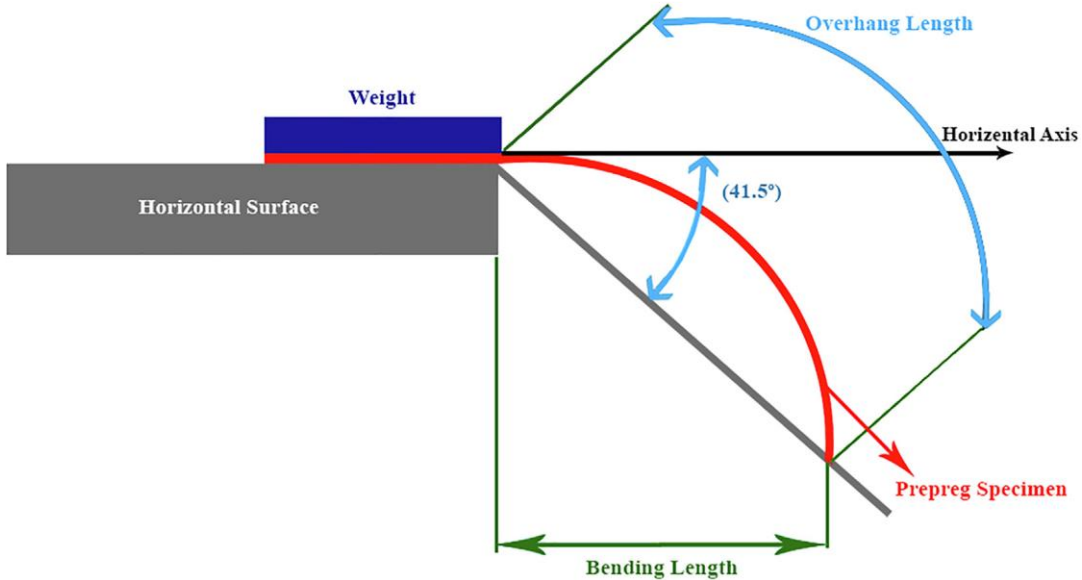


Figure 13. Drapeability measurement setup (Pouladvand et al., 2020a)

The tackiness measurements are carried out through universal tensile machines (UTM). The prepreg is placed onto a flat plate such as aluminum and fixed on left and right edges with hinges that are connected to the UTM machine. A circular compression fixture is used for this test, where the 50x50 mm prepgs were stuck on each compression plate manually and then for a minute with 100 N force they were compressed for a good adhesion. Further, they were debonded with a rate of 4 mm/s from each other. The calculated debonding force is plotted vs time and the maximum value will be regarded as the debonding force. The higher

the force is the tackier the prepreg will be. The tackiness and drapeability results will be linked to the viscosity and degree of cure through an equation as a linear relation between them is expected. Thus, this method can further be used to optimize the tackiness and drapeability of the prepgs for formulation studies.

Drapeability was measured according to ASTM D 1388 standard, which is used for measuring the stiffness of the fabrics. The manufactured prepgs were hang over with a 41.5° angle from a setup as shown in **Figure 13** and the overhang length of the fabric will be measured. The prepreg was placed onto the horizontal axis of the setup and it should be moved by hand with an approximate rate of 120 mm/min. Then, the rigidity of the fabric was calculated using **Equation 2**.

$$G = 1.421 \times 10^{-5} \times W \times c^3$$

Equation 2. Flexural rigidity of fabrics

3. MECHANICAL PROPERTIES

EXPECTED/PROPOSED OUTPUTS: Influence of TLCs on mechanical properties,

Mechanical properties of the manufactured composites will be investigated through tensile, compressive, and flexural tests. The standards for these tests are ASTM D 3039 for the tensile test, ASTM D 3410 for the compressive test, ASTM D 2344 for the interlaminar shear stress (ILSS) and ASTM D 790 for the 3-point bending test for flexural properties. The dimensions and test parameters are listed in **Table 3**.

The manufactured prepgs will be laid up accordingly to obtain the thicknesses that are required from the mechanical test standards. The direction and orientation of the prepreg lay-up is irrelevant as twill fabric provides isotropic properties both in x and y direction. The laid prepgs will be cured with the data obtained from curing studies in a laboratory oven where the lay-up is connected to a vacuum pump. A typical prepreg lay-up is shown in **Figure 14**. A tool is used to lay the prepgs on top of it but before lay-up, the tool is cleaned with a cleaning chemical, either acetone or isopropyl alcohol. Moreover, a mold release agent such

as Frekote NC 700 is used to remove the cured composite from the tool with ease. After stacking the preps, the preps are covered either with a peel ply or a release film to prevent impurities from getting into the layup, to release the cured composite, and an enhanced surface for secondary operations such as bonding or painting. On top of the peel ply or release film, a breather and/or a bleeder fabric is used for the lay-up to breathe and remove its air bubbles. If the lay-up has excess resin the bleeder fabric eases resin flow and lets the resin get out of the lay-up. Both fabrics might be necessary for different applications as sometimes the air bubbles can only be removed with the resin. Finally, the vacuum film is used to cover the whole lay-up and therefore the lay-up can be vacuumed. A vacuum valve is placed inside the lay-up through a cut hole and then is fixed, sealed, and squeezed through a rotating gauge. The sides of the lay-up are sealed with sealant tapes to ensure there is no air penetration into the lay-up. The whole lay-up is checked for any leakage and if there is none it is connected to a vacuum pump and the tool is placed into the oven and is cured with the determined parameter in the curing kinetics work package.

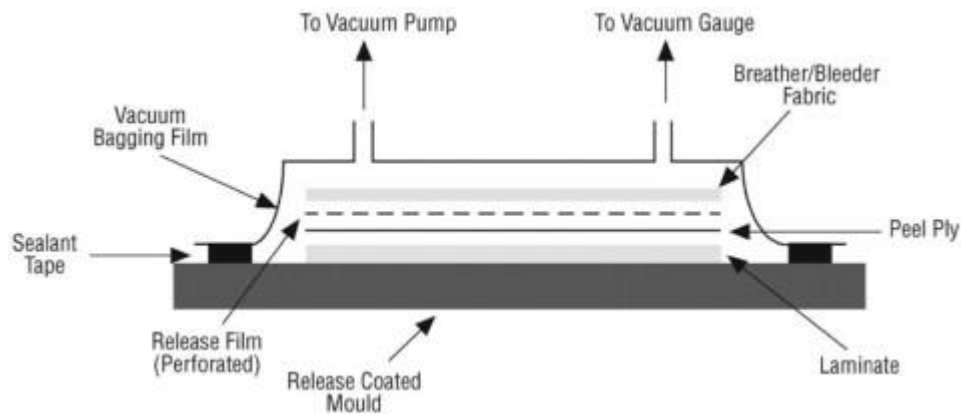


Figure 14. Prepreg lay-up scheme (CRIPPS et al., 2000)

The cured composites will be cut into the required dimensions of the test standards via water jet cutting. The dimensions of the test samples are listed in **Table 3**. The samples will be conditioned per the test standard requirements before testing. The influence of the TLCs on the mechanical performance of the cured composites will be investigated. Fracture mechanisms will be photographed and compared to the neat reference system. The same procedure will be applied to the preps that are stored at room temperature to observe the efficiency of the latency.

Table 3. Mechanical test dimensions

Standard	Length (mm)	Width (mm)	Thickness (mm)	# of specimens
ASTM D 3039	250	25	2-2,5	5-6
ASTM D 3410	145	25	2-2,5	5-6
ASTM D 2344	6h	2h	h	5-6

CHAPTER 2

2. Synthesis and characterization of 1-(3-aminopropyl)imidazole-phenyl isocyanate adduct and its application as a thermal latent curing agent for diglycidylether bisphenol A resin

2.1. Introduction

Composites have become indispensable for various engineering applications in industries such as aerospace, automotive, and coatings due to their exceptional mechanical properties and tailored performance characteristics. (Pouladvand et al., 2020b) They consist of a matrix material that encapsulates and binds a reinforcing phase, resulting in a material with enhanced properties beyond those of its individual components. One important subclass of composites is "prepreg composites," where the reinforcing fibers are pre-impregnated with matrix material (prepreg) prior to the fabrication process. (Hassan, 2021) This pre-impregnation ensures uniform distribution of the matrix within the reinforcement, enabling precise control over the composite's thermal and mechanical properties. The matrix material in prepreg is often in a tacky, partially cured state, facilitating ease of handling during layup and subsequent processing. In advanced composite manufacturing, epoxy prepgs have emerged as a crucial material, playing a pivotal role in industries ranging from aerospace to

automotive due to their exceptional mechanical properties, dimensional stability, and ease of application. (M R et al., 2022; Parameswaranpillai et al., 2021)

In the preparation of prepgs, both two-component and one-component epoxy resins are utilized. In two-component epoxy resins, the resin and hardener components are kept separate and mixed just prior to application. Conversely, in one-component epoxy resins (OCERs), the resin and a latent curing agent are pre-formulated together in a single package, simplifying handling and application processes. (Jee et al., 2020). OCERs have gained importance in commercial applications due to their increased manufacturing efficiency and improved storage conditions compared to conventional two-component resins. (Banks et al., 2004a; Hassan, 2021; M R et al., 2022; Pouladvand et al., 2020b) The inclusion of latent curing agents in OCERs prevents curing at room temperature and helps reach targeted cure temperatures. Latent curing agents can be classified according to their sources of stimuli such as thermal, ultrasonic, electron beam, and photo irradiation. (Li et al., 2017) Among these, thermal latent curing agents (TLCs) have been extensively investigated for their stability performance and handling properties. (J. Chen et al., 2020; Yen et al., 2016) TLCs contribute to the room temperature stability of epoxy resins and can be activated upon application of heat, reacting with epoxy resins at desired temperatures. Various TLCs including dicyandiamide (DICY), dihydrazides, aminoacids, and imidazole derivatives have been employed in OCERs in the literature. (Hesabi et al., 2019; Lee, 2021; Tomuta et al., 2012; Yu et al., 2021; P. Zhang et al., 2019) These TLCs enhance the application and performance of epoxy prepreg systems, enabling controlled curing kinetics as well as tailorabile prepreg properties such as drapeability and tackiness. (Banks et al., 2004a; Budelmann et al., 2020; Dubois & Beakou, 2009; Pouladvand et al., 2020b)

TLCs can offer physical or chemical latency. In physical latency, a curing agent is either encapsulated within a polymer, preventing its reaction with epoxy resin, or an insoluble curing agent is employed, which can only be activated following its melting and dissolution in epoxy resin. In chemical latency, either the active site of the curing agent is sterically hindered, or the curing agent is conjugated to another small molecule or polymer to reduce its reactivity with epoxy resin. Two commonly used curing agents with epoxy resins are DICY and imidazole (or its derivatives). DICY is an insoluble TLC in epoxy resin at room

temperature, with a melting temperature typically ranging from 208 to 212 °C. (Gilbert et al., 1991) The high melting point of DICY prevents its dissolution at room temperature, thereby providing thermal latency. However, DICY can be activated at very high temperatures during curing, typically exceeding 170°C, (> 170 °C), which necessitates high energy for curing and can lead to issues such as explosive evolution of ammonia and other gases, particularly in large part manufacturing processes such as composite parts. Consequently, DICY is typically suitable only for applications involving thin parts. (Gilbert et al., 1991). Additionally, concerns arise regarding the variation in dispersion quality of DICY in epoxy resin, which can result in challenges related to cure kinetics and heterogeneity in the final product properties.

While imidazole readily reacts with epoxy groups at room temperature, several less reactive imidazole derivatives have been developed as TLCs. (K.-L. Chen et al., 2012; Ham et al., 2010; Shi et al., 2019b; B. Yang et al., 2022) Strategies such as encapsulation of imidazole, utilization of 1-substituted imidazole derivatives, and restraining of the tertiary amine via metal-organic coordination or hydrogen bond have been employed to reduce imidazole reactivity. (Shi et al., 2019b) Behroozi Kohlan et. al. conducted a study on imidazole-epoxy reactions and discovered that the curing onset temperature of an OCER formulated with 5 wt. % of imidazole encapsulated in a copolymer and diglycidylether bisphenol A (DGEBA) resin is at 78 °C (Behroozi Kohlan et al., 2023). The encapsulation method has been reported to be inefficient due to challenges such as difficulty in mixing encapsulation materials with epoxy, and the potential for premature release of curing agent, leading to stability issues. Furthermore, as encapsulated agents remain within the crosslinked network, they can adversely affect the thermal and mechanical performance of cured epoxy matrices. (Shi et al., 2019b) Yin et al. demonstrated prolonged shelf life by encapsulating a thermal latent curing agent using urea-formaldehyde capsules. (Yin et al., 2007) Li et al. introduced a novel method for encapsulating imidazole adducts through thio-click reaction in an oil-water emulsion, claiming stability for up to 30 days with the encapsulated imidazole. (Li et al., 2017).

Our study involves the synthesis and characterization of PUPI, its incorporation into DGEBA to formulate an OCER, and the investigation of the curing behavior and stability of the OCER

via DSC and rheology studies. The novelty of this work stems from the utilization of the prepared PUPI as a thermal latent curing agent for one-component epoxy resins (OCERs). Although synthesized previously, PUPI has not been investigated in detail as a thermal latent curing agent for OCERs. In this study, in addition to providing a simple method for the synthesis and an extensive characterization of PUPI, the curing behavior of PUPI as a thermal latent curing agent alone and as a catalyst for DICY in the curing of DGEBA resin and the stability of the OCERs were thoroughly investigated.

2.2. Experimental

2.2.1. Materials

DGEBA (EEW: 170.2 g/mol), phenyl isocyanate ($\geq 99.8\%$), 1-(3-aminopropyl)imidazole ($\geq 97\%$), and dichloromethane (DCM) ($\geq 99.8\%$) were purchased from Merck Corporation Sigma-Aldrich. DICY was purchased from Ataman Chemicals.

2.2.2. Instruments

^1H NMR spectra are recorded in CD_3OD and CDCl_3 on a 500 MHz Varian spectrometer. FTIR spectra are obtained with a ThermoScientific Nicolet iS50 FTIR spectrometer using an attenuated total reflectance (ATR) accessory, employing transmission mode with a resolution of 4 cm^{-1} . DSC measurements are conducted using a Mettler Toledo DSC 3+ instrument with sample sizes of 8-10 mg. For dynamic DSC measurements, the temperature range spans from 25 to 250°C , with heating and nitrogen flow rates set at $10^\circ\text{C}/\text{min}$ and 50 mL/min., respectively. Isothermal DSC measurements are performed for 3h at various temperatures, followed by dynamic DSC tests from 25°C to 300°C at a heating rate of $10^\circ\text{C}/\text{min}$ to measure residual enthalpy. TGA measurements are executed on a Mettler Toledo TGA/DSC 3+ instrument within a temperature range of 25– 800°C . Samples weighing 10-100 mg are heated at $10^\circ\text{C}/\text{min}$ under a nitrogen atmosphere with a flow rate of 100 mL/min. Optical microscope images are captured using a Nikon Eclipse LV100ND optical microscope equipped with CFI60-2 lenses at magnifications of 25x, 50x, 100x and 200x. Bright field illumination is applied from beneath the material during imaging. Viscosity measurements

are conducted using a Brookfield DV2T viscometer with a SC4-2 1 type spindle at 40°C for 10 min. and a rotation speed of 100 rpm. Data is collected at 30-second intervals, with reported accuracy of ± 5 mPa.s. Following each measurement, the sample is retrieved and stored at room temperature in a sealed vial. The vial is purged with nitrogen for one minute before being sealed with parafilm.

2.3. Methods

2.3.1. Synthesis of phenyl urea propyl imidazole (PUPI)

PUPI is synthesized by reacting 1-(3-aminopropyl)imidazole (3.75 g, 0.029 mol, 1 equiv.) with phenyl isocyanate (3.57 g, 0.029 mol, 1 equiv.) in 60 mL of dichloromethane (DCM) (**Figure 15**). Initially, 1-(3-aminopropyl)imidazole is added to DCM in a 100 mL round-bottom flask equipped with a magnetic stir bar, and the solution is cooled to 0°C using an ice bath. Subsequently, phenyl isocyanate is added dropwise into the flask. The solution is then allowed to gradually warm up to room temperature and stirred for 24 h. Upon completion of the reaction, DCM is evaporated with a rotary evaporator at room temperature to yield a white powdery product (6.83 g, yield: 93%).

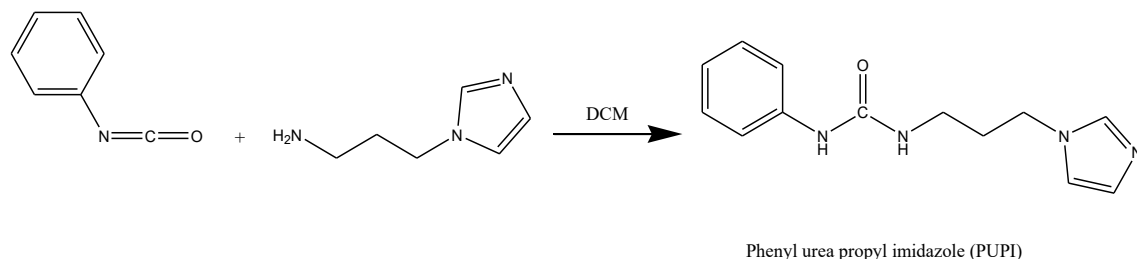


Figure 15. Synthesis of PUPI

2.3.2. Preparation of the OCER

PUPI (0.35 g) and DGEBA (5.0 g, EEW: 170.2 g/mol) are mixed for 5 min. at 1,000 rpm using a homogenizer in a glass vial to achieve a 5 mol% concentration of PUPI in the mixture.

Following mixing, the vial is purged with nitrogen, sealed with a cap, and covered with parafilm to ensure safe storage at room temperature.

2.4. Results

2.4.1. ^1H NMR Analysis of PUPI

The ^1H NMR spectrum of PUPI, along with the peak assignments, is presented in **Figure 16**.

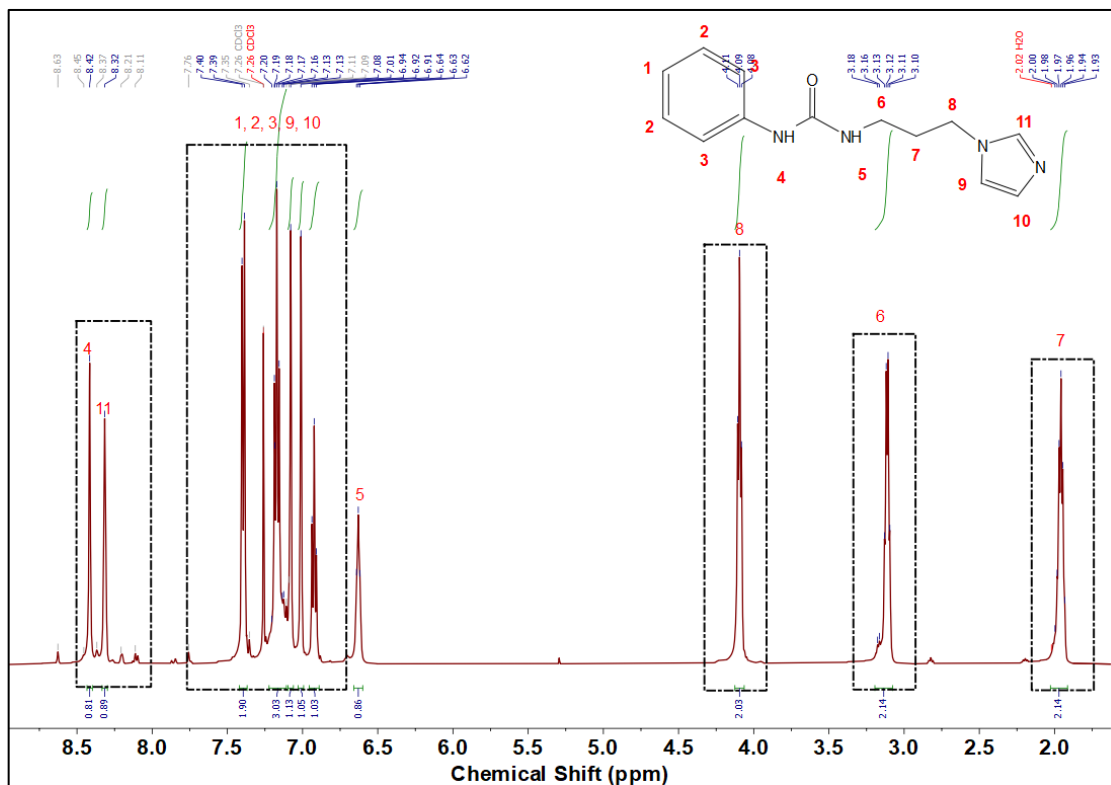


Figure 16. ^1H NMR spectrum of PUPI (in CDCl_3)

The presence of urea -NH peaks at 8.42 ppm (peak 4) and 6.63 ppm (peak 5), along with the shift of CH_2 peaks of 1-(3-aminopropyl) imidazole adjacent to -NH₂ from 1.85 and 2.64 ppm to 1.97 (peak 7) and 3.11 ppm (peak 6) in PUPI, indicates the successful progression of the reaction. Additionally, the absence of the -NH₂ peak of 1-(3-aminopropyl)imidazole at 7.69 ppm confirms its complete reaction with phenyl isocyanate. The Imidazole -CH peak (peak 11) shifted from 7.47 to 8.32 ppm due to hydrogen bonding with the urea group. Furthermore, all other peaks of 1-(3-aminopropyl)imidazole (peaks 8, 9, 10) and aromatic peaks (peaks 1,

2, 3) of phenyl isocyanate were observed in the spectrum. In **Figure 16**, the peaks 4, 5, 6, 7, 8, 11 were separately integrated, whereas the peaks 1, 2, 3, 9, 10 were integrated together in the NMR spectrum of PUPI. The corresponding integral values were included in the figure. The integration of the assigned peaks shows that the intended structure (PUPI) was obtained.

2.4.2. FTIR Analysis of PUPI

FTIR spectra of 1-(3-aminopropyl)imidazole, phenyl isocyanate, and PUPI are shown in **Figure 17**. The peak observed at $2,246\text{ cm}^{-1}$ for phenyl isocyanate corresponds to the isocyanate ($-\text{N}=\text{C}=\text{O}$) group, which is absent in the spectrum of PUPI due to its reaction with 1-(3-aminopropyl)imidazole. In the FTIR spectra of 1-(3-aminopropyl)imidazole, peaks associated with N-H bending and stretching are observed at $1,597\text{ cm}^{-1}$ and $3,358\text{ cm}^{-1}$, respectively. Additionally, the urea N-H peak of PUPI is observed around $3,350\text{ cm}^{-1}$. The appearance of the urea carbonyl peak ($-\text{NH}-\text{CO}-\text{NH}-$) at $1,693\text{ cm}^{-1}$ in the PUPI spectrum confirms the successful synthesis of the product. (Attaei et al., 2020; Manivannan & Rajendran, 2011)

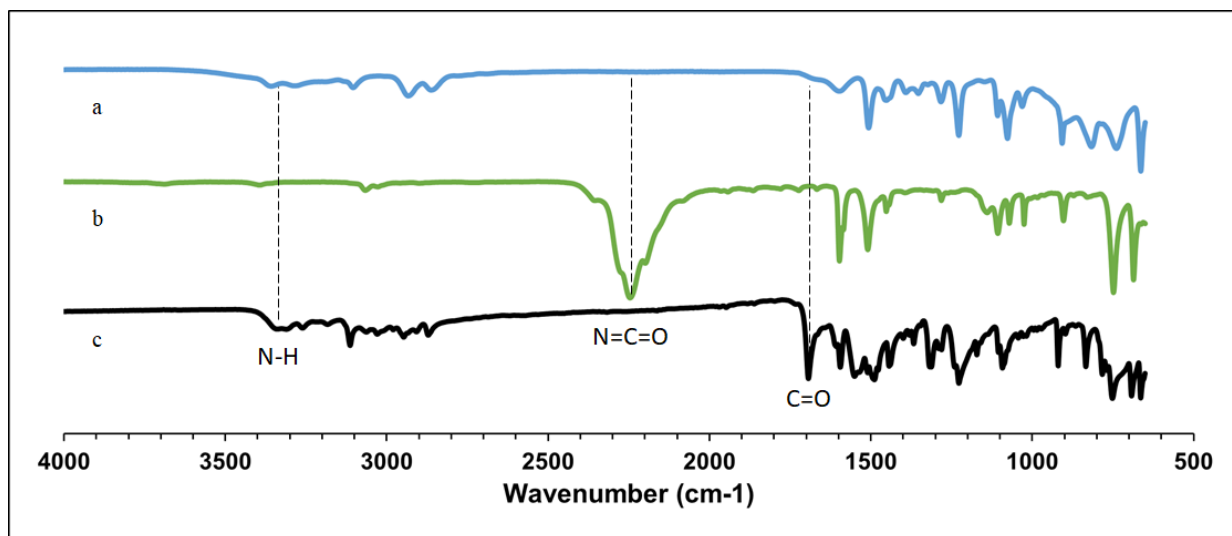


Figure 17. FTIR spectra of (a) 1-(3-aminopropyl)imidazole, (b) phenyl isocyanate, and (c) PUPI

2.4.3. TGA Analysis of PUPI

The TGA thermogram of PUPI and its derivative are shown in **Figure 18**. PUPI undergoes two main decomposition steps: the first occurs between 180-330°C, resulting in a 45% weight loss, while the second takes place within the range of 330-500°C, leading to a 50% weight loss. The initial decomposition is attributed to the breakage of the urea bond and the evaporation of the released phenyl isocyanate, while the subsequent decomposition is associated with the degradation of 1-(3-aminopropyl)imidazole. The weight loss percentages align with the molecular weight ratios of phenyl isocyanate (119.12 g/mol / 244.29 g/mol = 48.8%) and 1-(3-aminopropyl)imidazole (125.17 g/mol / 244.29 g/mol = 51.2%) in PUPI (molecular weight: 244.29 g/mol).

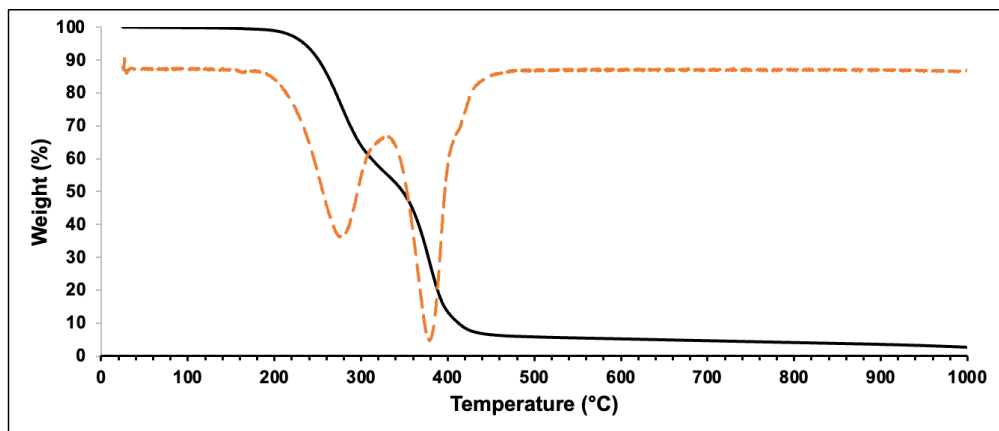


Figure 18. TGA profile of PUPI

2.4.4. DSC Analysis of PUPI

In the DSC thermogram of PUPI (**Figure 19**), the melting temperature of PUPI is observed in the range of 145-175 °C, with a peak temperature at 162 °C. PUPI starts to decompose at around 200 °C, a finding consistent with the TGA results.

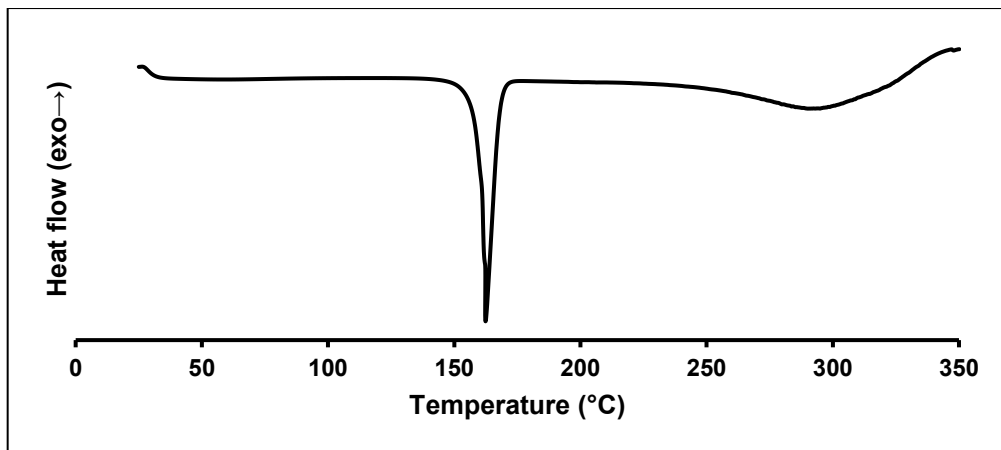


Figure 19. DSC thermogram of PUPI

2.4.4.1. Dynamic DSC Analysis of the OCER formulated with PUPI

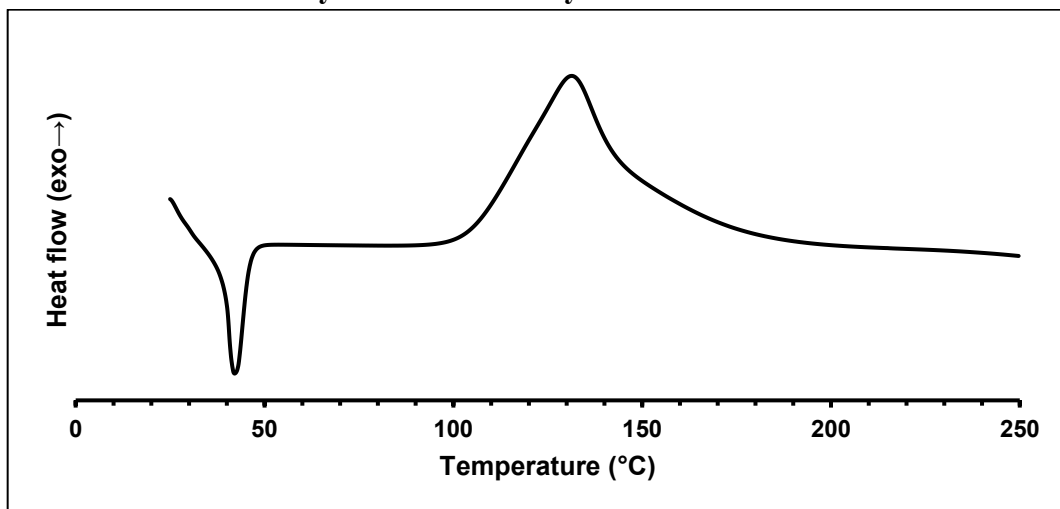


Figure 20. Dynamic DSC thermogram of the OCER formulated with PUPI

The dynamic DSC thermogram of the OCER is shown in **Figure 20**. Upon mixing PUPI with DGEBA at 5% mole concentration, the resin solidifies after cooling down to room temperature. Consequently, the initial peak around 40 °C corresponds to the melting of DGEBA. The left-limit, onset, peak, and right-limit temperatures of curing are observed at 82, 104, 131, 215 °C, respectively. The curing reaction enthalpy is 439.62 J/g.

2.4.4.2. Isothermal DSC Results of the OCER formulated with PUPI

The isothermal DSC thermograms of the OCER (5% PUPI in DGEBA) are shown at varying temperatures in **Figure 21**. At 140 °C and 120 °C, sharp and narrow curing peaks are observed, with curing completion times of 1.97 and 5.17 minutes, respectively. In contrast, the curing profiles at 100°C and 80°C are broader, with incomplete curing after 15.50 and 38.65 minutes, respectively. No curing is observed at 60°C even after 180 minutes.

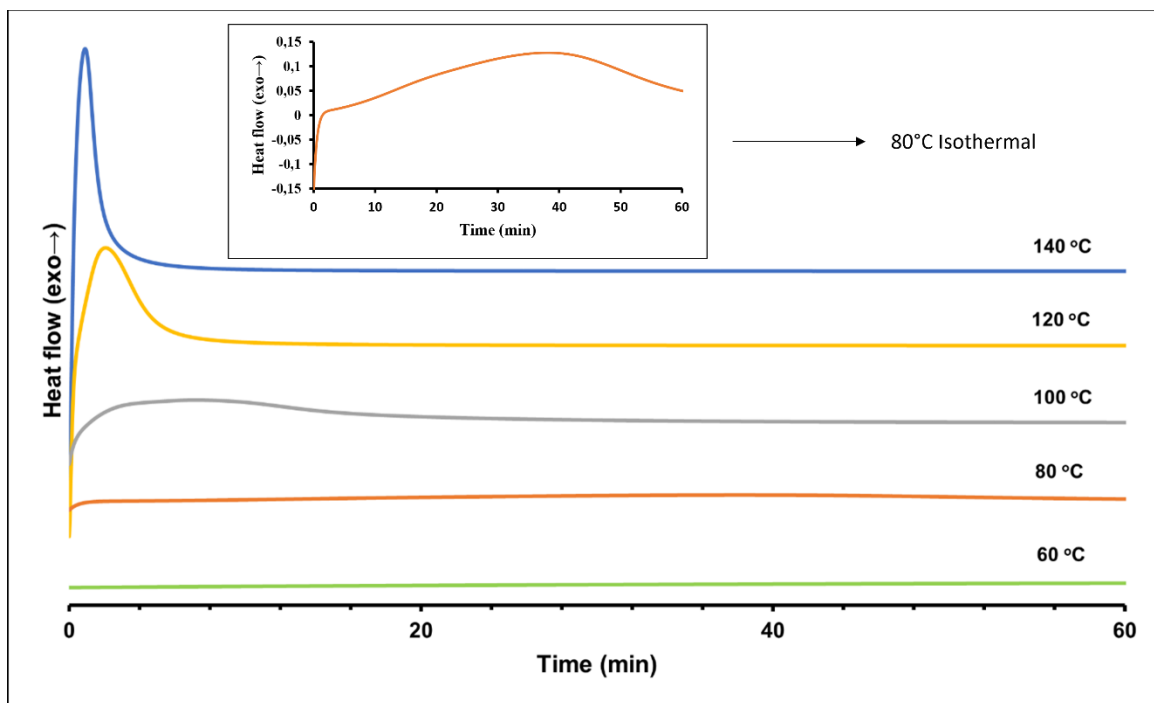


Figure 21. Isothermal curing profile of the OCER formulated with 5% PUPI

2.4.4.3. Dynamic DSC Results of the OCER formulated with 5% PUPI after Isothermal Curing

Dynamic DSC tests are conducted following the isothermal tests to determine residual curing enthalpy values at each temperature, as shown in **Figure 22**.

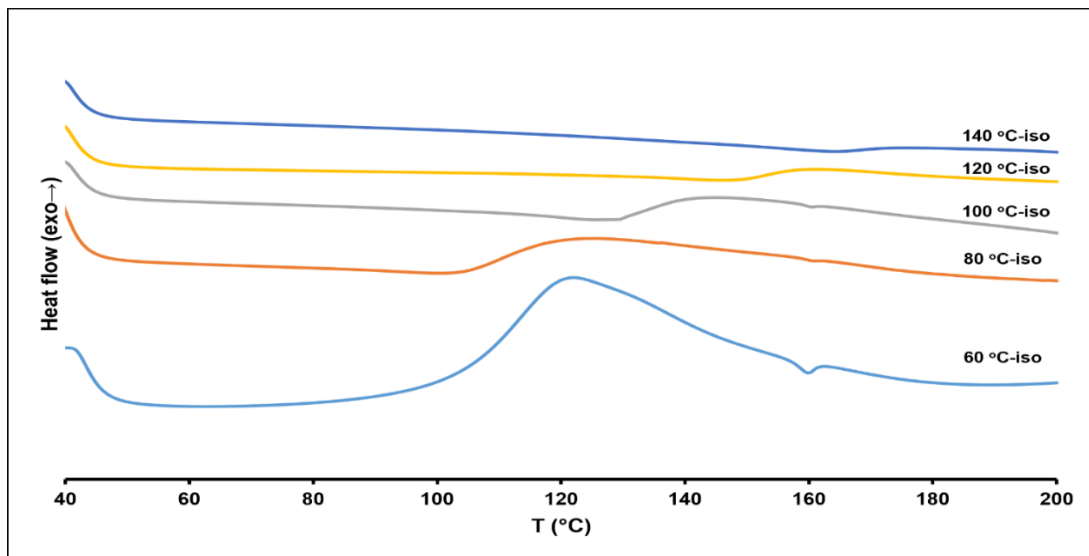


Figure 22. Dynamic DSC tests performed after isothermal curing to obtain residual curing data

The residual curing enthalpy values are summarized in **Table 4** along with conversion values. Isothermal curing at 140 °C for 3 h exhibits a conversion of %99.20, while the conversion at 80 °C for 3 h drops to %82.85. No curing is observed at 60 °C, and the dynamic DSC curing following the isothermal curing at 60 °C shows a residual enthalpy value of 149.52 J/g.

In **Figure 21**, the isothermal DSC tests at various temperatures (60-140 °C) are shown. At higher temperatures (120 and 140 °C), a sharp exothermic peak is observed in a very short time, indicating that the epoxy curing reaction takes place rapidly at these temperatures. As the temperature is lowered, the exothermic peak is broadened, which is indicative of a slower reaction and at an even lower temperature (i.e., 60 °C) the exotherm is not observed, a sign of either a very slow reaction or no reaction.

In isothermal DSC runs, the conversions depend on the cure temperature. At lower temperatures, if the isothermal DSC test time is not long enough, uncured resin will remain as residue. To determine the amount of residual unreacted epoxy resin, a dynamic DSC run is performed after the isothermal DSC tests. **Figure 22** in the manuscript is a follow-up test for the isothermal tests performed in **Figure 21**. After the isothermal DSC tests, the samples are cooled to room temperature and a dynamic DSC scan is performed at a specific heating rate to cure the unreacted resin. As shown in **Figure 22** and **Table 4**, the residual peaks at

lower temperatures have higher enthalpy values, indicating that there is unreacted epoxy resin. Through this analysis, the conversions at isothermal temperatures are determined.

Table 4. Isothermal and dynamic DSC curing analysis of PUPI-DGEBA

Isothermal temperature (°C)	Normalized curing enthalpy (J/g)	Residual enthalpy (J/g)	Conversion (%)
60°C	-	149.52	-
80°C	334	58.97	86.44
100°C	429	25.58	100
120°C	411	10.29	92.67
140°C	406	2.88	89.94

2.4.5. Optical Microscopy Images of the OCER

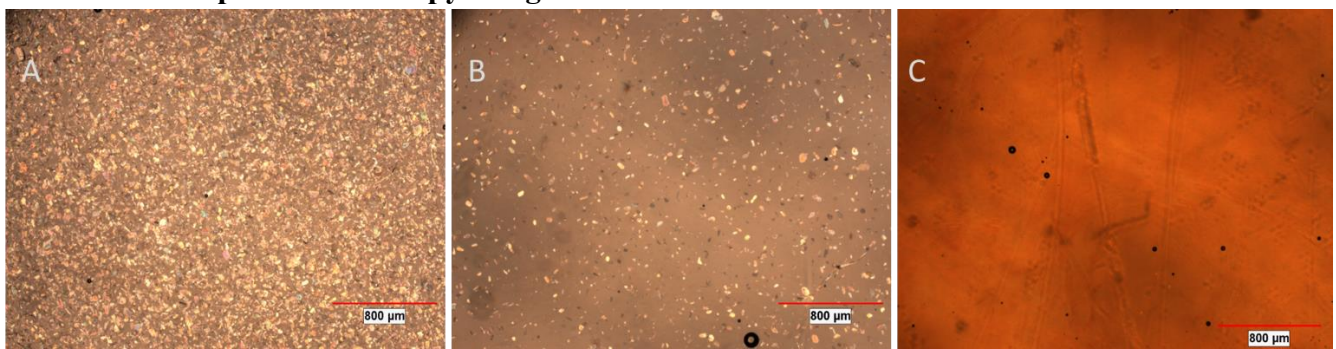


Figure 23. Optical microscopy images (25x) of the OCER (5% PUPI in DGEBA) (A: 25°C, B: 80°C 2 min, C: 60°C 6 hours)

Optical microscopy images of the OCER (5% PUPI in DGEBA) are captured at 25°C, 60°C and 80°C to observe the distribution of PUPI in DGEBA. The initial image is taken at 25°C immediately after mixing PUPI and DGEBA, while the image at 80°C is acquired after

heating the OCER on a hot plate until the thermocouple reads 80°C. At 80°C, the mixture loses its fluidity, and the formation of a film is observed, indicating the onset of curing (**Figure 23**). In the image captured at 80°C, there appears to be no significant decrease in the amount of PUPI, suggesting that the reaction is still in its initial stages. Therefore, at 60°C, to observe the homogeneity of the mixture the reaction time is extended and a film formation at 60°C with fewer particles have been observed under optical microscope. Moreover, in **Figure 24**, a clear reduction in the amount of solid material is observed, particularly noticeable when tracking the images from left to right over time. This decrease indicates the progression of the reaction over time at 60°C.

The black spots observed in the optical microscopy images at room temperature may be due to the voids present in the resin. At 80 °C, the resin is more mobile and less viscous, hence the voids are filled with the resin, but trapped air may leave bubbles as they are burst, thus leaving black spots at 80 °C. The bright spots observed at room temperature correspond to the DGEBA crystals and the curing agent. As the temperature is increased to 80 °C, DGEBA crystals melt (at 35-50 °C range as shown in Figure 6), thus only PUPI crystals are observed as the bright spots at 80 °C. This is one of the reasons for observing less bright spots at 80 °C. The other reason is the dissolution of PUPI at 80 °C and its curing reaction with DGEBA. The DGEBA crystals dissolve and reacts with DGEBA, thus bright spots gradually turn to darker spots as they dissolve and eventually disappear as they react with DGEBA. Moreover, PUPI is insoluble in DGEBA at room temperature, but it dissolves as the temperature increases. **Figure 24** illustrates the morphological change of the OCER at 60°C over a period of 5 h. As heating time at 60°C increases from 1 to 5 h, less PUPI remains in the mixture, indicating its gradual dissolution and involvement in the curing of DGEBA. However, complete dissolution of PUPI is not achieved at this temperature within this period. We included 6 h and 7 h data at 60°C to show that complete dissolution occurs at 60°C within 7 h, where all PUPI dissolves in DGEBA. In fact, this temperature-dependent solubility of PUPI in DGEBA imparts latency to the curing process of DGEBA, which we exploit in this study.

On the other hand, to ensure the strength and stability of the cured resin, we have performed the following optimizations in this study:

1. **Decreasing particle size:** PUPI was ground to a powdery form to decrease its size before its use with DGEBA. This decrease in size helped dissolve PUPI in DGEBA more easily at higher temperatures by increasing its surface area.
2. **Uniform dispersion of PUPI:** High shear mixing was utilized to achieve a homogeneous dispersion of PUPI within DGEBA. The ground PUPI and DGEBA were mixed at room temperature using a homogenizer for 15 minutes. The process conditions were optimized by studying various mixing times and rates.
3. **Optimal resin formulation:** The resin formulation was designed with the appropriate ratio of DGEBA to PUPI. In our previous studies, we found that imidazole concentrations above 3% in DGEBA ensure complete curing at 120-140°C. Thus, we used 5% PUPI in DGEBA in this work.
4. **Investigation of curing behavior of the OCER:** The optimal curing conditions (temperatures, times, etc.) were investigated for the OCER.

Although not studied here, post-curing treatments such as heat aging may optimize crosslinking density and improve the overall performance of the resin. In **Figure 24**, 11b-11d represent different magnifications of the sample 10a (50x, 100x, and 200x, respectively). In each raw, the optical microscopy images were taken with respect to time, which ranges between 1h and 5h. As the mixture is kept at 60 °C longer times, the dissolution of PUPI in epoxy resin and the curing reaction is observed, evidenced by the decrease in the number of bright spots, which are observed for PUPI in the optical microscopy images. The differences in the colors of the crystals stem from the different size and orientation of the crystals causing light to diffract in several diffraction patterns.

The image on the far-right side exhibits a sticky substance resulting from the curing process, making it challenging to spread across the microscope slide. This observation aligns with the viscosity data presented in **Figure 12**, where a notable surge in viscosity is recorded at 60°C after 250 minutes, indicating the progression of curing.

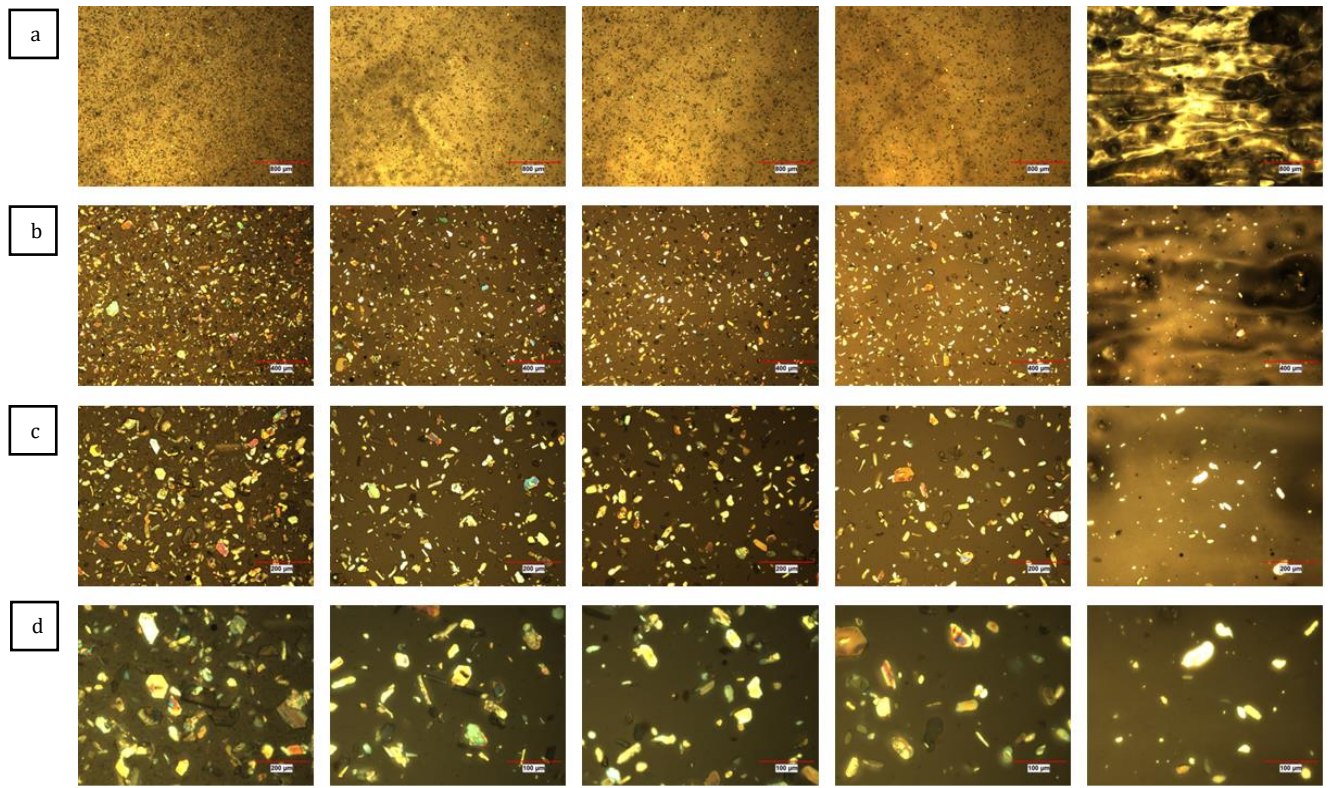


Figure 24. Optical microscopy images of the OCER (5% PUPI in DGEBA) at 60°C at different magnifications a: 25x, b:50x, c:100x, d:200x (left to right: 1, 2, 3, 4, 5 h)

2.4.6. Rheology Results

2.4.6.1. Storage and Loss Moduli of PUPI:DGEBA

In temperature sweep rheology test of the OCER (5% PUPI in DGEBA), as shown in **Figure 25**, the storage and loss modulus intersect each other around 110°C, indicative of the onset of the curing reaction. The fluctuations observed in the storage modulus prior to curing are attributed to the low viscosity of the liquid mixture (4.5 Pa.s at 25°C). The viscosity data is smoothed to get rid of the noisy appearance through a moving average method with 30 smoothing steps.

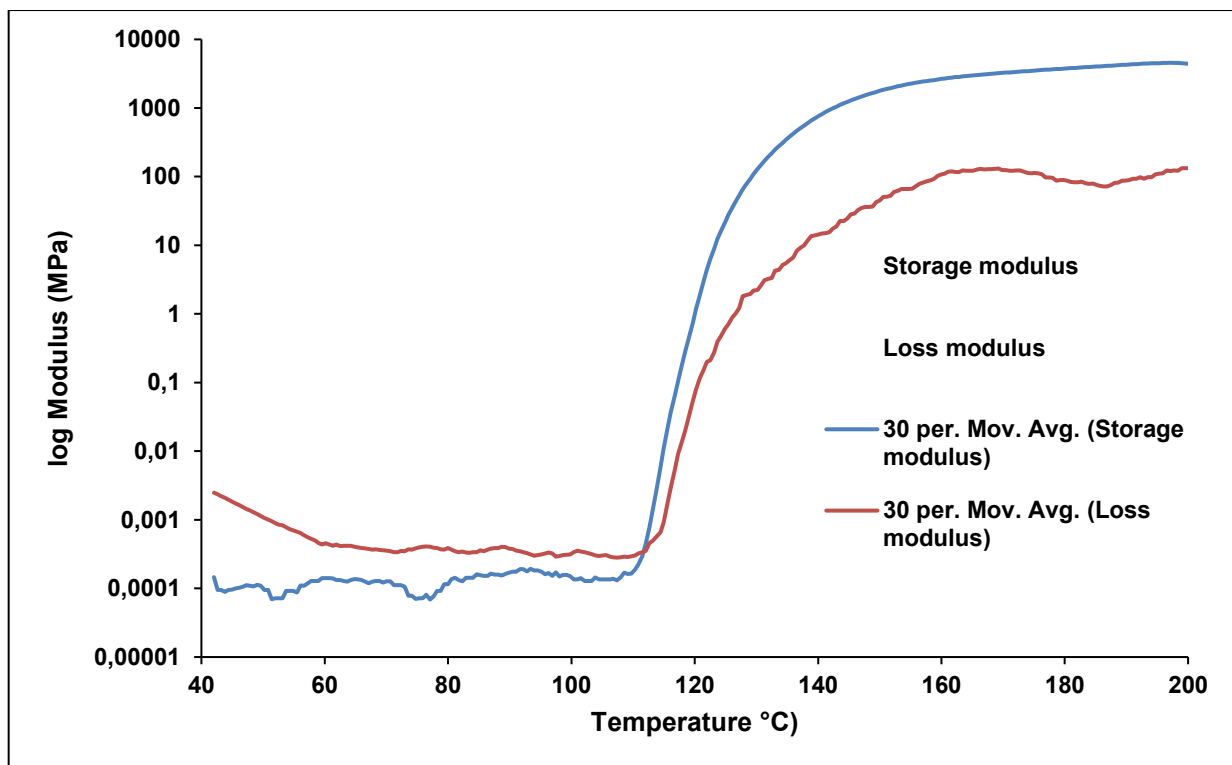


Figure 25. Storage and loss moduli in temperature sweep rheology test of the OCER formulated with 5% PUPI

2.4.6.2. Viscosity Profile of the OCER formulated with 5% PUPI

Figure 26 illustrates the isothermal viscosity data at various temperatures, revealing distinct gel times corresponding to each temperature. Additionally, both dynamic DSC and temperature sweep rheology studies exhibit the onset of curing around 110°C, observed as the initiation of exothermic peaks in dynamic DSC and the crossover point in the rheological temperature sweep study. Furthermore, rheology data obtained at 40°C suggests that the OCER remains stable for up to 20 h. Viscosity increases exponentially with temperature increase in isothermal rheology studies, especially after 80 °C where the dynamic DSC data confirms the left limit of curing is near 80°C.

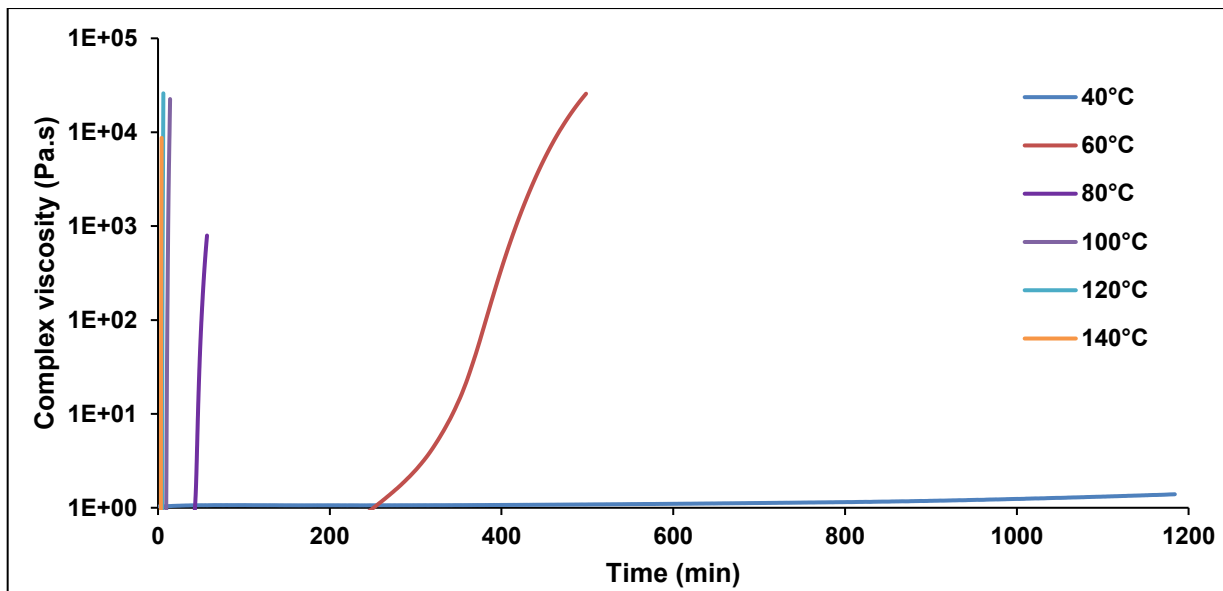


Figure 26. Complex viscosity profile of the OCER at isothermal rheology tests

Gel times (process times) and shelf-life times (times at which complex viscosity doubles) were obtained from complex viscosity data in rheology tests. The conversions corresponding to these times were found in isothermal DSC tests. Applying the first-order reaction kinetics for epoxy curing with PUPI and using Arrhenius equation **Equation 3** and **Equation 4**, the rate constants (k values) at different temperatures were determined. The following equations were used to find k values:

$$\alpha = ([A]_0 - [A]_t) / [A]_0 = (\Delta H_t / \Delta H_{\text{total}}) \times 100\%$$

Equation 3. Conversion calculation using enthalpy values

$$[A]_t / [A]_0 = 1 - \alpha$$

$$\ln ([A]_t / [A]_0) = \ln (1 - \alpha) = -kt$$

$$k = -\ln (1 - \alpha) / t$$

Equation 4. Arrhenius equation for the 1st order reaction in natural logarithmic form

where α is the conversion calculated using isothermal DSC data, $[A]_t$ and $[A]_0$ are concentrations at time = t and time = 0, k is the rate constant, t is either gel time or shelf-life time.

Ln k values were then calculated and lnk vs 1/T graphs (green-color graphs) were plotted to obtain an equation using a linear fit. Using this equation, ln k values at lower temperatures were estimated and plotted against 1/T (blue-color graphs). k values were then calculated and used to estimate process times and shelf-life times at lower temperatures (average of the $-kt$ values obtained at higher temperatures were used here, which means average of the conversions obtained at higher temperatures were utilized here). Using the equation $t = -\ln(1 - \alpha) / k$, the t values (process times and shelf-life times) at lower temperatures. The results are displayed in **Figure 27**.

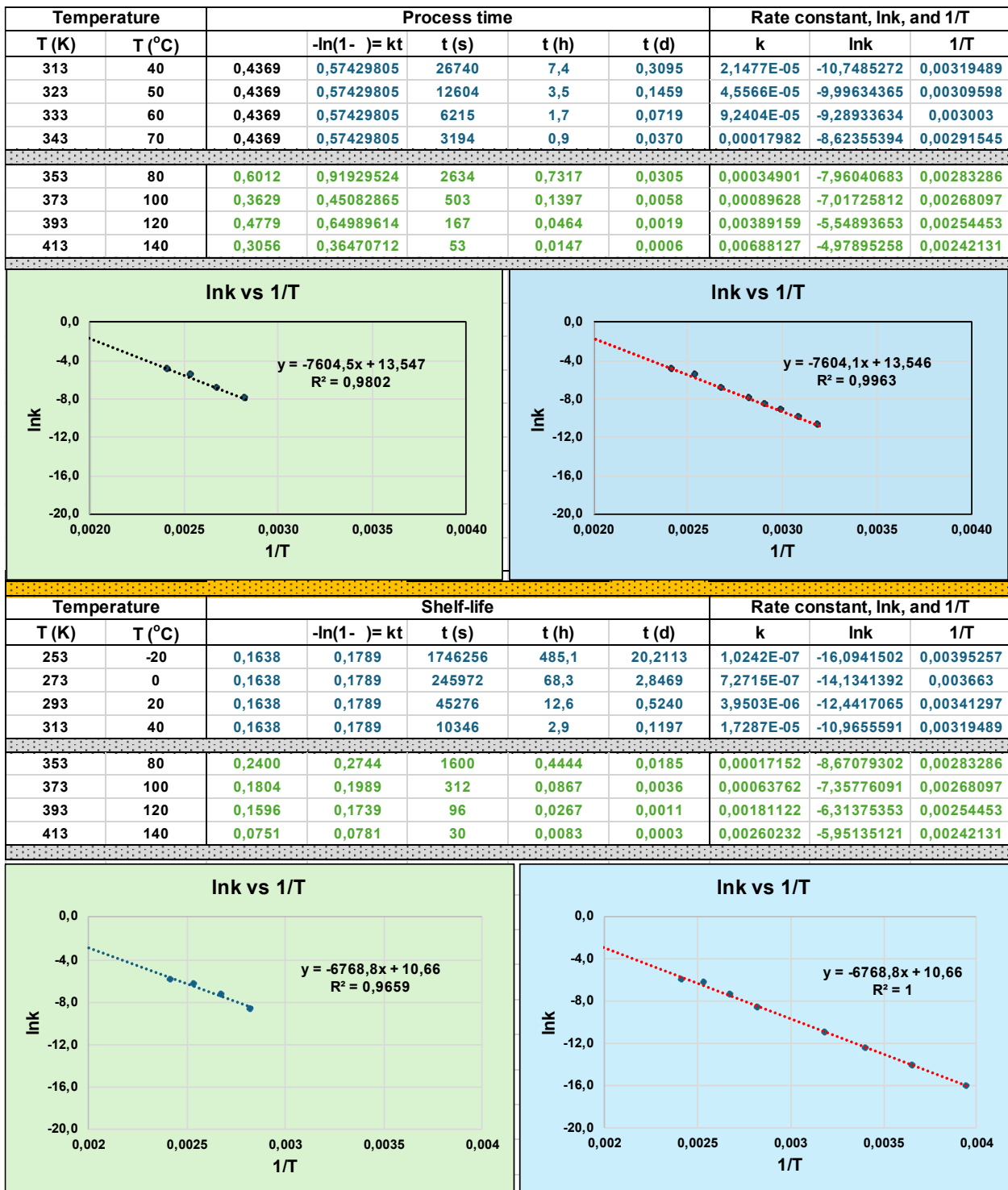


Figure 27. Estimation of process times (upper data and graphs) and shelf-life times (lower data and graphs) at lower temperatures (shown in blue color) using rheology and isothermal DSC data obtained at higher temperatures (shown in green color)

2.4.7. Room Temperature Stability Tests

Stability tests are conducted with a Brookfield viscometer at 40°C with 3 day intervals. The initial absolute viscosity was measured at 132.1 mPa.s. Over a span of 6 days of storage at room temperature, this value increased to 493.6 mPa.s. The results are depicted in **Figure 28**, indicating that the OCER maintained a pot-life of at least 3 days.

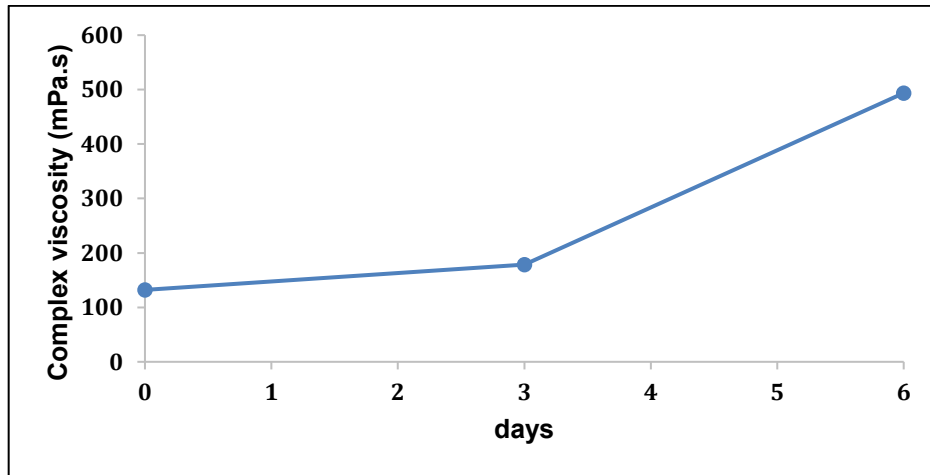


Figure 28. Complex viscosity results at room temperature storage

2.4.8. PUPI as catalyst for DICY

PUPI is combined with DICY to observe its effect on the reaction kinetics of DICY at varying ratios, as depicted in **Figure 29**. DICY's functionality is selected as 4, resulting in a 1:2 mole ratio of DICY:DGEBA. PUPI:DGEBA ratios are adjusted to 1%, 5%, and 10% moles of PUPI relative to the epoxy groups in DGEBA. For 1% of PUPI, the reaction left-limit and peak temperatures are measured at 111°C and 155°C, respectively. In the case of 5% PUPI + DICY, the onset and peak temperatures of curing are observed at 97°C and 135°C, respectively. With 10% mole of PUPI + DICY, the onset and peak temperatures of curing were slightly lower, at 72°C and 122°C, respectively, owing to the increased presence of imidazole groups compared to the epoxy groups. The corresponding reaction enthalpies are 503.54 J/g for 1% PUPI, 417.22 J/g for 5% PUPI, and 291.96 J/g for 10% PUPI.

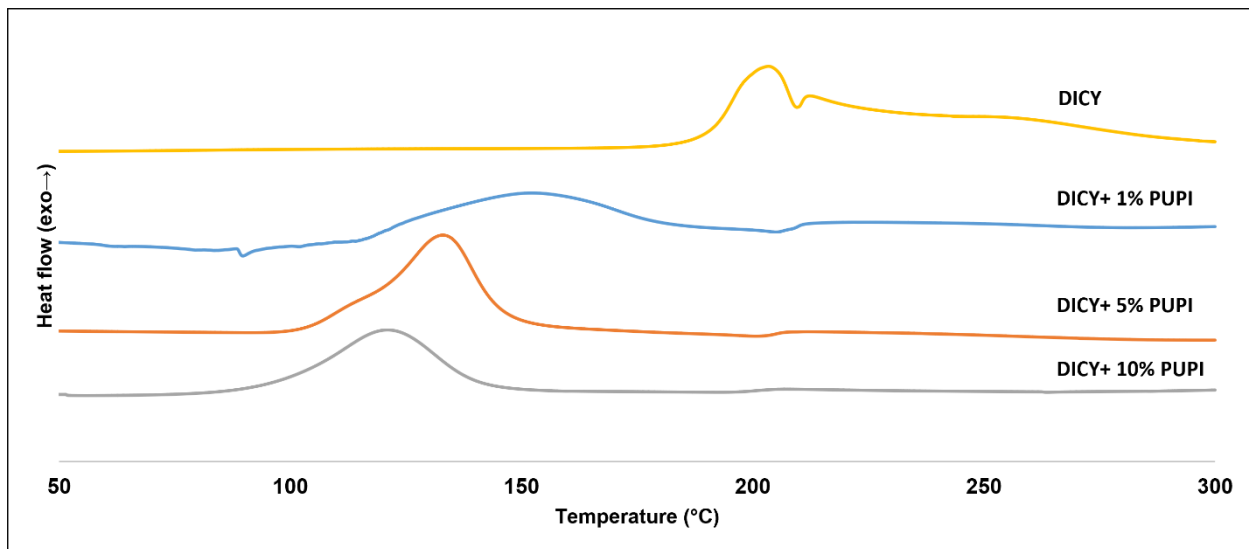


Figure 29. Dynamic DSC results of the OCERs formulated with 1% PUPI + DICY (blue), 5% PUPI + DICY (red), and 10% PUPI + DICY (green)

The left-limit, peak, and right-limit temperatures as well as enthalpy values are listed in **Table 5**. The dynamic DSC curing data for the OCERs formulated with 1% PUPI + DICY, 5% PUPI + DICY, and 10% PUPI + DICY

Table 5. Enthalpy, limit and peak temperature values of DICY:PUPI cured DGEBA formulations

PUPI:DGEBA Ratio (%)	Reaction left limit temperature (°C)	Reaction peak temperature (°C)	Reaction right limit temperature (°C)	Enthalpy (J/g)
1	111	155	205	503.54
5	97	135	179	417.22
10	72	122	161	291.96

Isothermal curing of OCER formulated with 5% PUPI+DICY indicates that curing is completed in 9 minutes with no residual enthalpy peak showing a T_g 152°C of, which is consistent with the T_g 's obtained with DICY+DGEBA resin. (Gilbert, 1988)

Imidazole and its derivatives are used as catalysts to accelerate the reaction between epoxy groups and DICY. Imidazole group functions as both a nucleophile and a base, facilitating the ring-opening of the epoxy resin by attacking the less sterically hindered carbon atom in the oxirane ring, forming an imidazole-epoxy adduct. The imidazole-activated epoxy can react with the active hydrogen atoms of the DICY, leading to the formation of crosslinked polymer networks. The catalytic action of imidazole (or imidazole derivatives) allows curing to take place at lower temperatures and increases the rate of curing, which reduces curing temperature and time as shown in **Figure 29** and **Table 5**.

Dareh and et. al. studied the acceleration effect of imidazole derivatives for epoxy curing with dicy and found out that methyl imidazole accelerated dicy curing most whereas regarding pot life and highest T_g , carbonyldiimidazole displayed the best results. (Dareh et al., 2020) Reuther et. al. investigated the effect of imidazole derivatives on the acceleration of dicy curing of DGEBA resin. Tertiary amines such as imidazole can attack to the energy-rich secondary carbon of oxirane of epoxy groups (Reuther et al., 2022). This results in the chain oligomerization which produces positive charged amine groups and negative charged alkoxylate end groups. Further, alkoxylate can deprotonate dicy which increases its reactivity at lower temperatures. Reuther et. al. concluded that above a critical temperature, the polymeric imidazole derivatives became soluble in epoxy and displayed high reactivities (Reuther et al., 2022). Rodošek et. al. researched three different accelerators to observe the effect on T_g of the cured epoxy with dicy. They found that the imidazole compound that they used, 2-methyl imidazole, decreased the cured epoxy T_g whereas other compounds such as N,N-benzyl dimethylamine (BDMA) and a commercial product Curezol increased the T_g of the cured epoxy (Rodošek et al., 2020). Olson filed a patent for a composition which included imidazole, dicy and a reactivity controller for imidazole to achieve a one component epoxy composition. He claims that the cured epoxy has a T_g of 135°C (Olson, 1994). Gilbert stated that tertiary amines have been used to accelerate dicy curing, however it refutes the room temperature latency (Gilbert, 1988).

2.5. Conclusion

In conclusion, phenylurea propyl imidazole (PUPI) was successfully synthesized using a one-pot, easy, and scalable synthesis method and characterized for its role as a TLC in OCER formulations with DGEBA. PUPI effectively delayed the onset of curing in OCER, allowing precise control over the process. Dynamic DSC showed high conversion rates at 120°C and 140°C, with PUPI providing stability to the OCER for up to three days at room temperature. Furthermore, PUPI acted as an accelerator for DICY, lowering its curing temperature significantly. Overall, PUPI presents as a promising TLC for OCERs, offering control over curing kinetics and stability. Further research could optimize PUPI formulations for specific applications and explore its compatibility with other resins.

CHAPTER 3

3. Para-toluene sulfonyl isocyanate-ethylene diamine adduct as a thermal latent curing agent for epoxy resins

3.1. Introduction

One-component epoxy resins (OCERs), composed of an epoxy resin and a latent curing agent, remain stable at room temperature and are activated by external stimuli such as heat, ultrasonic waves, electron beams, or photo-irradiation (Jee et al., 2020; Li et al., 2017). This unique stability-activation behavior, combined with ease of handling, makes OCERs highly desirable for various applications in adhesives, grouting materials, coatings, and molding compounds across industries such as automotive, construction, electronics, defense, and aerospace (Banks et al., 2004b; Fang et al., 2021; Hassan, 2021; M R et al., 2022; Pouladvand et al., 2020b). The inclusion of latent curing agents ensures controlled curing, maintaining stability at room or slightly elevated temperatures (Gotro, 2022), a critical advantage for applications such as prepreg manufacturing. This reduces the need for cold storage and transportation, resulting in significant cost savings (Kim et al., 2021).

Thermal latent curing agents (TLCs) are the most widely used class of latent curing agents in epoxy formulations. Notable examples include dicyandiamide (DICY), dihydrazides, amino acids, imidazole derivatives, ionic liquids, and urea-based compounds (Hesabi et al., 2019; Lee, 2021; Tomuta et al., 2012; Yu et al., 2021; P. Zhang et al., 2019). Moreover, urea-based compounds have gained particular attention due to their unique properties and effectiveness in controlling the curing process. Ying et al. explored the dynamic reversibility and self-healing properties of urea bonds, noting that introducing bulky groups into carbonyl-amine structures disrupted the co-planarity of amide bonds, weakening carbonyl-amine

interactions. They emphasized the importance of stabilizing molecules and identified isocyanates-highly reactive with amines-as key components in such systems (Ying et al., 2014).

Urea-based catalysts are commonly used in epoxy curing (Holbery & Bordia, 2001; Hübner et al., 2021; Robert P. Kretow, 1996). These catalysts are often combined with TLCs, like DICY, to produce high-quality prepgs and tapes under manufacturing conditions (Hübner et al., 2021; Robert P. Kretow, 1996). Hübner et al. studied the ambient aging of prepgs formulated with urea and DICY and found that tackiness, linked to the viscosity of the prepg, played a crucial role in the mechanical properties of the cured composite. They also observed that urea formed clusters in the prepg, causing viscosity to increase after 42 days (Hübner et al., 2021). Similarly, Kretow investigated the shelf lives of mixtures containing DICY and substituted ureas, finding that substituted ureas exhibited significantly longer shelf lives at ambient temperatures compared to alternatives like monuron and diuron (Robert P. Kretow, 1996). Gotro reported that some ureas, used as accelerators for DICY, displayed no viscosity increase for over 60 weeks, while others showed an increase in viscosity after just 8 weeks at room temperature (Gotro, 2022). An amine based curing agent, ethylenediamine, is preferred over other curing agents, such as organophosphorus, due to amine's good mechanical and thermal properties as well as low shrinkage, ease of processing and low cost. (Nassiet et al., 2006)

Despite these advances, issues such as the control of viscosity increase over time and the optimization of curing temperature remain significant challenges. Additionally, there is room for improvement in developing TLCs that offer better activation characteristics and more stable curing profiles. Pearce et al. addressed these concerns by showing that a novel substituted urea-an adduct of p-phenylene diisocyanate and dimethylamine (PDI-DMA)-alongside DICY, bisphenol S, and a toughener, reduced the curing temperature to 120°C compared to approximately 175°C for formulations using DICY alone. They also demonstrated that sulfonyl groups, through hydrogen bonding with hydroxyl groups, enhanced the stiffness of the polymer chain in diglycidyl ether of bisphenol A (DGEBA) (Pearce & Ennis, 1993).

This paper introduces a new TLC, p-toluene sulfonyl urea-ethylene diamine (PTSU-EDA). The TLC was synthesized by reacting p-toluene sulfonyl isocyanate with ethylene diamine and thoroughly characterized using ¹H NMR, FTIR, TGA, and DSC. The TLC was incorporated into DGEBA to formulate an OCER, which was analyzed using FTIR, DSC, DMA, rheometry, and optical microscopy. The curing kinetics of the OCER were investigated through dynamic and isothermal DSC analyses to address existing challenges in curing temperature control and stability. Finally, DMA samples were fabricated to assess the glass transition temperature (T_g), storage and loss moduli of the cured polymer, providing a comprehensive understanding of the material's performance.

3.2. Experimental

3.2.1. Materials

DGEBA (EEW: 170.2 g/mol), p-toluene sulfonyl isocyanate (PTSI) (96.0%), ethylene diamine (EDA) (\geq 99.5%), and dichloromethane (DCM) (\geq 99.8%) were purchased from Merck Corporation Sigma-Aldrich and used as received. Loctite Frekote 700 NC mold release was used for DMA sample mold.

3.2.2. Synthesis of PTSU-EDA

PTSU-EDA was synthesized by reacting p-toluene sulfonyl isocyanate (15.75 g, 0.078 mol, 2 equiv.) with ethylene diamine (2.34 g, 0.039 mol, 1 equiv.) in 100 mL of dichloromethane (DCM) (**Figure 30**). Initially, the flask was purged with N₂ to provide an inert atmosphere, and then p-toluene sulfonyl isocyanate was added to DCM in a 250 mL round-bottom flask equipped with a magnetic stir bar, and the solution was cooled to 0°C using an ice bath. Subsequently, ethylene diamine was added dropwise into the flask. The solution was then allowed to gradually warm up to room temperature and stirred for 24 h. Upon completion of

the reaction, DCM was evaporated at room temperature with a rotary evaporator to yield a white powdery product (17.45 g, yield: 96.4%).

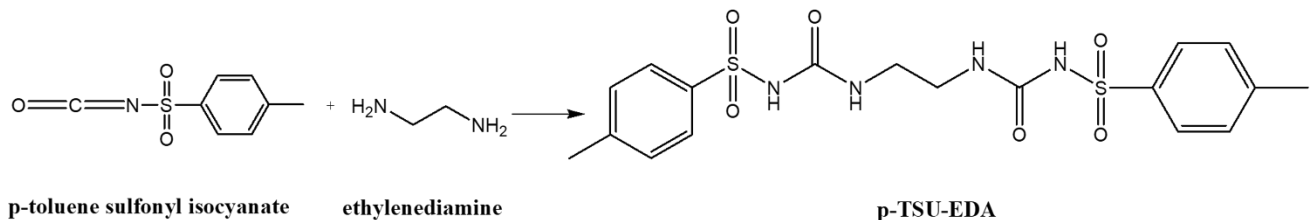


Figure 30. Synthesis of PTSU-EDA

3.2.3. Preparation of the OCER

OCER was prepared with a ratio of 2.26 g:1 g for DGEBA: PTSU-EDA. The epoxy equivalent weight (EEW) of used epoxy was 170.2 and the amine hydrogen equivalent weight (AHEW) of PTSU-EDA was 75.3. The functionality of PTSU-EDA was assumed to be six considering that upon heating each mole of urea decomposes to form one mole of EDA with four functionalities and two moles of PTSI having a total of two functionalities. The OCER was prepared using a homogenizer at 1000 rpm at room temperature for several durations (5, 10, and 15 min). The highest temperature measured after mixing the mixture was recorded as 40°C.

3.2.4. Preparation of DMA samples

DMA samples were prepared using an aluminum mold with dimensions complying with ASTM D 4065 standard for tension mode. Before molding, a mold release agent was applied onto the aluminum mold twice to ensure easy removal of the sample, which was left at room temperature until it dried. There was 15 min between each application to ensure film formation. The OCER was heated in an oven at 80°C for 1 h and when it became moldable,

it was poured into aluminum mold cavities and degassed in a vacuum oven for 4 h at 50°C and 1 h at 80°C. Once the gas pressure was measured between 1-10 mbars and no bubble formation was observed through the glass cover of the vacuum oven, the mixture was cured at 140°C for 4 h to complete the curing. DMA test was conducted between 25-250°C with a 3K/min heating rate at 1 Hz frequency and in single cantilever bending mode.

3.2.5. Preparation of optical microscopy samples

Microscope slides were cleaned with isopropyl alcohol and used as received at room temperature. 1-2 drops of the OCER mixture were taken using 1 mL plastic pipette and dispensed onto a prepared slide. To ensure uniform distribution and minimize thickness variation, a second slide was placed on top and gently pressed. To remove trapped air, the top slide was moved horizontally at $\pm 45^\circ$ relative to the bottom slide before placing the assembly under the microscope for observation.

3.3. Methods/Characterization

^1H NMR spectra were recorded in DMSO-d₆ for PTSU-EDA on a 500 MHz Varian spectrometer. Fourier transform infrared (FTIR) spectra were obtained with a Thermo Scientific Nicolet iS50 FTIR spectrometer using a Smart iTR Accessory, employing transmission mode with a resolution of 16 cm^{-1} . DSC measurements were conducted using a Mettler Toledo DSC 3+ instrument with 8-10 mg sample amounts. For dynamic DSC measurements, the temperature range spanned from 25 to 250 °C, with heating and nitrogen flow rates set at 3 °C/min and 50 mL/min, respectively to obtain an accurate window of curing reactions. Isothermal DSC measurements were performed for 3 h at various

temperatures, followed by dynamic DSC tests from 25 to 300 °C at a heating rate of 10 °C/min to measure residual enthalpy. Horizontal right baseline was used for enthalpy calculations. Thermogravimetric analysis (TGA) measurements were executed on a Mettler Toledo TGA/DSC 3+ instrument within a 25-800 °C temperature range. Samples with weights ranging between 10-100 mg were heated at 10 °C/min under a nitrogen atmosphere with a 100 mL/min flow rate. Optical microscope images were captured using a Nikon Eclipse LV100ND optical microscope equipped with CFI60–2 lenses at magnifications of 25x, 50x, 100x, and 200x. Bright-field illumination was applied from beneath the material during imaging. Zeiss / Leo Supra VP35 SEM was used to obtain a better resolution and topography of the sample. Rheological properties are tested at Anton Paar MCR 302 with a ± 0.1 strain rate, which is determined by an amplitude sweep test prior to temperature sweep, and an initial gap of 0.5 mm. The temperature range is 25-200 °C and the heating rate for temperature sweep is 2°C/min.

3.4. Results and Discussion

The synthesis of PTSU-EDA (TLC) is shown in **Figure 30**. The reaction was conducted at room temperature under N_2 atmosphere for 24 h.

3.4.1. NMR Analysis

The ^1H NMR spectrum of PTSU-EDA, along with the peak assignments, is presented in **Figure 31**. The presence of urea -NH peaks at 10.28 ppm (peak 4) and 6.50 ppm (peak 5), along with the shift of CH_2 peaks of ethylene diamine adjacent to -NH₂ (peak 6) at 3.01 ppm to 2.95 ppm indicated the successful completion of the reaction. The -NH peak is magnified

and broadened as its peak intensity is very low compared to other peaks, which is observed around 10 ppm. Furthermore, methyl (peak 1) and phenyl peaks (peaks 2 and 3) were observed at 2.37 ppm (singlet), 7.37-7.38 (doublet) and 7.75-7.77 (doublet), respectively. The integral values of the assigned peaks 1, 2, 3, 4, 5, 6 were 7.12: 4.74: 4.63: 2.02: 2: 4.38, corresponding to 6H: 4H: 4H: 2H: 2H: 4H, showed that the intended structure (PTSU-EDA) was obtained.

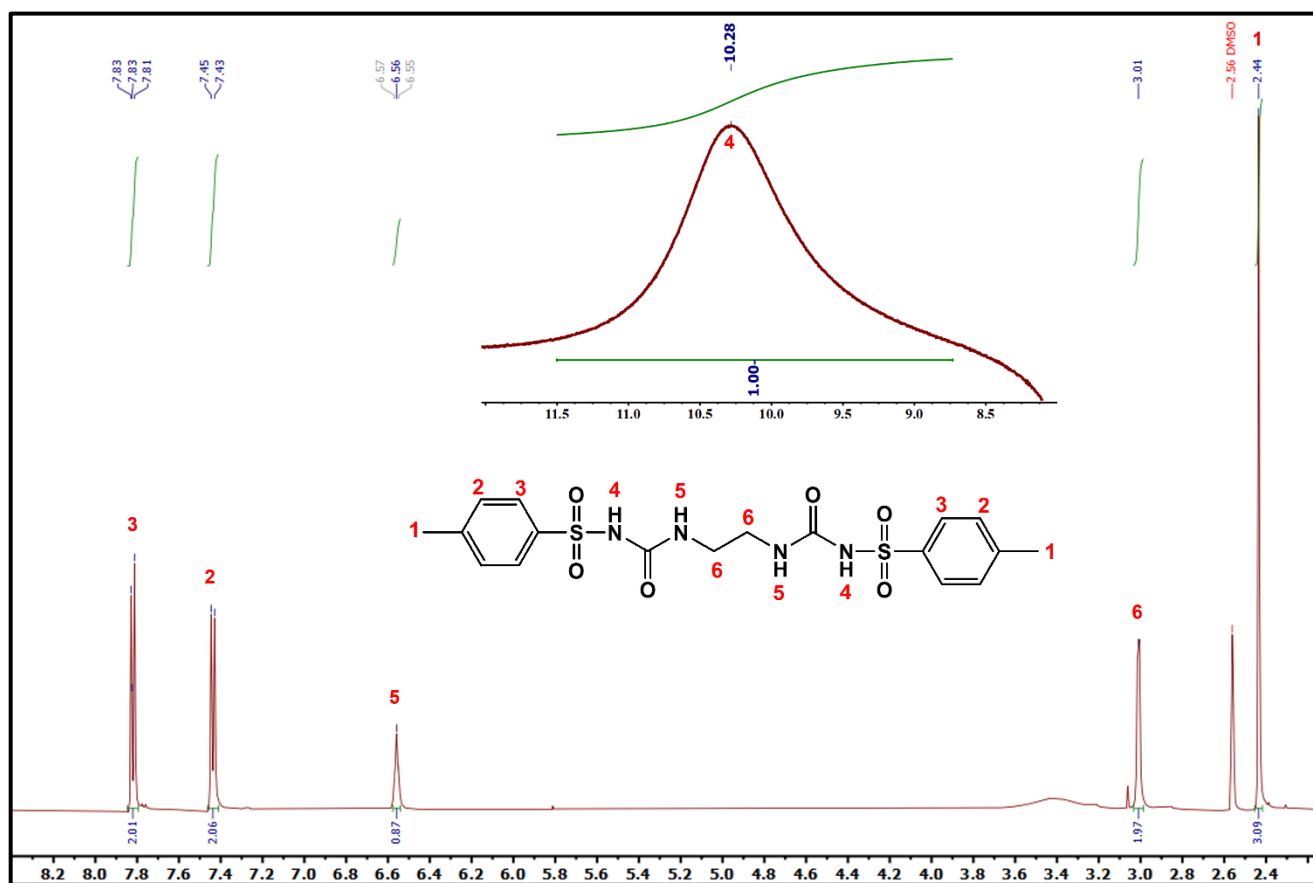


Figure 31. NMR spectrum of PTSU-EDA in DMSO-d6

3.4.2. FTIR analysis

FTIR spectrum of PTSU-EDA is shown in **Figure 32**. The peaks associated with N-H bending and stretching were observed at 1597 cm^{-1} and 3358 cm^{-1} for ethylenediamine (EDA), respectively where both peaks seem to have shifted towards left in PTSU-EDA which might be associated with sulfonyl peak's inclusion in PTSU-EDA. The peak associated with isocyanate groups (-N=C=O), generally appearing at 2246 cm^{-1} , was not observed in the spectrum, which indicated a complete reaction of PTSI with EDA. The appearance of the urea carbonyl peak (-NH-CO-NH-) at 1693 cm^{-1} in the PTSU-EDA spectrum confirmed the successful synthesis of the product (Attaei et al., 2020; Manivannan & Rajendran, 2011). In **Figure 33a and 20b**, the compared FTIR spectrums of DGEBA, PTSU-EDA (TLC), uncured and cured epoxy are displayed. 20a shows the full spectrum ranging between $500\text{-}3500\text{ cm}^{-1}$ wavenumber and 4b is a zoomed version of the full spectrum ranging between $500\text{-}1800\text{ cm}^{-1}$. The oxirane groups of DGEBA show C-O and C-O-C stretching peaks at 915 cm^{-1} and 831 cm^{-1} , respectively (Pouladvand et al., 2020b). The carbonyl group of urea was seen for PTSU-EDA and the uncured mixture, but it disappeared when the product was cured, which can be interpreted as the successful reaction of the urea with DGEBA.

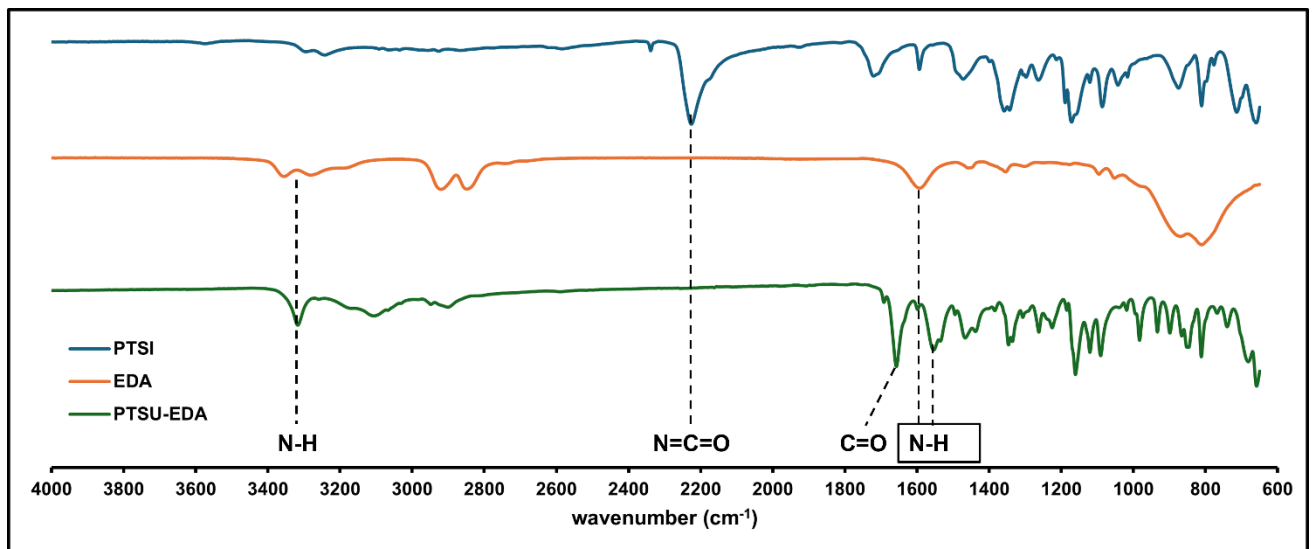


Figure 32. FTIR spectra of PTSI, EDA and PTSU-EDA

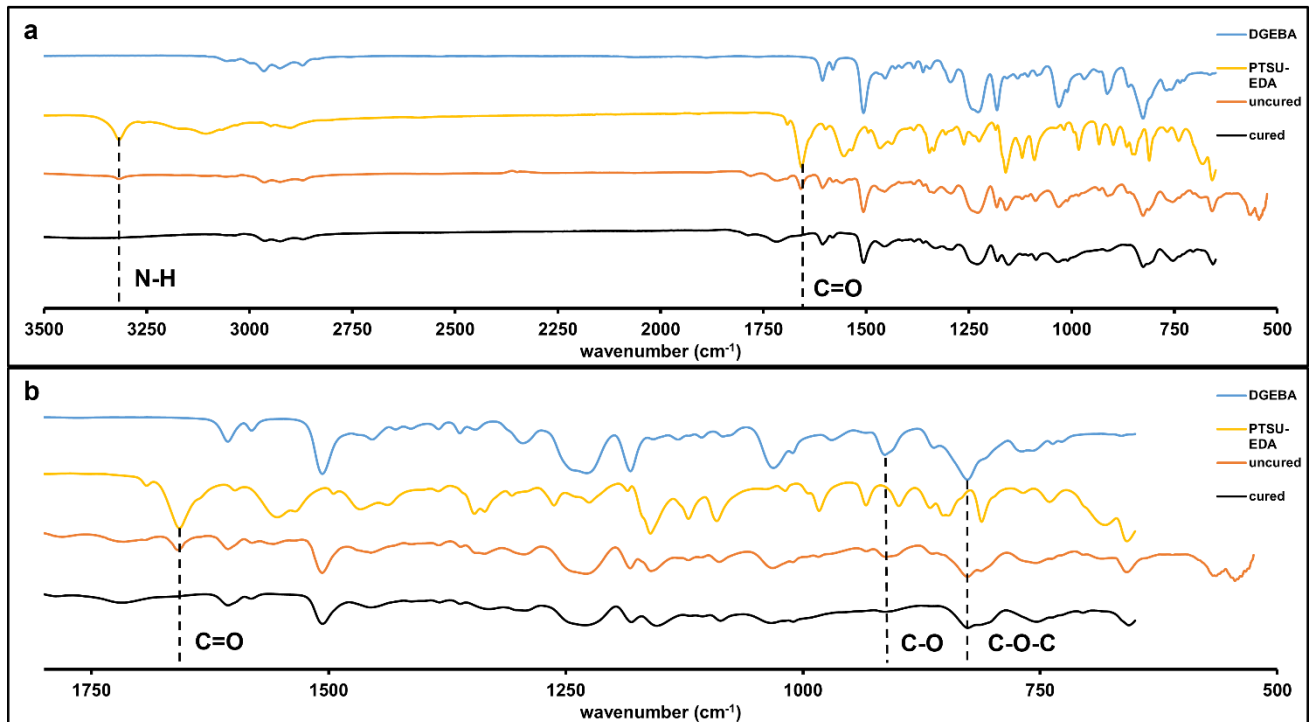


Figure 33. FTIR spectrum comparisons of DGEBA, PTSU-EDA, uncured and cured mixture

3.4.3. TGA analysis

TGA thermogram of PTSU-EDA (black line) and the differential form of the peak (red dotted line) are shown in **Figure 34a and 21b**. A single-step decomposition of PTSU-EDA with an onset temperature of 262 °C was observed. Same test is repeated under air flow and the onset is 5 % weight loss of the TLC was measured at 228 °C under nitrogen and 259 °C under air flow and the decomposition was completed at 431°C and 527°C respectively. The difference between nitrogen and air flows can be explained via the reaction between phenolic and sulphur groups with oxygen causing thermal stability as well as mass gain (Yee Low & Ishida, 1999). The mass gain is also pronounced at the char yield of % 4.13 under air flow test compared to none under nitrogen flow. Weh et. al. studied the thermal decomposition of various sulfone group attached aliphatic and aromatic compounds and concluded that the onset of thermal decomposition of acyclic aliphatic and sulfones attached to aromatic groups is above 350°C under air (Weh & de Klerk, 2017). Under nitrogen flow, there was no residual mass left, indicating the high purity of the molecule. Zamani has reported that a urea model compound, which is composed of phenyl isocyanate and aniline, has decomposed over 350°C (Zamani et al., 2023). This high decomposition temperature might be due to the aromatic nature of aniline contributing to the thermal stability of urea.

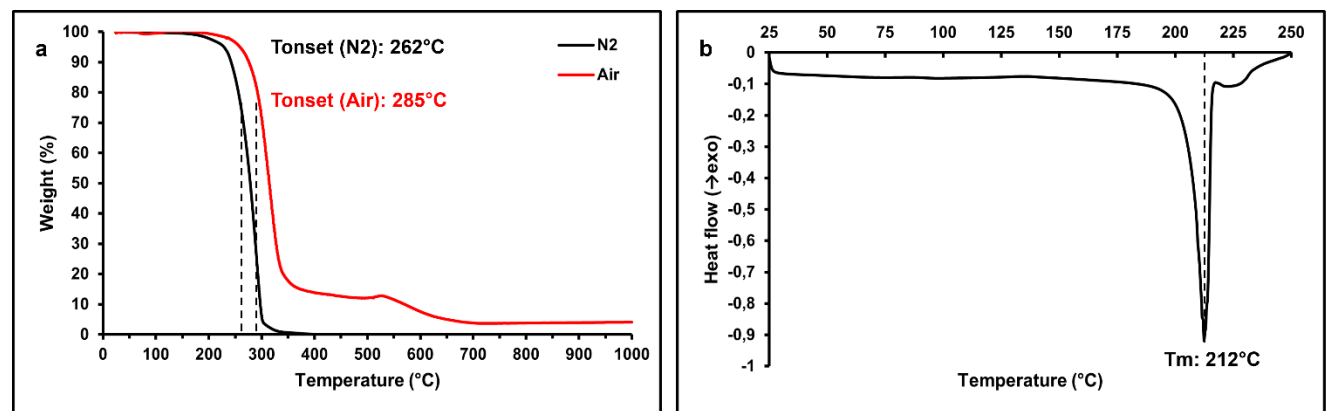


Figure 34. a) TGA thermogram of PTSU-EDA, b) DSC thermogram of PTSU-EDA

3.4.4. DSC analysis

DSC analysis was performed with a 3°C/min heating rate to have a pronounced display of the thermal changes occurring in the TLC and the OCER.

3.4.4.1. DSC thermogram of the TLC

A sharp endotherm appeared in the heating profile of PTSU-EDA as shown in **Figure 34b**. The onset temperature of melting started at 207 °C and the peak temperature is recorded at 212 °C whereas the left and right limit temperatures are 168 and 217 °C. The melting enthalpy of the molecule is 124 J/g. Above 230 °C, an exotherm seems to start rapidly which might be interpreted as the initiation of decomposition of the material which coincides with the results of TGA.

3.4.4.2. DSC thermogram of the OCER

Dynamic DSC curing profile of the OCER is shown in **Figure 35a and 22b**. The left limit, peak, and right limit temperatures of the reaction were 141, 173, and 222°C, respectively. The measured enthalpy of the curing reaction was 115 J/g. The TLC started to dissociate at around 140°C to form EDA and PTSI, both of which reacted with DGEBA. As the temperature increased, the dissociation and curing rate increased. Riccardi et. al. examined the mechanism and kinetics of ethylene diamine and epoxy reactions. They proposed a simple addition reaction mechanism of hydrogens present in the ethylene diamine with the epoxy group of DGEBA. In addition, they stated that at high temperatures only the non-catalytic

reaction pathway was active as the ternary transition complex would be difficult to form (Riccardi et al., 1984). Moreover, they found that the reactivity of the amines varied with the particular diamine (hexamethylene diamine and ethylene diamine) used. The conversion of the curing reaction with EDA at the gelation point was 57.7% and there was more pronounced steric hindrance for the reaction with EDA (Riccardi et al., 1984). Scott et. al. investigated the crack propagation in epoxy resins using four different diamines including EDA. They found out that the increase in molecular weight of the curing agent caused the cross-linking density to decrease (Scott et al., 1980). Thus, for small molecules such as EDA, the cross-linking density is expected to be high, which can cause brittleness in the cured resin. Isocyanates and epoxies can form ureas, carbodiimides, isocyanurates and oxazolidones depending on the reaction temperature. Kadurina et. al. reported that the reaction of epoxy resins and isocyanates yield oxazolidones and urethanes (Kadurina et al., 1992). Moreover, they reported the lowest temperature needed for oxazolidone formation as 140°C. Chian et. al. studied DGEBA reaction with isocyanates and found that stoichiometric ratio determined whether isocyanurates or oxazolidones were formed. Furthermore, they stated that especially the formation of isocyanurates yielded highly cross-linked structures forming brittle materials (Chian & Yi, 2001).

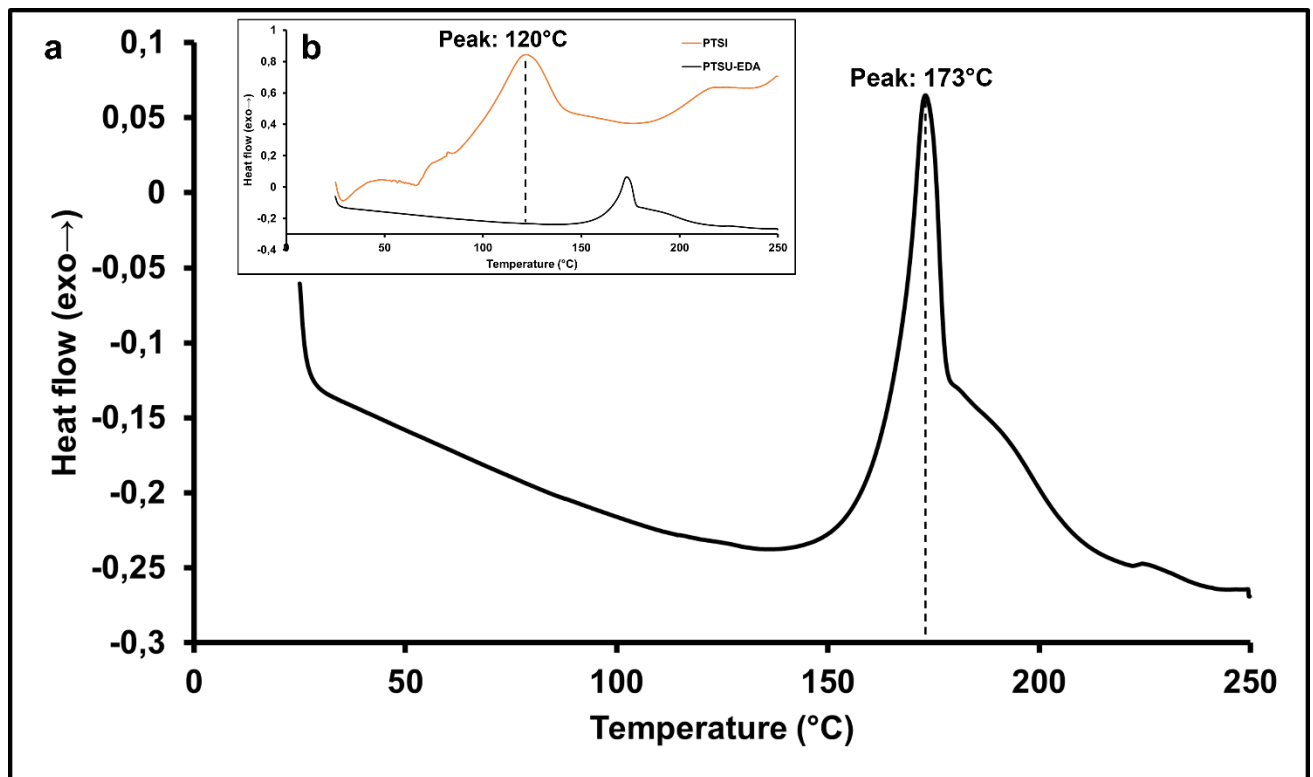


Figure 35. a) Dynamic DSC curing profile of PTSU-EDA-DGEBA mixture (OCER), b) Dynamic DSC curing profiles of PTSI-DGEBA (red line) and PTSU-EDA-DGEBA (black line) mixtures

3.4.4.3. DSC thermograms of PTSI-DGEBA vs. PTSU-EDA-DGEBA mixtures

p-Toluene sulfonyl isocyanate was solely used to cure DGEBA resin at 2:1 mole ratio of isocyanate:epoxy. The dynamic DSC curing profile is shown in **Figure 35b**. The left limit, peak, right limit temperatures of curing were 73, 120, and 176 °C. The curing enthalpy for the PTSI-DGEBA reaction was 128 J/g. PTSI cured epoxy resin at about 50 °C lower than the curing temperature of the PTSU-EDA, meaning that the PTSI formed upon dissociation of PTSU-EDA above 140 °C would react with DGEBA right away. Although isocyanate-epoxy reactions were reported to proceed at temperatures above 160 °C (Chian & Yi, 2001;

Kadurina et al., 1992), the presence of sulfonyl groups in PTSI resulted in reaction with DGEBA at lower temperatures.

3.4.4.4. Isothermal DSC thermograms of the OCER

Isothermal DSC thermograms of the OCER at different temperatures are shown in **Figure 36a**. The leftover curing enthalpies were measured after isothermal curing as shown in **Figure 36b**.

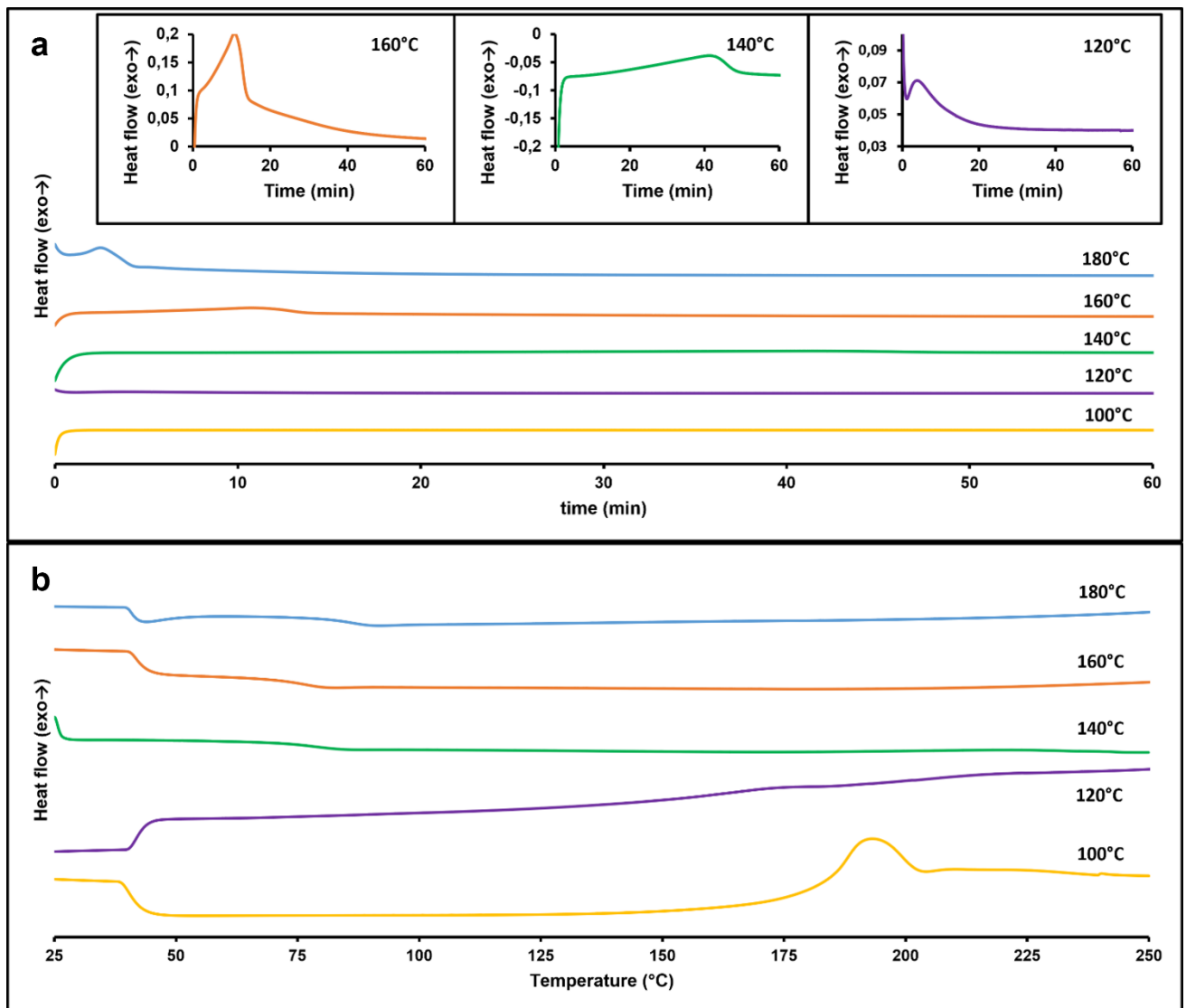


Figure 36. a) Isothermal DSC thermograms of the OCER and b) dynamic leftover curing profile of PTSU-EDA and DGEBA after isothermal curing

The enthalpy values of isothermal and residual dynamic DSC curing are shown in **Table 6**.

The residual enthalpy curves were observed after isothermal curing at 100 and 120°C. No residual enthalpy curves were observed for the samples that were isothermally cured at 140, 160, and 180°C, indicating that the reactions were completed. At 100°C, there was no reaction. The curing times increased as the temperature decreased from 180°C to 120°C as shown in Figure 6. T_g values of the cured samples were 70, 77, and 89°C for the samples cured at 140, 160, and 180°C, respectively (**Figure 36**). The differences between T_g values

in DMA and DSC stemmed from the cure duration as for DSC measurements 3 h of isothermal curing was applied whereas for DMA sample 4 h at 140°C was applied for curing. Moreover, for DMA samples the mixture was degassed and held under vacuum for 5 h, which should influence the T_g of the sample positively whereas in DSC samples no vacuum was applied.

Table 6. Enthalpy values for isothermal and dynamic DSC curing of PTSI-DGEBA mixture and OCER

Mixture	Curing method	Temperature/ Temperature range (°C)	Normalized curing enthalpy (J/g)	Residual enthalpy (J/g)
PTSI-DGEBA	Dynamic	25-250	128	NA
OCER	Dynamic	25-250	115	NA
OCER	Isothermal	100	-	36
OCER	Isothermal	120	14	-
OCER	Isothermal	140	171	-
OCER	Isothermal	160	237	-
OCER	Isothermal	180	239	-

3.4.5. Rheology results of the OCER

The rheological properties of the OCER were analyzed using a rheometer temperature sweep method. Before the temperature sweep, an amplitude sweep test was conducted to determine the linear viscoelastic region of the mixture. The temperature range and initial gap were set to 25–200°C and 0.5 mm, respectively. A strain rate of 0.1% was applied based on the amplitude sweep results. The gel point could not be directly determined due to the absence of a clear crossover between the storage and loss modulus. The y-axis values were reported on a logarithmic scale.

The complex viscosity profile of the OCER is shown in **Figure 37**. At room temperature, the OCER appeared as a creamy product with a complex viscosity of 481 Pa·s. The viscosity steadily increased until approximately 145°C, likely due to the increased solubility of the TLC in DGEBA [26]. Beyond this point, the viscosity decreased rapidly, continuing until 180°C.

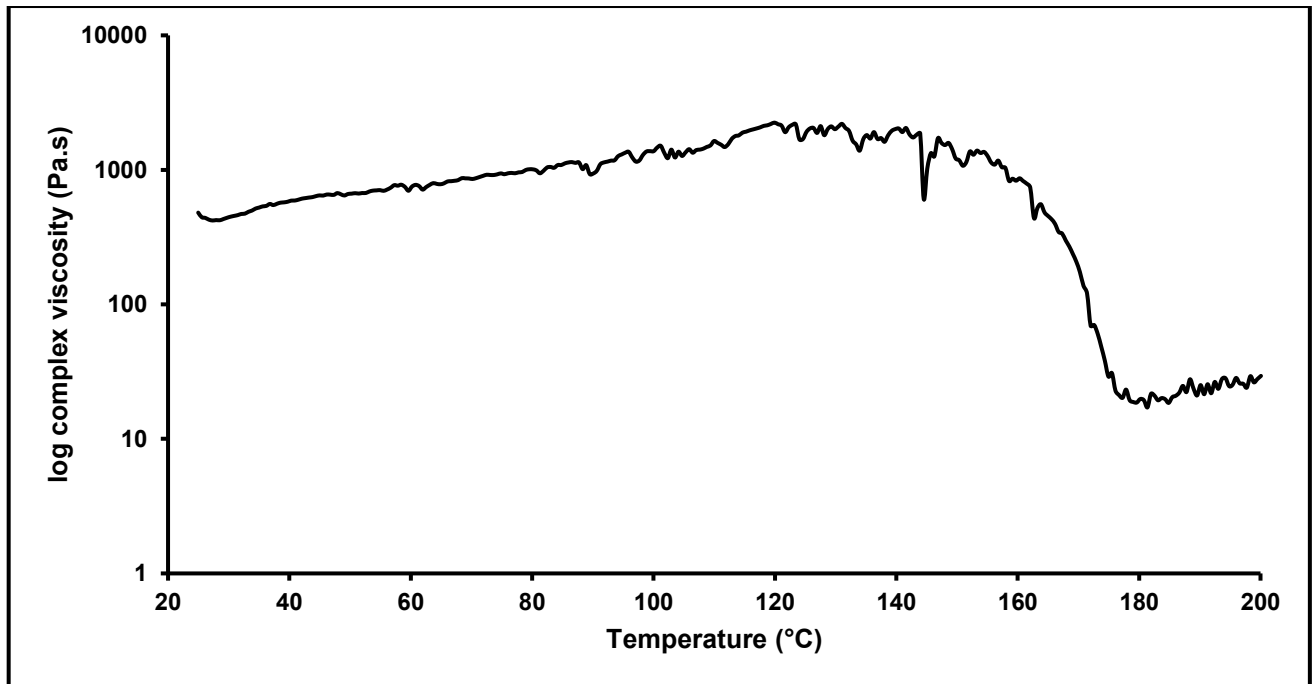


Figure 37. Complex viscosity profile of the OCER

The change in storage and loss modulus of the OCER with respect to temperature is shown in **Figure 38**. Both properties increased up to 140°C and then began to decrease simultaneously. Although a definite crossover (gel) point was not observed, the storage and loss modulus values intersected and decreased together between 144°C and approximately 175°C. Beyond 175°C, the loss modulus continued to decrease, while the storage modulus remained steady. The steadiness of the viscosity and storage modulus makes the OCER ideal

for applications such as self-healing and repair applications as over a wide range of temperature, the OCER remains stable and is only activated at a certain temperature.

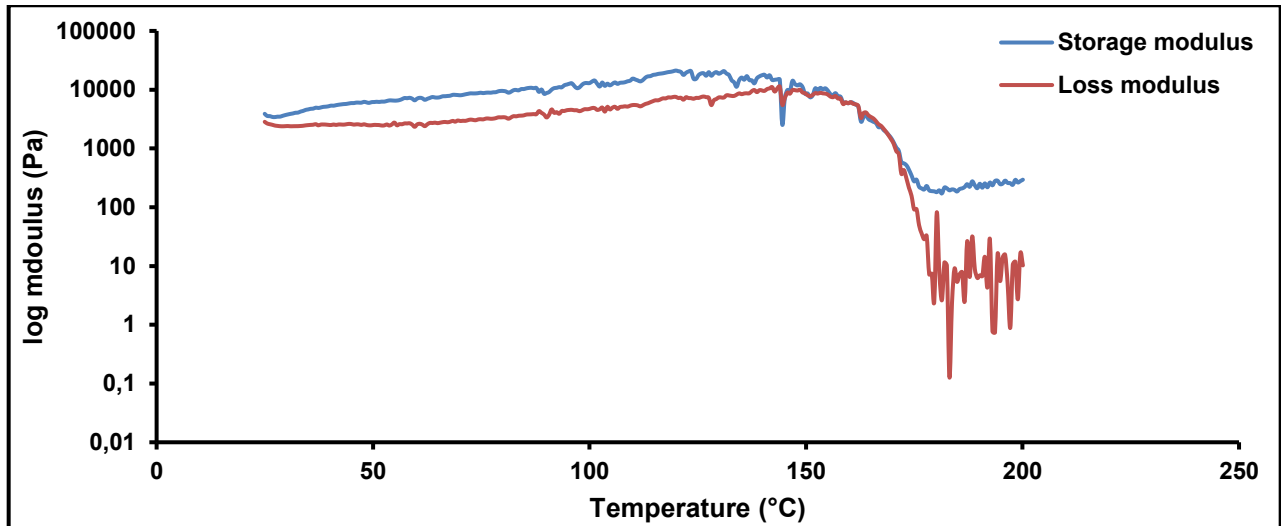


Figure 38. Storage and loss modulus of the OCER

3.4.6. Optical Microscopy Analysis of the OCER

The optical microscopy images of PTSU-EDA (ground and unground) and the OCER are shown in **Figure 39**. A clear morphological difference was observed between the ground and unground PTSU-EDA samples. The ground samples exhibited a rounded shape (**Figure 39b**), whereas the unground samples appeared as flake-type particles (**Figure 39a**). The ground samples contained a higher number of smaller-diameter particles, indicating an increased surface area. This enhanced surface area likely facilitated better interaction and distribution of PTSU-EDA particles within the DGEBA matrix. The optical microscopy image of the OCER at 200x magnification indicated that a homogeneous distribution of TLC particles was achieved when the OCER was mixed at 40°C for 10 min (**Figure 39c**).

The optimum mixing duration to prepare the OCER was studied, and the results are shown in **Figure 40**. Mixing for 5 min at room temperature was insufficient, as unmixed crystals of

the TLC were observed under an optical microscope, and no temperature increase was recorded. While TLC was mostly distributed in the matrix, dispersion was not optimal. Mixing for 10 min resulted in a homogeneous mixture, with the bottom of the mixture vial reaching 35°C and smooth surface images observed at 100x magnification. However, when mixed for 15 min, crystals of DGEBA appeared.

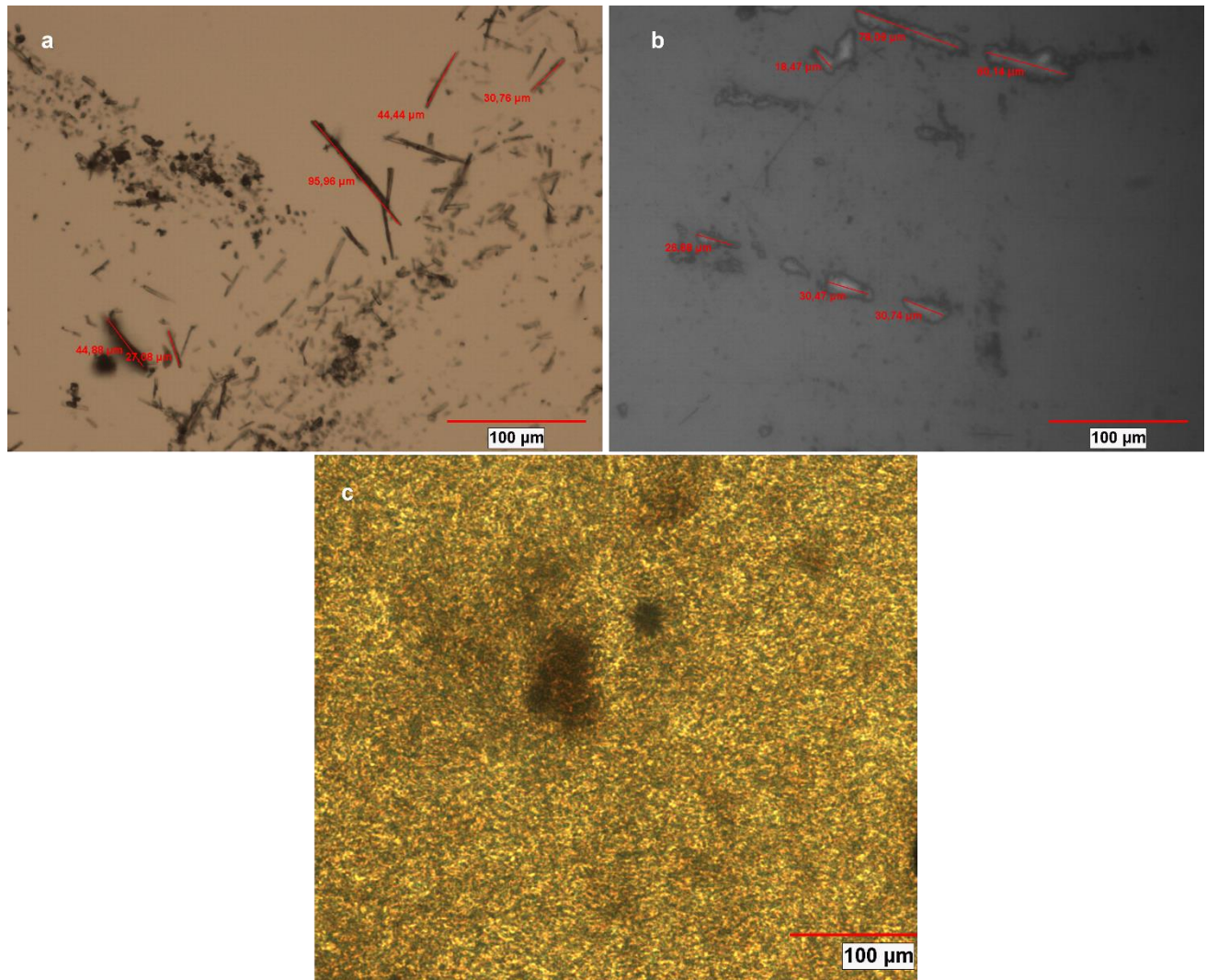


Figure 39. Optical microscopy images of unground PTSU-EDA (a), ground PTSU-EDA (b), and the OCER after mixing at 40°C for 10 mins (c) under 200x magnification.

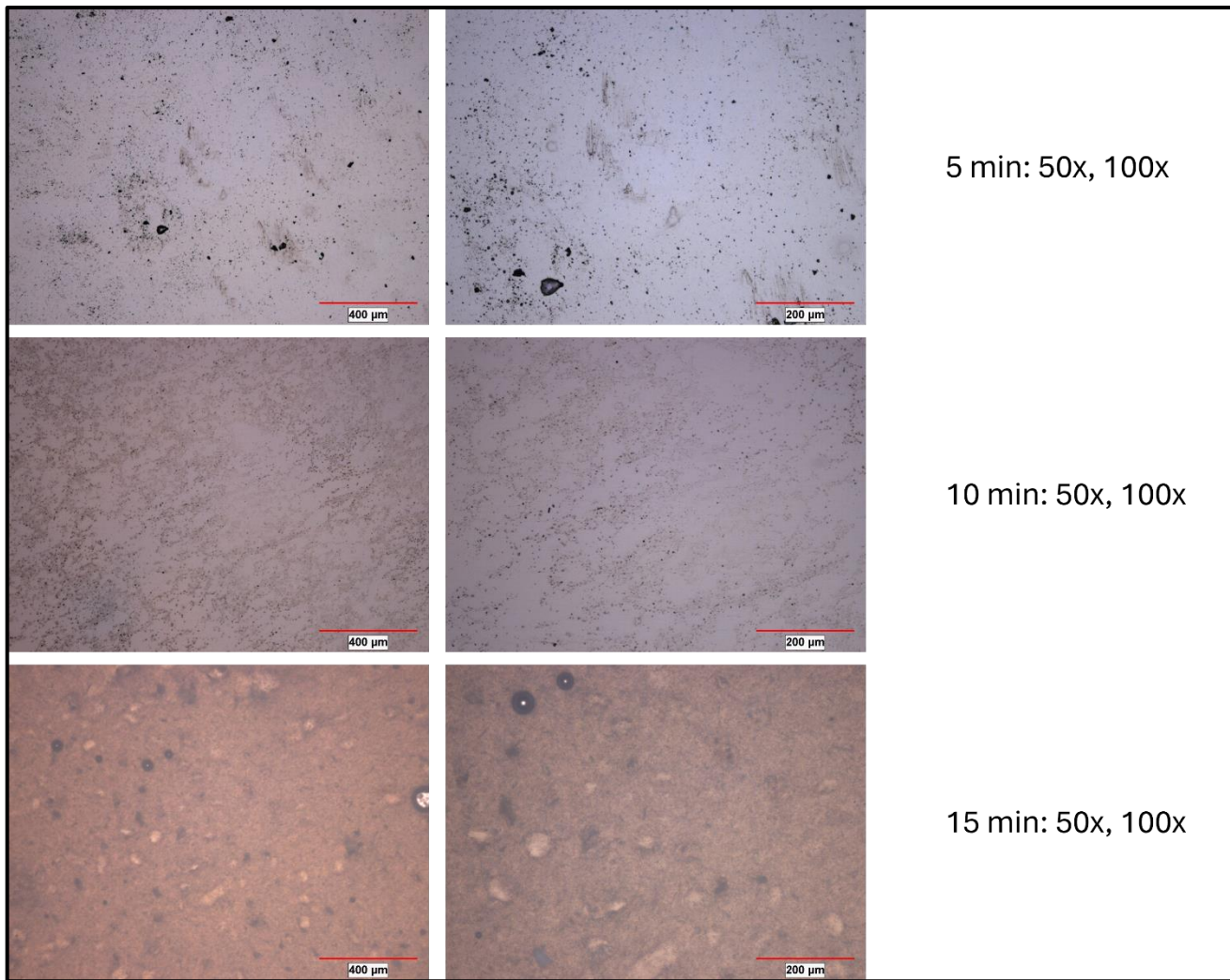


Figure 40. Optical microscope images of the OCER at different mixing durations (5, 10, 15 min)

3.4.7. DMA analysis

The OCER was prepared using liquid molding in a metal mold for DMA testing. It was first heated to 80°C in a vacuum oven, a temperature at which the curing reaction does not occur and then poured into a mold maintained at ambient temperature. Consequently, the temperature of the mixture dropped to 50°C. The OCER was degassed at 50°C for 4h and then at 80°C for 1h. After degassing, the mixture was slowly poured into another mold and cured at 140°C for 4 h to complete the curing reaction. Before molding, a mold release agent

was applied twice to facilitate the removal of the cured product. The DMA sample was removed from the metal mold while still hot and left in the oven over the mold to cool gradually. The cured samples were then processed to meet the dimensional requirements of the DMA test standard. The glass transition temperature (T_g) determined from the $\tan \delta$ peak was measured at 115°C, while the T_g values from the storage modulus curve (onset) and the loss modulus (peak point) were 96°C and 104°C, respectively, as shown in **Figure 41**. Since T_g was lower than T_{cure} , the cured polymer was considered to be in a gelled state rather than fully cured (Lange et al., 2000). The storage modulus decreased rapidly around T_g , while the loss modulus exhibited a Gaussian distribution, rising to its maximum at T_g . The loss modulus remained low (~10 MPa) until T_g was reached. Beyond T_g , $\tan \delta$ and loss modulus values became noisy, likely due to increased dynamic flexibility of the polymer chains, leading to rapid variations in storage and loss modulus values.

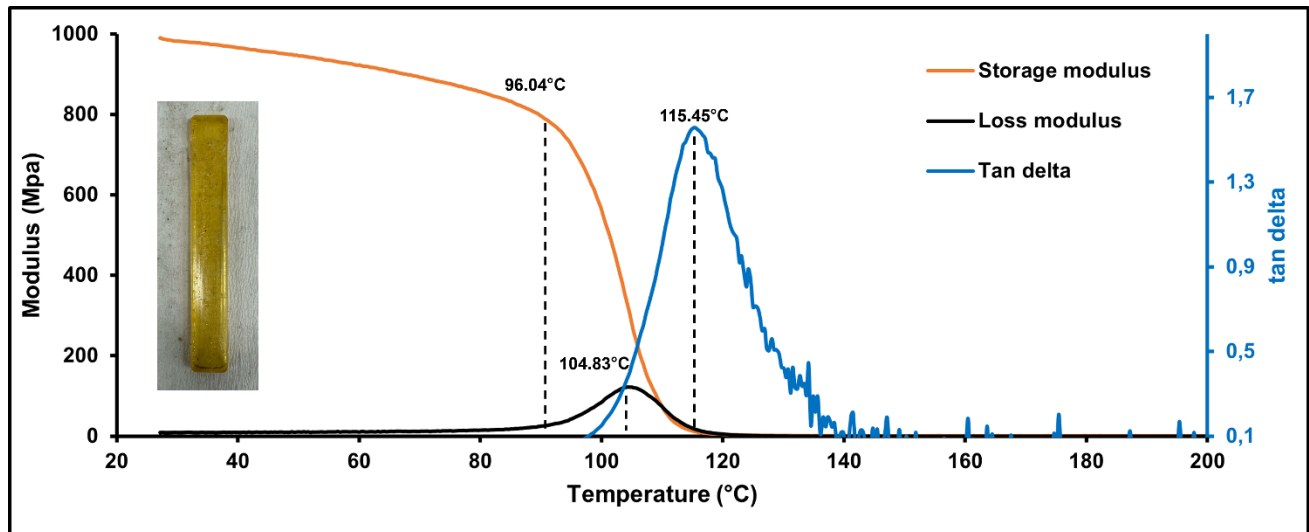


Figure 41. The DMA results of the cured OCER

The crosslink density of the cured OCER was calculated using the equation below (J. Huang et al., 2022; Klein et al., 2024):

$$Vc = \frac{E'}{3RT} = \frac{1.18 \text{ MPa}}{3 * 8.314 \text{ cm}^3 \cdot \frac{\text{MPa}}{\text{K}} \cdot \text{mol} * 438.182 \text{ K}} = 0.108 \frac{\text{mol}^{-1}}{\text{cm}^3}$$

Storage modulus (E') at the temperature T (selected as $T_g + 50^\circ\text{C}$ as stated by Huang et.al. (J. Huang et al., 2022) was used in the equation. The crosslinking density was calculated to be $0.108 \text{ mol}^{-1}/\text{cm}^3$. The crosslink density value was low compared to the results in literature (J. Huang et al., 2022; J. Huang & Nie, 2016; K. Huang et al., 2013; Klein et al., 2024). This may be since the PTSI formed upon dissociation of the TLC reacted with the epoxy group of the DGEBA, which potentially interrupted the crosslinking reaction, limiting the formation of a fully crosslinked network.

3.5. Conclusions

In conclusion, the PTSU-EDA adduct was successfully synthesized through a simple, one-pot, and scalable method and characterized for its role as a TLC in OCER formulations with DGEBA. PTSU-EDA effectively delayed the onset of curing, providing precise control over the curing process. DSC results revealed that the lower limit of the reaction occurred at 141°C , with PTSU-EDA maintaining stability in the OCER up to 100°C . Optical microscopy confirmed the homogeneous distribution of the TLC within the OCER. DMA results showed that the cured OCER exhibited a glass transition temperature (T_g) of 115°C . PTSU-EDA offers reversibility which can be beneficial for applications such as self-healing and use the cured epoxy as a vitrimer candidate. The inclusion of sulfonyl group contributed to the flexibility of the urea chain and it can be further utilized for applications such as flame retardancy due to the sulphur's properties such as thermal stability, improved fire resistance and increasing or maintaining mechanical properties of epoxy resins (Battig et al., 2020; P. Wang, Chen, et al., 2020; P. Wang, Xiao, et al., 2020). Overall, PTSU-EDA proves to be a promising TLC for OCERs, offering control over curing kinetics and stability. Future work could focus on optimizing PTSU-EDA formulations for specific applications and investigating its compatibility with other resin systems.

CHAPTER 4

4. Ambient-Temperature-Stable Epoxy Prepregs with Tunable Processability and Curing Behavior: Correlating Prepreg Structure with Composite Performance

4.1. Introduction

One-component epoxy resins (OCERs) are in high demand in composite manufacturing due to their ease of processing, extended shelf life, and controlled curing behavior. OCERs contain latent curing agents that are activated through various stimuli such as heat, photo-irradiation, ultrasonic waves, and electron beams (Jee et al., 2020; Li et al., 2017). Thermal latent curing agents are commonly used in composite applications to obtain OCERs as they significantly improve prepreg manufacturing conditions due to controlled curing (Aoki et al., 2024). The control over curing provides a broader process window, with regards to temperature, pressure and time, for prepreg manufacturing and further, and the cold storage needed to prevent reactions at room temperature is eliminated (Kim et al., 2021).

Thermal latent curing agents (TLC) are incorporated into OCERs where they offer activity only at high temperatures. Thus, TLCs provide prolonged room temperature stability as well as high catalytic activity for cross-linking at elevated temperatures (Gotro, 2022; J. Wang et al., 2016). Dicyandiamide (DICY), chemically modified amines, urea compounds, amino acids, imidazole derivatives and ionic liquids which are used for different applications and

needs, are the most common thermal latent curing agents (Hesabi et al., 2019; Hübner et al., 2021; Kim et al., 2021; Lee, 2021; Tomuta et al., 2012; Yao et al., 2017b; Yu et al., 2021; P. Zhang et al., 2019).

Prepregs are materials that yield the highest quality composites as they can be manufactured in autoclaves and compression molding resulting in minimal voids in the cured part. Prepregs are mainly carbon, glass or aramid fiber reinforced and they can serve to industrial sectors such as automotive, aerospace and marine as they offer good resin distribution, high fiber volume ratios and therefore excellent mechanical properties (Banks et al., 2004a; Budelmann et al., 2022; Somarathne et al., 2024). Somarathna et al. claimed that B-staging, viscosity and tack are the most critical parameters for epoxy prepreg manufacturing (Somarathne et al., 2024).

Dual cure prepgs utilize two distinct curing agents as one curing agent is used for B-staging and adjusting drape and tack properties whereas the other curing agent is used for the complete cure at elevated temperatures. They can be prepared either by B-staging over a certain time or via off-stoichiometric ratios to obtain a desired degree of cure which can be adjusted regarding properties such as tack, drape and viscosity (Pouladvand et al., 2020b). Pouladvand et al. promoted dual cure prepgs as strong candidates for eliminating the cold storage conditions due to use of TLCs at off-stoichiometric ratios as well as optimizing the prepg properties for better processing (Pouladvand et al., 2020b). Moreover, Khamidullin et al. stated that via the use of dual cure epoxy systems, exothermic peaks are lowered by selecting appropriate curing agents (Khamidullin et al., 2025). Tack and drapability properties are addressed as crucial processing parameters by several authors (Banks et al., 2004a; Budelmann et al., 2020, 2022; Lammens et al., 2014; Pouladvand et al., 2020b; Somarathne et al., 2024) for part manufacturing but for establishing structure-property relationships only tackiness is considered. Drapability is the ability of a material to conform to the shape of a structure without wrinkling or bridging and tackiness is a measure of adhesion of a material onto another substrate (Banks et al., 2004a; Budelmann et al., 2019, 2022; Gay & Leibler, 1999; Han & Chang, 2021; Joesbury et al., 2025; Y. Wang et al., 2023). Han et al. stated that drapability of prepgs can be characterized via a uniaxial tensile test, a picture frame shear test mechanically, and the drapability performance of it can be tested

with bending test according to ASTM D 1388 standard (Han & Chang, 2021). They later introduced a model to predict the out-of plane deformations of the prepgs using a FE method called lay-up shell modelling. Budelmann et al. investigated the tack properties of a formulated epoxy aerospace-grade prepg with respect to resin formulation, toughening and B-staging (Budelmann et al., 2022). Wang et al. introduced a new test probe method for tack measurement of inter and intraplies during AFP manufacturing. They studied the influence of AFP manufacturing parameters such as contact time, temperature, pressure and pull-off rate on the tack of the prepgs (Y. Wang et al., 2023). Pouladvand et al. linked drapability and tack properties to the stability of the prepg via the inclusion of off-stoichiometric low temperature curing agent, DETA and tracked it through methods such as FTIR and DSC (Pouladvand et al., 2020b). There has been no attempt, so far, to link the drapability and tackiness properties to mechanical properties of cured composites.

Mechanical properties of composites depend on factors such as resin system, type of reinforcement, the fiber to resin volume ratio and manufacturing conditions (Budelmann et al., 2019, 2020; Grunenfelder et al., 2017; Kheradpisheh et al., 2025; Schmidt et al., 2018). Manufacturing conditions influences the cured composites mechanical performance drastically, which is reported by several researchers (Belhaj et al., 2021; Kheradpisheh et al., 2025; Mbotto Tonye & Buet Gautier, 2021; Schmidt et al., 2018). ILSS is a critical mechanical property for composites as it is a measure how good the adhesion between the layers of the layup is (Budelmann et al., 2019; João Pedro Martins de Silva Luis, 2014). ILSS performance is mainly researched for the ageing of the prepgs as there is a linear relationship between the two but relating it directly to the tackiness or drapability of the prepg is often overlooked as for each system a new model should be proposed.

This paper investigates the relationship between prepg properties such as drapability and tackiness with mechanical properties of cured composites such as ILSS and void content. Prepgs are manufactured with varying degree of cures using a off-stoichiometric curing agent, TETA, and further cured at an elevated temperature using DICY, a commercial TLC. Rheological, thermomechanical (T_g), drapability and tack properties of the manufactured prepgs are measured. Prepgs are further cured to yield composites and ILSS, void content are measured and optical cross section images of the cured composites are observed. A

relationship between drapability and tackiness is constructed through their relative ratios such as DTR (Drapability to tackiness ratio). A model based on this relationship is constructed and presented. The model can be used to evaluate the ageing performance of prepgs as well as choosing the optimum prepg properties such as OCER formulation, fiber to resin ratio and degree of cure tailored to the type of composite manufacturing.

4.2. Experimental

4.2.1. Materials

Araldite LY 1564 (EEW: 165.2-172.4 g/mol) is purchased from Huntsman. Triethylenetetramine (TETA) (AHEW: 24.3 g/mol, ≥%95) is purchased from Merck Corporation Sigma-Aldrich. DICY (MW: 84 g/mol, AHEW: 21 g/mol) is purchased from Ataman Chemicals. 245 GSM twill 3K fabric with 1000 mm width is acquired from Kordsa. Loctite Frekote 700 NC mold release used as a release agent for the steel tool is purchased from Henkel. Stretchlon HT-350 vacuum bag, AT- 200Y vacuum sealant, Wrightlon 5200 release film, Airweave N10 breather & bleeder, Vac Valve 401C vacuum valve, DVP RC.8D vacuum pump are used from Airtech Europe Sarl and DVP brands.

4.2.2. Resin preparation

Resins are formulated equally regarding their respective amine hydrogen equivalent weight (AHEW). For the resin that contains %10 TETA, the remaining 90% AHEW is calculated for determining the DICY amount. Resin densities are measured to calculate the void content of the cured composites.

Stochiometric ratio of curing agents and epoxy resin, which are listed in **Table 7**, were weighed and mixed via a homogenizer for 10 min. at 1000 rpm for an initial mix of DICY and DGEBA. Prior to mixing, initially DICY was weighed and poured into the cup followed by the inclusion of DGEBA and TETA, respectively. The mixture temperature was recorded

as $40^{\circ}\text{C}\pm2$ after mixing for each of the mixtures. Then, the mixtures are degassed for 5 min. at a vacuum chamber as the lowest and highest vacuum pressure levels were recorded between 10 and 20 mbar.

For epoxy resin formulation, the resin, curing agent and accelerator amounts are shown in **Table 7**.

4.2.3. Prepreg manufacturing

245 GSM twill carbon fabrics were cut to 320x380 mm dimensions for drapability and tackiness measurements and then cut according to the sample dimensions complying the test requirements after composite manufacturing. Mixed and degassed resins were manually applied at room temperature using a plastic scraper for resin distribution as the fabrics were placed onto the silicone paper. Layups are partially cured at 70°C for 30 min. Prepregs were covered with a silicone release paper from top side as well after curing and vacuum bagged to ensure the safe storage of preps at room temperature and kept for at least 24 h prior to any test to ensure they are cooled and kept at lab conditions. The preps were not rolled to prevent resin accumulation and stored flatwise on top of each other. For prepreg manufacturing, the curing parameters are shown in **Table 7**. The resin to fiber ratio of 45:55 is applied for prepreg manufacturing to ensure enough wetting and to observe the effect of drapability property better as it is linked to the resin viscosity.

4.2.4. Composite manufacturing

The preps were cut to 40x300 mm (width x length) size layers and 9 layers were used to yield ILSS and void content composite test samples. The steel tool was cleaned with a cloth wetted with isopropyl alcohol and then Loctite Frekote 700 NC mold release was applied to ensure the easy removal of the cured composite. Prepregs were laid up onto the steel mold and compaction was done manually. After the prepreg lay-up, the manufacturing lay-up was in the following order: perforated release film-breather-vacuum bag. Manufactured twill

carbon prepregs were laid up to achieve a predicted minimum thickness of 2 mm, equal to 9 layers, which is desired for the ILSS test.

4.3. Methods/Characterization

DSC measurements were conducted using a Mettler Toledo DSC 3+ instrument with 10-15 mg sample amounts. For dynamic DSC measurements, the temperature range spanned from 25 to 250 °C, with heating and nitrogen flow rates set at 10 °C/min and 50 mL/min, respectively. Isothermal DSC measurements were performed for 3 h at various temperatures, followed by dynamic DSC tests from 25 to 300 °C at a heating rate of 10 °C/min to measure residual enthalpy. Brookfield viscometer is used for viscosity measurements with a 5-rpm speed, SC4-21 spindle, shear rate of 4650 s⁻¹ and a data collection interval of 5 seconds and test time of 30 min. at room temperature. Optical microscope images were captured using a Nikon Eclipse LV100ND optical microscope equipped with CFI60-2 lenses at a magnification of 100x. Bright-field illumination was applied from beneath the material during imaging. Drapability of the prepregs was measured according to ASTM D 1388 with an in-house made apparatus according to the standard requirements. A total of 32 measurements for 8 samples (4 warp, 4 weft) are done where 4 measurements of a single sample is done in the directions of top, bottom, reverse top and reverse bottom of the sample. Flexural rigidity (μJ/m) is reported as well as taking the inverse of the value is taken as a measure of drapability. Tackiness is measured with an Instron 100 kN UTM which has a 100 N compression fixture. Two 10x10 cm samples are adhered onto each other from top to bottom, representing composite manufacturing. The layup is compressed under 100 N force for 60 seconds and then the measurement started with a speed of 4 mm/min. The maximum debonding force (N) is noted as the tackiness value. The viscosity of the OCER was analyzed using an Anton Paar MCR 302 rheometer at room temperature. Test conditions were selected as a strain rate of 0.1 %, initial gap of 1 mm with a frequency of 1 Hz. Void content is measured according to ASTM D 3171-B standard and ILSS is measured according to ASTM D 2344 standard.

Table 7. Curing agent and TLC ratios

Configuration	Curing agent	TLC	Degree of cure (%)	Curing agent amount (phr)	TLC (phr)	Curing temperature (°C)	Curing duration (h)
C1	TETA	DICY	10	1.43	4.5	70	0.5
C2	TETA	DICY	15	2.14	4.25	70	0.5
C3	TETA	DICY	20	2.86	4	70	0.5
C4	TETA	DICY	25	3.57	3.75	70	0.5

4.4. Results and discussion

4.4.1. Characterization of Prepreg

4.4.1.1. DSC results

Prepregs are manufactured as described in section 4.1.3. Their T_g 's are measured in DSC starting at -60°C up to 100°C . The graph is shown below in **Figure 42**. T_g increase with respect to an increase in degree of cure (DoC) is evident. There is almost a perfect linear relationship between the increasing T_g of the prepregs for each 5 % of DoC increase (**Figure 43**). The values of T_g 's are listed in **Table 8**.

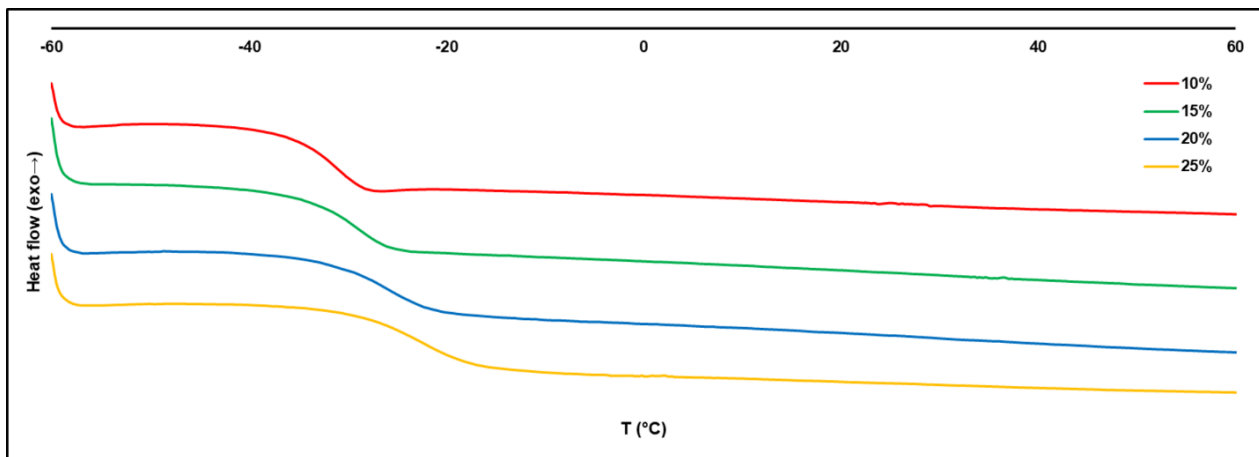


Figure 42. Prepreg T_g for different DoC prepregs

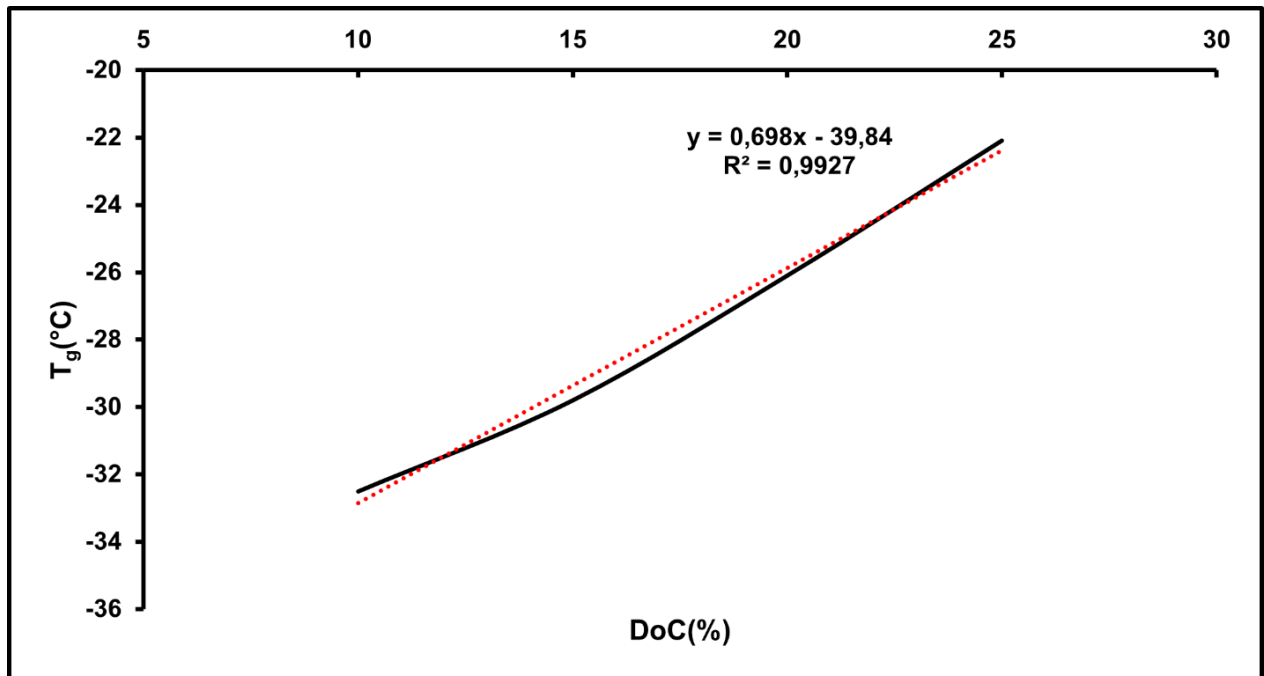


Figure 43. T_g vs degree of cure (DoC)

Table 8. Properties of the B-staged prepreg and mechanical properties of the cured composites

Properties	C1	C2	C3	C4
Viscosity (mPa.s)	6.4	16	31	112
Prepreg T_g ($^{\circ}$ C)	-32.5	-29.8	-26.1	-22.1
Flexural Rigidity (μ J/m)	878.04	875.28	901.26	1252.85
1/FR (Drapability) (m/ μ J)	1,14	1,14	1,11	0,80

Tackiness (N)	74.98	82.27	111.45	90.04
---------------	-------	-------	--------	-------

Table 9. ILSS and void content results

Properties	C1	C2	C3	C4
ILSS (MPa)	62.24	63.44	62.53	57.26
Void Content (%)	-1.21	0.23	0.36	-0.92

4.4.1.2. Rheology results

Room temperature viscosities of the resin mixtures were measured via a rheometer with a 0.1 % of strain rate, 1 mm initial gap and 1 Hz. There is a linear increase until 20 % degree of cure resin but above this ratio, when the degree of cure increases to 25 %, there is a sharp increase in the viscosity, which also resembles the increase in drapability. Thus, to illustrate the similarity in the behavior of viscosity and drapability with respect to degree of cure, both results are shown in the same figure (Figure 44). Especially, beginning with 15 % there is almost an identical behavior of increase in the values. Considering the bleed during composite manufacturing of 10 % cured prepreg, and therefore excluding it, it can be concluded that the viscosity can be linked directly to the drapability for this system. Above a certain viscosity threshold, this relationship seems promising, which corresponds to the viscosities of above 10 % cured prepgs for this study.

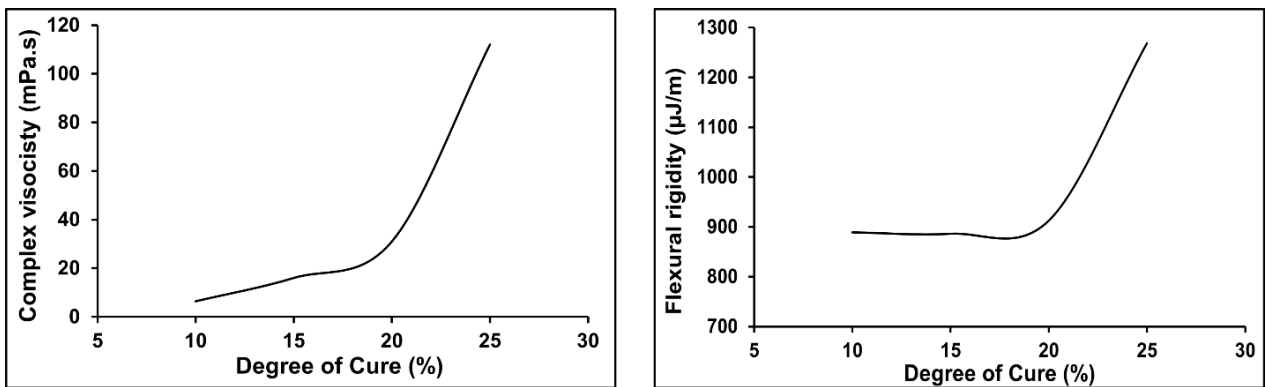


Figure 44. Viscosity of resin mixtures at room temperature and flexural rigidity (inverse drapability) values of preprints

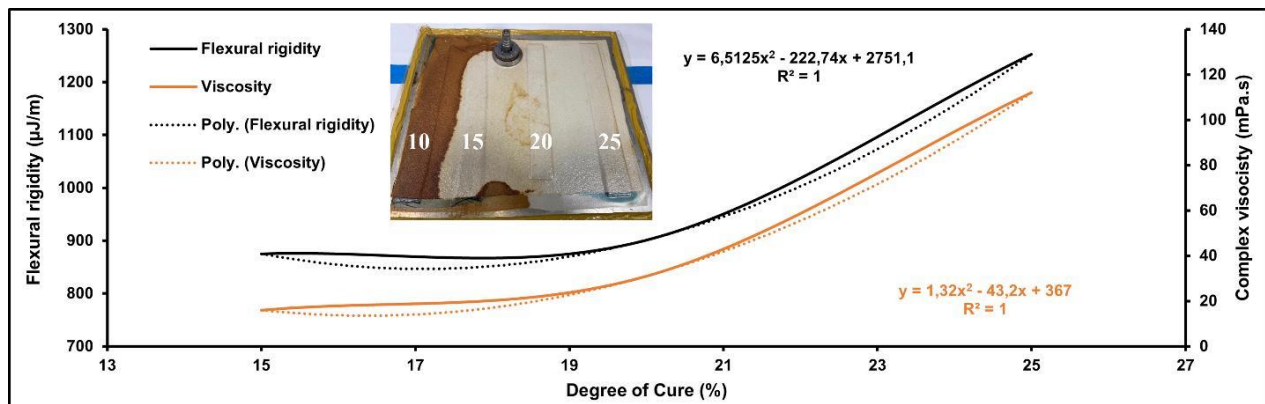


Figure 45. Drapability vs viscosity behavior above 10 % and bleeding of resin for 10 % cured preprint

4.4.1.3. Drapability and tackiness results

Drapability and tackiness values compared to ILSS values with respect to varying degree of cures are displayed in **Figure 46** and **Figure 47** respectively. There is already an established relationship between drapability and tackiness values, when 10 % of cure is excluded again as it occurred for viscosity results. The change in values of drapability and ILSS is not dramatic until 20 % of cure. However, beyond 20 % there is a sudden decrease in both values as seen in **Figure 46**.

The graph **Figure 46** illustrates the relationship between the Degree of Cure (DoC%) and two performance parameters: Interlaminar Shear Strength (ILSS), represented by the blue line on the left y-axis, and Drapability, shown by the orange line on the right y-axis.

Interpretation:

ILSS Trend:

ILSS increases as the Degree of Cure rises, reaching its maximum around 15–17% DoC. Beyond approximately 20% DoC, ILSS drops significantly. This suggests that a moderate level of cure improves interlaminar bonding likely due to better resin flow and interface adhesion, whereas excessive curing introduces brittleness or residual stresses, which weaken shear strength.

Drapability Trend:

Drapability remains stable or improves slightly up to around 17% DoC. However, between 17–20% DoC and beyond, it declines sharply. This indicates that higher cure levels increase material stiffness, making it less capable of conforming to complex geometries. As a result, high DoC reduces formability due to increased rigidity. Overall, both ILSS and drapability exhibit optimal performance at intermediate Degree of Cure levels, approximately between 15–17%. Outside of this range, further increases in DoC have a detrimental impact on both properties.

In summary, a trade-off exists between mechanical strength (ILSS) and processing ease (drapability) as DoC varies. Maintaining DoC within the 15–17% range appears to offer the most favorable compromise between structural performance and manufacturability for the composite system analyzed.

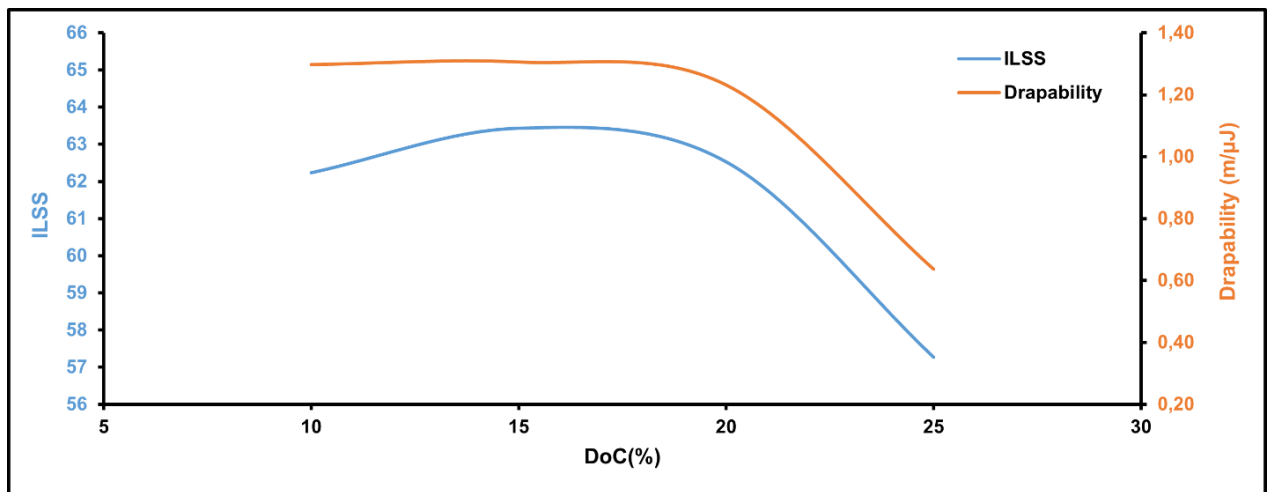


Figure 46. ILSS vs Drapability values for varying DoC (10-15-20-25%)

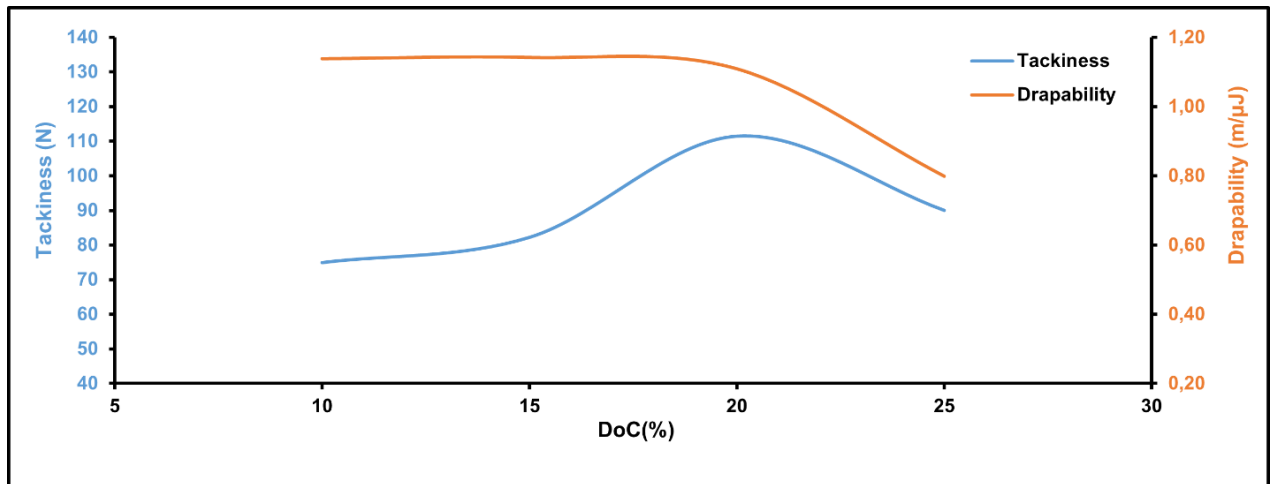


Figure 47. Tackiness vs Drapability values for varying DoC (10-15-20-25%)

Drapability values are reported as m/μJ as they are taken the inverse of the flexural rigidity values per ASTM D 1388 standard. The standard measures the flexural rigidity of the prepgs yielding an energy value as a measure of how difficult bending the fabrics/prepgs where taking the reverse would mean how easy the fabrics are pliable as a measure of their drapability. For ease of calculation and presentation, the values are also multiplied with 1000.

The graph **Figure 47** illustrates the relationship between the Degree of Cure (DoC%) and two key properties: Tackiness (measured in Newtons on the left Y-axis) and Drapability (measured in $\text{m}/\mu\text{J}$ on the right Y-axis). Drapability is determined as the inverse of flexural rigidity (measured according to ASTM D1388) and scaled by a factor of 1000, with higher values indicating greater fabric conformability (i.e., improved drapability). Tackiness increases with DoC, reaching a peak of approximately 110 N around 20% DoC, before declining to about 95 N at 25% DoC. Drapability remains relatively stable between 10–15% DoC, shows a slight increase at 20%, and then drops sharply, falling below 0.9 $\text{m}/\mu\text{J}$ at 25% DoC. The rise in tackiness up to 20% DoC suggests that moderate curing promotes adhesive behavior—likely due to the partial formation of a polymer network that enhances resin cohesion while maintaining surface tack.

When the Degree of Cure exceeds 20% continued crosslinking likely limits surface mobility, leading to a reduction in tackiness. Drapability is highest at low to moderate DoC levels, reflecting the material's greater ease of deformation when less cured. As DoC surpasses 20%, increased crosslink density results in greater stiffness, reducing the material's flexibility and thus its drapability.

In summary, the optimal processing window lies between 15–20% DoC, where both tackiness and drapability remain favorable. Beyond this range, stiffness induced by further curing negatively impacts both adhesion and formability. These findings highlight the critical need to control the Degree of Cure during prepreg storage and forming stages to maintain desirable handling and processing characteristics.

4.4.2. Mechanical testing

4.4.2.1. ILSS Results

Interlaminar shear strength (ILSS) test is conducted per ASTM D 2344 standard and the test results are listed in **Table 10**. For 10, 15 and 20 % of cured preangs, the values are very close to each other, however there is a definite difference between 25 % of cured prepreg with the other three.

Interpretation of ILSS Values in Relation to Degree of Cure (DoC):

Initial Rise (10–15% DoC):

ILSS increases from 62.24 MPa to 63.44 MPa, indicating that partial curing enhances interfacial bonding and matrix cohesion. This improvement is likely due to adequate resin flow for effective fiber wetting and bonding, combined with the onset of polymer network formation. Moreover, the resin bleed that is observed at 10% DoC during curing, could have decreased the ratio of the resin in the interlayer of each ply causing load distribution to be less than compared to 15%.

Moderate Decline (15–20% DoC):

ILSS slightly decreases to 62.53 MPa, remaining relatively high but suggesting that continued curing may begin to introduce internal stresses or limit molecular mobility, subtly impacting mechanical strength.

Significant Drop (25% DoC):

ILSS falls sharply to 57.26 MPa, pointing to a marked reduction in interlaminar strength. This decline is likely caused by increased brittleness from extensive crosslinking, reduced fiber wetting due to premature curing, or the development of microcracks during testing as a result of internal stress buildup.

Table 10. Drapability, tackiness and ILSS results

DoC (%)	Drapeability (μJ/m)	Tackiness (N)	ILSS (MPa)	UPT (mm)	CPT (mm)
10	1,12	74,98	62,24	0,34	1,92
15	1,13	82,27	63,44	0,37	2,46
20	1,10	111,45	62,53	0,44	2,54
25	0,79	90,04	57,26	0,42	2,78

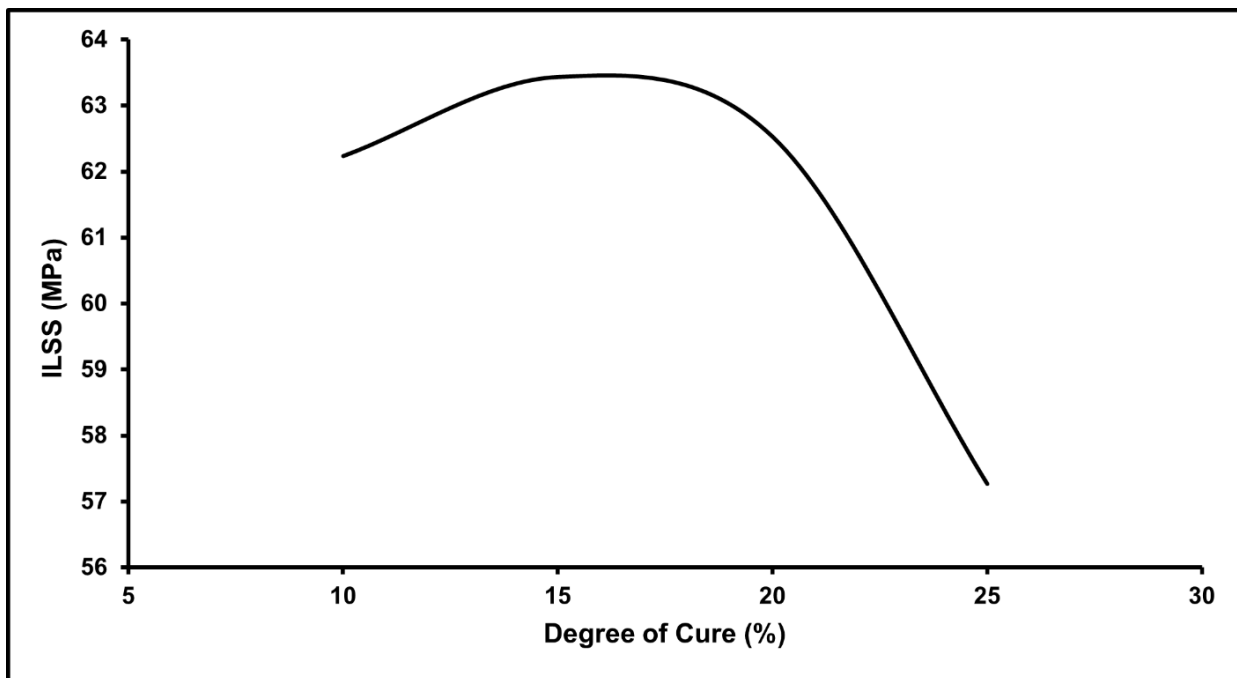


Figure 48. ILSS values with varying DoC

4.5. Conclusions

In this study, a dual-curing epoxy prepreg system stable at ambient conditions was developed using DGEBA-based resin, TETA as a low-temperature reactive curing agent, and DICY as a thermal latent curing agent. By systematically varying the degree of cure, key prepreg characteristics namely viscosity, drapability, and tackiness—were tuned, revealing strong

interdependencies among these parameters. The developed prepgs demonstrated stable handling properties, with tack and drape behaviors aligning closely with the rheological characteristics of the system.

Notably, the study introduced and validated a practical approach for quantifying prepreg drapability using ASTM D1388-based testing and established a strong correlation between drapability, and composite performance, specifically with interlaminar shear strength (ILSS). A critical threshold for viscosity and drapability was identified, beyond which composite quality, especially ILSS, declined—highlighting the importance of controlling early-stage resin behavior. Overall, the findings contribute a comprehensive structure–property–performance relationship model for dual-cure epoxy prepgs, enabling optimization of processability without compromising final composite integrity. This approach has potential for guiding the formulation of advanced prepreg systems for high-performance composite applications in aerospace, automotive, and related sectors.

CHAPTER 5

5. Mechanical properties of epoxy composites cured with dicyandiamide and polyphenyloxazolineimidazole as an accelerator for dicyandiamide

5.1. Introduction

Epoxy resins are thermoset materials known for their excellent chemical resistance, mechanical strength, thermal stability, and versatility in applications such as coatings, adhesives, composites, and electronic encapsulants (Atespare et al., 2024, 2025; Salamatgharamaleki et al., 2025; Ucar & Dizman, 2024; Uçar & Dizman, 2025). Curing of epoxy resins typically involves various type of curing agents, namely: amines, acid anhydrides, imidazoles, etc. that initiate either step-growth or chain-growth polymerization. Among these, imidazoles are notable for their efficiency in catalyzing chain-growth curing even in small amounts. However, their high reactivity at room temperature limits their use in one-component epoxy resins (OCERs) due to poor shelf stability.

To address the drawbacks of conventional two-component systems such as storage instability, short pot life, and energy inefficiency, OCERs employing thermal latent curing agents (TLCs) have been developed. TLCs are designed to remain inactive at ambient temperatures but initiate curing at elevated temperatures, improving shelf life and processing

control. TLCs operate primarily via two strategies: (1) the use of crystalline agents that melt and activate at high temperatures (e.g., DICY), and (2) the encapsulation or conjugation of curing agents with small molecules or polymers.

Recent research has turned to poly(2-oxazoline)s (POZs) a class of polymers that can be precisely synthesized via cationic ring-opening polymerization (Atespare et al., 2024, 2025; Kohlan et al., 2022; Salamatgharamaleki et al., 2025; Viegas et al., 2011). POZs are notable for their structural versatility, amphiphilic nature, tunable thermal properties, and functional side-chain variability. These properties make them highly promising for tailoring curing behavior and compatibility with various epoxy systems.

In particular, homopolymer POZs have been explored as novel polymer matrices for encapsulating imidazoles in TLC formulations. Homopolymer POZs allow for fine tuning of polarity, adjustable thermal behavior (e.g., melting point, T_g), and miscibility with epoxy resins by altering monomer composition and side chains. This approach enhances latency (preventing premature curing), improves storage stability, and enables controlled activation at desired curing temperatures, positioning homopolymer POZs as a next-generation platform for efficient and customizable thermal latent curing systems in advanced epoxy formulations. Out of the POZ polymers synthesized by the other research group members (**Figure 49**), the most optimum latent cure performing PPhOZ-IM was selected for further studies.

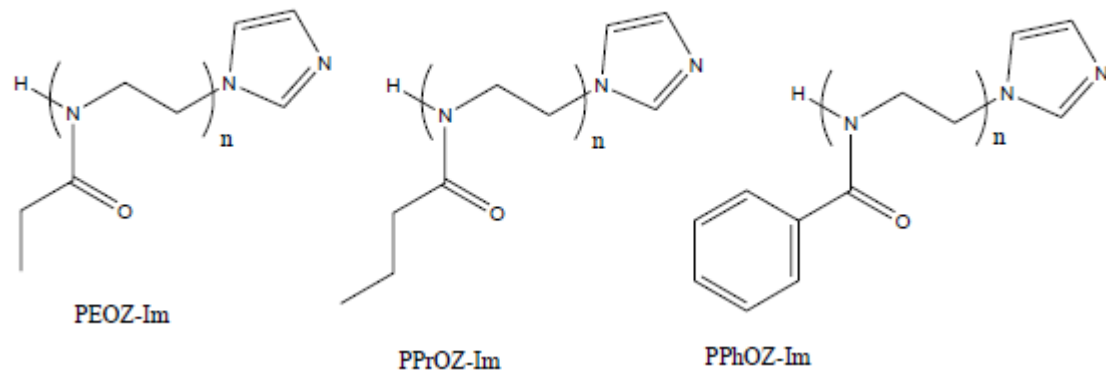


Figure 49. Thermal latent curing POZ based polymers with imidazole group covalently attached



Figure 50. Stages of hand lay-up and vacuum bagging during composite manufacturing

5.2. Composite Manufacturing

DGEBA epoxy resin was heated to 80°C and then allowed to cool to room temperature to melt the crystals and liquify the resin. DICY and DGEBA were weighed in a 1:2 molar stoichiometric ratio and mixed in a homogenizer at 1500 rpm for 10 min. Twill carbon fabric was cut to 380x320 mm to obtain test samples for tensile, compression, DMA, and void content testing. The fabrics used were 2x2 3K twill type with a weight of 245 GSM. The steel lay-up mold was cleaned with a cloth soaked in isopropyl alcohol, and then Loctite Frekote 700 NC mold release agent was applied three times at different angles to ensure easy removal of the cured composite. The fabrics were laid onto the steel mold and wetted with epoxy resin mixtures at a fabric/resin ratio of 55:45. Resin on each layer was applied and compacted using a plastic scraper. After composite lay-up, the manufacturing sequence proceeded as follows: Steel mold - Fabric+resin layup - Peel ply - Perforated release film - Breather fabric - Vacuum bag (**Figure 50**). The vacuum level measured during composite production was approximately 40 mbar. The curing cycle was conducted in a fan-assisted oven at 140°C for 3 h for epoxy with PPhOZ-Im, and 180°C for epoxy with DICY. Both samples were kept under vacuum at 80°C for 1 h prior to curing to allow the resin to impregnate the fabric.

Mixtures containing PPhOZ-Im cured at temperatures 40°C lower than those with only DICY. Therefore, in addition to improved mechanical properties, the use of oxazoline polymers is advantageous over traditional curing agents due to benefits like energy efficiency and prevention of exothermic reactions.

5.3. Mechanical Test Results

Mechanical tests were performed using a 100 kN static UTM machine with a servohydraulic motor and measured using biaxial extensometers. Test standards and specimen dimensions are given in **Table 11**.

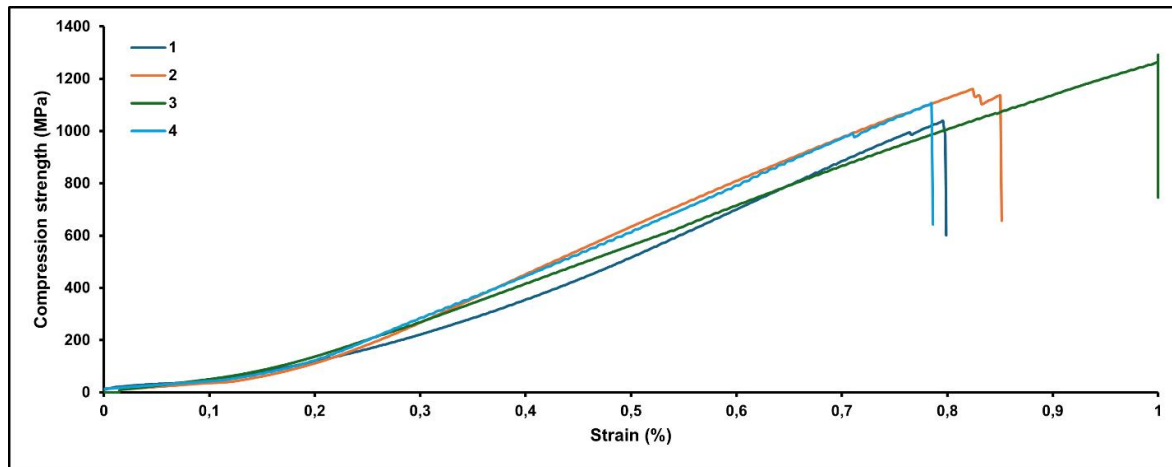


Figure 51. DICY + Epoxy compressive strength

The compressive strength results of DICY cured DGEBA is displayed in **Figure 51**. The results and the pictures taken after the test indicate that a brittle fracture (**Figure 55**) occurs with a 114.93 MPa strength and a strain of 0.86 %. The DICY is used 1:2 molar ratio with DGEBA thus when cured at 180°C it forms a complete network. This might have caused the chains in the network to be shorter compared to DGEBA chains which homopolymerize through tertiary amine accelerators such as imidazole.

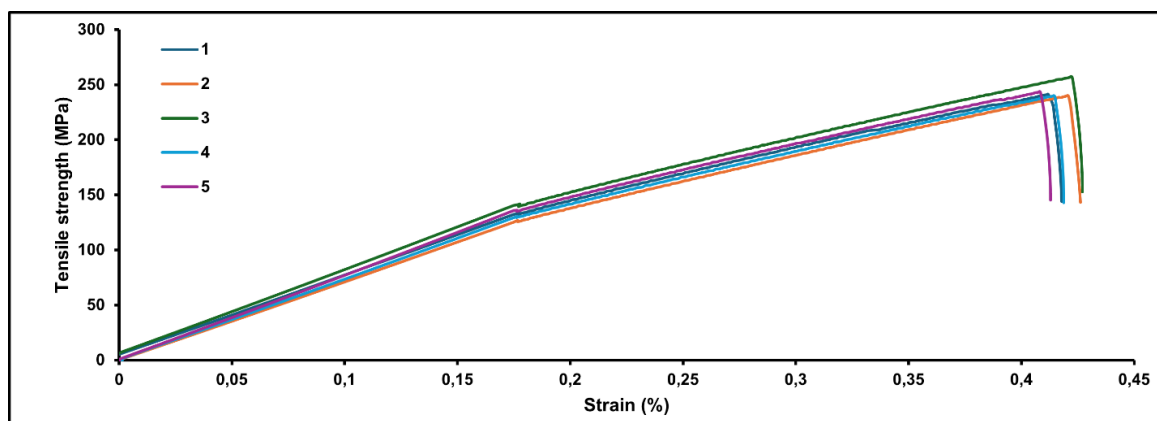


Figure 52. DICY + Epoxy tensile strength

The tensile strength results of DICY cured DGEBA is displayed in **Figure 52**. Tensile strength is measured as 244.12 and the strain is 0.83 %. The brittle fracture is observed once again, as in compressive strength, (**Figure 56**) in the tensile strength measurements.

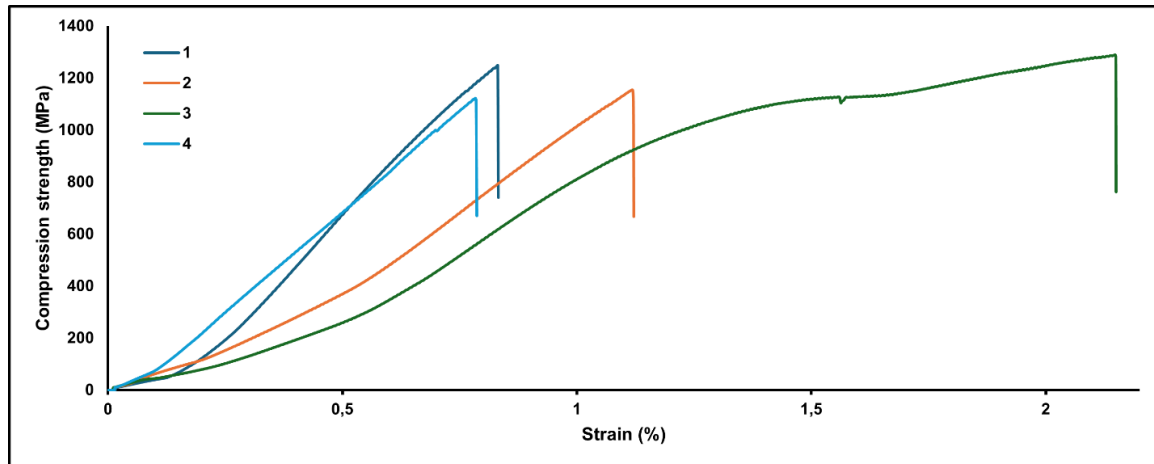


Figure 53. DICY+Epoxy+PPhOZ-Im compressive strength

The compressive strength results of DICY+PPhOZ-IM cured DGEBA is displayed in **Figure 53**. Compressive strength is measured as 120.39 and the strain is 1.22 %. Compressive strength of DICY+PPhOZ-IM system cured DGEBA has shown an increase of 4.75 % compared to DICY cured DGEBA. The compressive strength is fiber dominant and thus the average increase of 4.75 % of compressive strength is noticeable.

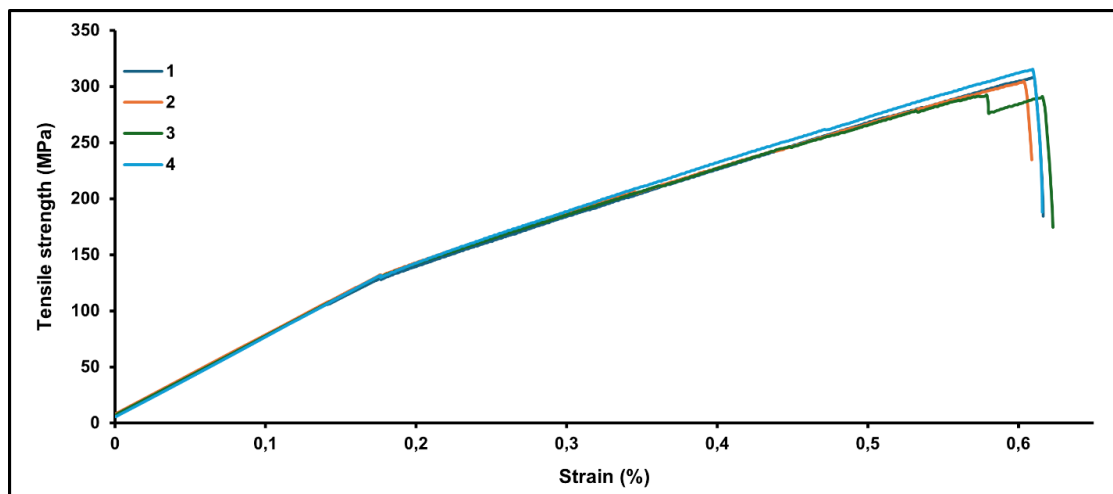


Figure 54. DICY+Epoxy+PPhOZ-Im tensile strength

The tensile strength results of DICY+PPhOZ-IM cured DGEBA is displayed in **Figure 54**. Tensile strength is measured as 320.68 and the strain is 1.20 %. Compressive strength of DICY+PPhOZ-IM system cured DGEBA has shown an increase of 31.3 % compared to DICY cured DGEBA. Thus, a major improvement is recorded and this might be explained through the homopolymerization contribution of imidazole accelerated cure.

Table 11. Tensile and compression test standards and dimensions

Test	Standard	Length (mm)	Width (mm)	Thickness (mm)
Tensile	ASTM D 3039	250	25	2-2,5
Compression	ASTM D 3410	145	25	2-2,5

Table 12. Compression modulus and strength results of DICY+Epoxy and DICY+Phenyl oxazoline-imidazole+Epoxy

Composite	Tensile modulus (GPa)	Tensile strength (MPa)	Tensile strain (%)	Compressive strength (MPa)	Compression strain (%)
DICY + Epoxy	37.27	244.12	0.83	114.93	0.86
Standard deviation	1.10	6.51	0.01	10.72	0.11
DICY + Epoxy + PPhOZ-Im	35.34	320.68	1.20	120.39	1.22

Standard deviation	0.40	8.29	0.02	7.83	0.63
---------------------------	------	------	------	------	------

When comparing compressive strengths, the epoxy cured with DICY has a compressive strength of 114.93 MPa, while in the PPhOZ-Im and DICY systems, this value increased to 120.39 MPa. The elongation values mentioned refer to the amount of movement in the Z-direction during the compression test. The compressive strength of the PPhOZ-Im and DICY samples increased by 4.75% compared to the DICY-only samples. Fractures occurred during compression in the DICY-only samples (**Figure 55**). This can be explained by the higher crosslinking density in DICY-cured epoxies, which makes them more brittle. In systems cured with PPhOZ-Im, homopolymerization is promoted, leading to the formation of longer chains that crosslink with each other. In systems like DICY-only, which rely solely on amine-epoxy reactions, shorter chain monomers crosslink with amines, resulting in higher crosslinking density. Similarly, the lower tensile strength of DICY-only samples compared to PPhOZ-Im and DICY systems can also be explained by their increased brittleness.

When comparing tensile strengths, the epoxy cured with DICY has a tensile strength of 244.12 MPa, while this value increases to 320.68 MPa in the systems containing PPhOZ-Im and DICY. In the epoxy cured with both PPhOZ-Im and DICY, a 31.3% increase in tensile strength was observed compared to the epoxy cured with only DICY. Additionally, the elongation at break increased by 44.5%. Regarding the elastic modulus values, the modulus of the samples with PPhOZ-Im and DICY decreased by only 5.1% compared to those with only DICY. This can be explained by the increased elongation in the epoxy samples cured with PPhOZ-Im and DICY. Moreover, with the increase in both tensile strength and elongation, it can be stated that the toughness of the PPhOZ-Im and DICY samples also improved. Therefore, in addition to accelerating the reaction and lowering the curing temperature, PPhOZ-Im also acts as a toughening agent in epoxy resins cured with DICY. In the tensile test results, delamination was observed in both types of samples, but improved interlayer bonding was especially noted in the systems containing PPhOZ-Im.

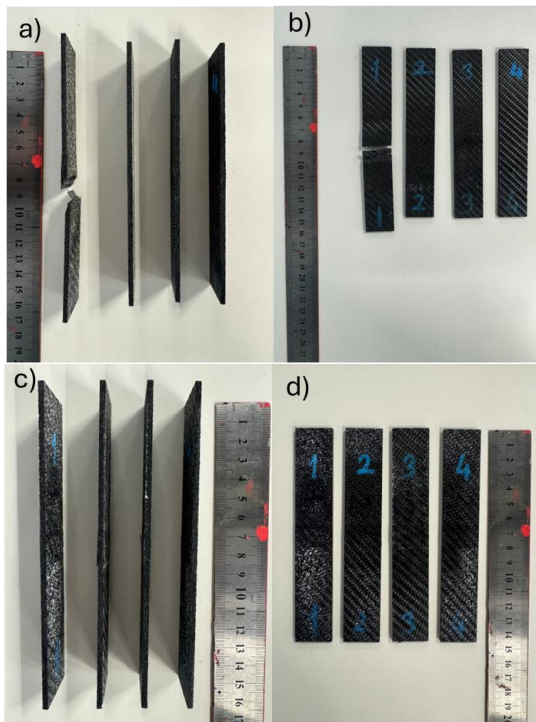


Figure 55. Compression Test Specimens of the Produced Composites **a&b)** DICY + DGEBA, **c&d)** PPhOZ-Im+DICY+DGEBA

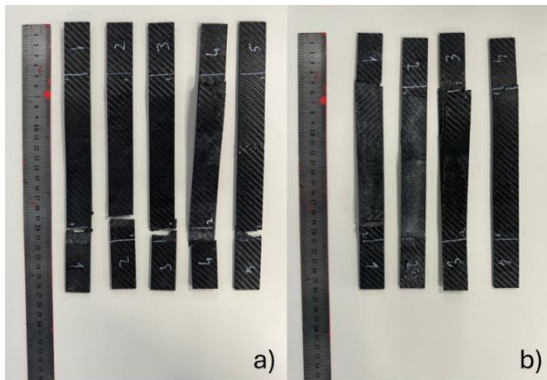


Figure 56. Tensile Test Specimens of the Produced Composites **a)** DICY+DGEBA, **b)** PPhOZ-Im+DICY+DGEBA

5.4. Conclusions

The incorporation of PPhOZ-Im into the epoxy curing system alongside DICY significantly enhances the mechanical performance of the resulting composites. Notably, a substantial

increase in tensile strength and elongation at break was achieved, indicating improved toughness. Although a slight reduction in elastic modulus was observed, this trade-off is offset by the material's enhanced ductility and resilience. In compression tests, PPhOZ-Im also contributed to modest strength gains and reduced brittleness, attributed to differences in polymer network structure and crosslinking behavior. Overall, PPhOZ-Im not only accelerates curing and reduces curing temperatures but also acts as an effective toughening agent, making it a promising additive for high-performance epoxy-based composites.

CHAPTER 6

6. CONCLUSIONS

This Ph.D. study presents the design, synthesis, and evaluation of novel thermal latent curing agents (TLCs) for developing one-component epoxy resin (OCER) systems, aimed at enhancing the stability and processability of carbon fiber-reinforced preangs. Through a systematic experimental approach, several small- and polymer-based TLCs including PUPI, PTSU-EDA, and PPhOZ-IM were successfully synthesized and characterized.

The key findings for each used systems are as below:

PUPI demonstrated stability up to three days at room temperature and showed acceleration of DICY-based curing, as it reduced the required curing temperatures for DICY noticeably. Thus, for improvement of stability urea based PTSU-EDA was considered to be a good alternative to continue for further studies.

PTSU-EDA provided improved thermal stability, increasing the reaction temperature more than 100°C, but yielded composites with relatively lower crosslink densities, indicating further optimization potential. Moreover, the reversibility due to the dynamic nature of urea bond was noticed which can be considered for recyclable thermoset applications. The low degree of cross-linking directed us to the use of imidazole based accelerators which promote homopolymerization where they yield better mechanical properties.

PPhOZ-IM significantly improved the mechanical properties of epoxy composites, particularly tensile and compressive strength, making it a promising accelerator for DICY. However, it still needs stabilization through use of molecules such as boric acid, which paved the way for further studies.

The study further emphasized the role of prepreg characteristics, particularly drapability and tackiness on the interlaminar shear strength (ILSS) of final composites. TETA and DICY were used as curing agent for prepreg manufacturing and as a TLC to cure completely at elevated temperatures. TETA was used at off-stoichiometric ratios to obtain different degree of cures for prepgs with different tack and drape properties. Notably, drapability, which inversely correlates with resin viscosity, showed a stronger influence on ILSS than tackiness, with varying degree of cured prepgs, establishing a meaningful processing-structure-property relationship.

In summary, this work contributes significantly to the field of latent curing systems and prepreg design by offering new insights into the synthesis-structure-property relationships of TLCs and their impact on the manufacturability and performance of composite materials. These findings pave the way for more cost-effective, ambient-stable prepreg solutions with tunable mechanical and processing properties for advanced structural applications.

6.1. FUTURE WORK

The following works can be investigated and developed further using the data and knowledge generated in this thesis:

- Imidazole systems can be stabilized with electrophiles such as boric acid or boronic acid
- Curing and mechanical properties of p-toluene sulphonyl urea cured epoxy can be enhanced with longer and branched amines (e.g. DETA, TETA, PEI)

- Upon stabilization polyphenyloxazoline imidazole can be a promising TLC for prepreg manufacturing due to its excellent curing properties and improvement in mechanical properties
- Drapability's relation with viscosity and ILSS need to be tested for different systems as it can be a very practical method to predict cured composite's ILSS value

Combining all these works, TLCs can be utilized to manufacture ambient temperature stable prepgs and these prepgs can be fine-tuned to match the requirements of manufacturing applications such as vacuum bag only (VBO) processes.

7. REFERENCES

Advani, S., Sozer, E., & Mishnaevsky Jr, L. (2003). Process Modeling in Composite Manufacturing. *Applied Mechanics Reviews - APPL MECH REV*, 56. <https://doi.org/10.1115/1.1584418>

Ahn, K. J., & Seferis, J. C. (1993). Prepreg process analysis. *Polymer Composites*, 14(4), 349–360. <https://doi.org/https://doi.org/10.1002/pc.750140411>

Amare, C., Mantaux, O., Gillet, A., Pedros, M., & Lacoste, E. (2022). Innovative test methodology for shelf life extension of carbon fibre prepgs. *IOP Conference Series: Materials Science and Engineering*, 1226(1), 12101. <https://doi.org/10.1088/1757-899X/1226/1/012101>

Aoki, D., Dogoshi, S., Ito, Y., & Arimitsu, K. (2024). Thermal curing of epoxy resins at lower temperature using 4-(methylamino)pyridine derivatives as novel thermal latent curing agents. *Journal of Polymer Science*, 62(19), 4406–4415. <https://doi.org/https://doi.org/10.1002/pol.20240379>

Atespare, A. E., Behroozi Kohlan, T., Salamatgharamaleki, S., Yildiz, M., Menceloglu, Y. Z., Unal, S., & Dizman, B. (2024). Poly(2-alkyl/aryl-2-oxazoline)-Imidazole Complexes as Thermal Latent Curing Agents for Epoxy Resins. *ACS Omega*, 9(34), 36398–36410. <https://doi.org/10.1021/acsomega.4c03904>

Atespare, A. E., Kohlan, T. B., Salamatgharamaleki, S., Yildiz, M., Menceloglu, Y. Z., Unal, S., & Dizman, B. (2025). Structure–property relationship and epoxy resin compatibility of poly(2-alkyl/aryl-2-oxazoline)s, alongside rheological properties of their blends. *Polymer Engineering & Science*, 65(6), 3193–3208. <https://doi.org/https://doi.org/10.1002/pen.27208>

Attaei, M., Vale, M., Shakoor, A., Kahraman, R., Montemor, M. F., & Marques, A. C. (2020). Hybrid shell microcapsules containing isophorone diisocyanate with high thermal and chemical stability for autonomous self-healing of epoxy coatings. *Journal of Applied Polymer Science*, 137(22), 48751. <https://doi.org/https://doi.org/10.1002/app.48751>

Banks, R., Mouritz, A. P., John, S., Coman, F., & Paton, R. (2004a). Development of a new structural prepreg: characterisation of handling, drape and tack properties. *Composite Structures*, 66(1–4), 169–174. <https://doi.org/10.1016/J.COMPSTRUCT.2004.04.034>

Banks, R., Mouritz, A. P., John, S., Coman, F., & Paton, R. (2004b). Development of a new structural prepreg: characterisation of handling, drape and tack properties. *Composite Structures*, 66(1–4), 169–174. <https://doi.org/10.1016/J.COMPSTRUCT.2004.04.034>

Bashir, M. A. (2023). Cure Kinetics of Commercial Epoxy-Amine Products with Iso-Conversional Methods. *Coatings*, 13(3). <https://doi.org/10.3390/coatings13030592>

Battig, A., Markwart, J. C., Wurm, F. R., & Schartel, B. (2020). Sulfur's role in the flame retardancy of thio-ether-linked hyperbranched polyphosphoesters in epoxy resins. *European Polymer Journal*, 122, 109390. <https://doi.org/https://doi.org/10.1016/j.eurpolymj.2019.109390>

Behroozi Kohlan, T., Atespare, A. E., Yildiz, M., Menceloglu, Y. Z., Unal, S., & Dizman, B. (2023). Amphiphilic Polyoxazoline Copolymer-Imidazole Complexes as Tailorable Thermal Latent Curing Agents for One-Component Epoxy Resins. *ACS Omega*, 8(49), 47173–47186. <https://doi.org/10.1021/acsomega.3c07177>

Belhaj, M., Dodangeh, A., & Hojjati, M. (2021). Experimental investigation of prepreg tackiness in automated fiber placement. *Composite Structures*, 262, 113602. <https://api.semanticscholar.org/CorpusID:234153278>

Bernath, A., Kärger, L., & Henning, F. (2016). Accurate Cure Modeling for Isothermal Processing of Fast Curing Epoxy Resins. *Polymers*, 8, 390. <https://doi.org/10.3390/polym8110390>

Budelmann, D., Detampel, H., Schmidt, C., & Meiners, D. (2019). Interaction of process parameters and material properties with regard to prepreg tack in automated lay-up and draping processes. *Composites Part A: Applied Science and Manufacturing*, 117, 308–316. <https://doi.org/https://doi.org/10.1016/j.compositesa.2018.12.001>

Budelmann, D., Schmidt, C., & Meiners, D. (2020). Prepreg tack: A review of mechanisms, measurement, and manufacturing implication. *Polymer Composites*, 41, 3440–3458. <https://doi.org/10.1002/pc.25642>

Budelmann, D., Schmidt, C., & Meiners, D. (2022). Tack of epoxy resin films for aerospace-grade prepgres: Influence of resin formulation, B-staging and toughening. *Polymer Testing*, 114, 107709. <https://doi.org/https://doi.org/10.1016/j.polymertesting.2022.107709>

Cem Özturk. (2019). *Whitespot, Waterspot and Visually Fault-Free Prepreg for Composite Materials*.

Chen, J., Chu, N., Zhao, M., Jin, F.-L., & Park, S.-J. (2020). Synthesis and application of thermal latent initiators of epoxy resins: A review. *Journal of Applied Polymer Science*, 137(48), 49592. <https://doi.org/https://doi.org/10.1002/app.49592>

Chen, K.-L., Shen, Y.-H., Yeh, M.-Y., & Wong, F. F. (2012). Complexes of imidazole with poly(ethylene glycol)s as the thermal latency catalysts for epoxy-phenolic resins. *Journal of the Taiwan Institute of Chemical Engineers*, 43(2), 306–312. <https://doi.org/https://doi.org/10.1016/j.jtice.2011.08.007>

Chian, K. S., & Yi, S. (2001). Synthesis and characterization of an isocyanurate-oxazolidone polymer: Effect of stoichiometry. *Journal of Applied Polymer Science*, 82(4), 879–888. <https://doi.org/https://doi.org/10.1002/app.1919>

Choe, Y., & Kim, W. (2002). Cure reactions of epoxy/anhydride/(polyamide copolymer) blends. *Macromolecular Research*, 10(5), 259–265. <https://doi.org/10.1007/BF03218315>

Cole, K. C., Noël, D., Hechler, J.-J., Chouliotis, A., & Overbury, K. C. (1989). Room temperature aging of Narmco 5208 carbon-epoxy prepreg. Part I: Physicochemical characterization. *Polymer Composites*, 10(3), 150–161. <https://doi.org/https://doi.org/10.1002/pc.750100303>

CRIPPS, D., SEARLE, T. J., & SUMMERSCALES, J. (2000). Open Mold Techniques for Thermoset Composites. *Comprehensive Composite Materials*, 737–761. <https://doi.org/10.1016/B0-08-042993-9/00188-1>

Dalle Vacche, S., Michaud, V., Demierre, M., Bourban, P.-E., & Månson, J.-A. (2016). Curing kinetics and thermomechanical properties of latent epoxy/carbon fiber composites. *IOP Conference Series: Materials Science and Engineering*, 139, 012049. <https://doi.org/10.1088/1757-899X/139/1/012049>

Dareh, M., Beheshty, M. H., & Bazgir, S. (2020). Effect of Type and Amount of Accelerator on Reactivity and Curing Behavior of Epoxy/Dicyandiamide/Accelerator System. *Iranian Journal of Polymer Science and Technology*, 33(4), 329–338. <https://doi.org/10.22063/jipst.2020.1751>

Deng, K., Zhang, C., Dong, X., & Fu, K. K. (2022). Rapid and energy-efficient manufacturing of thermoset prepreg via localized in-plane thermal assist (LITA) technique. *Composites Part A: Applied Science and Manufacturing*, 161, 107121. <https://doi.org/10.1016/J.COMPOSITESA.2022.107121>

Dubois, O., & Beakou, A. (2009). Experimental Analysis of Prepreg Tack. *Experimental Mechanics*, 50, 599–606. <https://doi.org/10.1007/s11340-009-9236-7>

Dušek, K. (1986). Network formation in curing of epoxy resins. In K. Dušek (Ed.), *Epoxy Resins and Composites III* (pp. 1–59). Springer Berlin Heidelberg.

Dušek, K., Ilavský, M., & Luňák, S. (1975). Curing of epoxy resins. I. Statistics of curing of diepoxides with diamines. *Journal of Polymer Science: Polymer Symposia*, 53(1), 29–44. <https://doi.org/https://doi.org/10.1002/polc.5070530107>

Dworak, A., Trzebicka, B., Kowalcuk, A., Tsvetanov, Ch., & Rangelov, S. (2014). Polyoxazolines — mechanism of synthesis and solution properties. *Polimery*, 59(1), 88–94. <https://doi.org/10.14314/polimery.2014.088>

Edith A. Turi. (1981). *Thermal Characterization of Polymeric Materials*. Academic Press.

Fang, Y., Ma, B., Wei, K., Wang, X., Kang, X., & Liu, F. (2021). Performance of single-component epoxy resin for crack repair of asphalt pavement. *Construction and Building Materials*, 304, 124625. <https://doi.org/https://doi.org/10.1016/j.conbuildmat.2021.124625>

Gay, C., & Leibler, L. (1999). Theory of Tackiness. *Physical Review Letters*, 82(5), 936–939. <https://doi.org/10.1103/PhysRevLett.82.936>

Gilbert, M. D. (1988). *Mechanism and kinetics of the dicyandiamide cure of epoxy resins*. <https://api.semanticscholar.org/CorpusID:135935474>

Gilbert, M. D., Schneider, N. S., & MacKnight, W. J. (1991). Mechanism of the dicyandiamide/epoxide reaction. *Macromolecules*, 24(2), 360–369. <https://doi.org/10.1021/ma00002a004>

Gotro, J. (2022, September 12). *Epoxy Curing Agents – Latent Curing Agents for One Component Systems*. <Https://Polymerinnovationblog.Com/Epoxy-Curing-Agents-Latent-Curing-Agents-for-One-Component-Systems/>.

Grunenfelder, L. K., Dills, A., Centea, T., & Nutt, S. (2017). Effect of prepreg format on defect control in out-of-autoclave processing. *Composites Part A: Applied Science and Manufacturing*, 93, 88–99. <https://doi.org/10.1016/J.COMPOSITESA.2016.10.027>

Ham, Y., Kim, S., Shin, Y., Lee, D., Yang, M., Min, J., & Shin, J. (2010). A comparison of some imidazoles in the curing of epoxy resin. *Journal of Industrial and Engineering Chemistry - IND ENG CHEM*, 16, 556–559. <https://doi.org/10.1016/j.jiec.2010.03.022>

Han, M. G., & Chang, S. H. (2021). Draping simulations of carbon/epoxy fabric prepgs using a non-orthogonal constitutive model considering bending behavior. *Composites Part A: Applied Science and Manufacturing*, 148, 106483. <https://doi.org/10.1016/J.COMPOSITESA.2021.106483>

Hassan, M. H. (2021). A mini review on manufacturing defects and performance assessments of complex shape prepreg-based composites. *The International Journal of Advanced Manufacturing Technology*, 115(11), 3393–3408. <https://doi.org/10.1007/s00170-021-07421-8>

Heise, M. S., & Martin, G. C. (1989). Curing mechanism and thermal properties of epoxy-imidazole systems. *Macromolecules*, 22(1), 99–104. <https://doi.org/10.1021/ma00191a020>

Hesabi, M., Salimi, A., & Beheshty, M. H. (2019). Development of amine-based latent accelerator for one-pot epoxy system with low curing temperature and high shelf life. *European Polymer Journal*, 112, 736–748. <https://doi.org/https://doi.org/10.1016/j.eurpolymj.2018.10.044>

Holbery, J., & Bordia, R. (2001). Accelerated cure of thermoset fiber composites utilizing latent cure agents. *Journal of Materials Science*, 36, 5301–5308. <https://doi.org/10.1023/A:1012474702397>

Huang, J., Fu, P., Li, W., Xiao, L., Chen, J., & Nie, X. (2022). Influence of crosslinking density on the mechanical and thermal properties of plant oil-based epoxy resin. *RSC Advances*, 12(36), 23048–23056. <https://doi.org/10.1039/D2RA04206A>

Huang, J., & Nie, X. (2016). A simple and novel method to design flexible and transparent epoxy resin with tunable mechanical properties. *Polymer International*, 65(7), 835–840. <https://doi.org/https://doi.org/10.1002/pi.5144>

Huang, K., Zhang, P., Zhang, J., Li, S., Li, M., Xia, J., & Zhou, Y. (2013). Preparation of biobased epoxies using tung oil fatty acid-derived C21 diacid and C22 triacid and study of epoxy properties. *Green Chemistry*, 15(9), 2466–2475. <https://doi.org/10.1039/C3GC40622A>

Hübner, F., Meuchelböck, J., Wolff-Fabris, F., Mühlbach, M., Altstädt, V., & Ruckdäschel, H. (2021). Fast curing unidirectional carbon epoxy prepgs based on a semi-latent hardener: The influence of ambient aging on the prepgs Tg0, processing behavior and thus derived interlaminar performance of the composite. *Composites Science and Technology*, 216, 109047. <https://doi.org/https://doi.org/10.1016/j.compscitech.2021.109047>

Ignatenko, V., Ilyin, S., Kostyuk, A., Bondarenko, G., & Antonov, S. (2020). Acceleration of epoxy resin curing by using a combination of aliphatic and aromatic amines. *Polymer Bulletin*, 77. <https://doi.org/10.1007/s00289-019-02815-x>

Jee, S. M., Ahn, C.-H., Park, J. H., Kim, T. A., & Park, M. (2020). Solvent-free encapsulation of curing agents for high performing one-component epoxy adhesives. *Composites Part B: Engineering*, 202, 108438. <https://doi.org/https://doi.org/10.1016/j.compositesb.2020.108438>

Jin, F.-L., Li, X., & Park, S.-J. (2015). Synthesis and application of epoxy resins: A review. *Journal of Industrial and Engineering Chemistry*, 29, 1–11. <https://doi.org/https://doi.org/10.1016/j.jiec.2015.03.026>

João Pedro Martins de Silva Luis. (2014). *Effect of out-time aging in composite prepg material*. Técnico Lisboa.

Joesbury, A. M., Endruweit, A., Budelmann, D., Giannis, S. P., De Focatiis, D. S. A., Call, D. B., Chan, C., Choong, G. Y. H., Clark, R. A., Collins, J. A., Fishpool, D. T., Garber, J. M., Ghose, S., Golding, J., Good, S. T., Jones, B. R., Meiners, D., Niitsoo, O., Palmer, C. T., ... Yuan, H. (2025). Repeatability and reproducibility of the measurement of prepg tack following ASTM D8336: Results of a round-robin study. *Composites Part A: Applied Science and Manufacturing*, 188, 108561. <https://doi.org/https://doi.org/10.1016/j.compositesa.2024.108561>

Jones, R. W., Ng, Y., & McClelland, J. F. (2008). Monitoring ambient-temperature aging of a carbon-fiber/epoxy composite prepg with photoacoustic spectroscopy. *Composites Part*

A: *Applied Science and Manufacturing*, 39(6), 965–971.
<https://doi.org/https://doi.org/10.1016/j.compositesa.2008.03.015>

Kadurina, T. I., Prokopenko, V. A., & Omelchenko, S. I. (1992). Curing of epoxy oligomers by isocyanates. *Polymer*, 33(18), 3858–3864.
[https://doi.org/https://doi.org/10.1016/0032-3861\(92\)90373-5](https://doi.org/https://doi.org/10.1016/0032-3861(92)90373-5)

Khamidullin, O. L., Andrianova, K. A., Nikitin, V. S., & Amirova, L. M. (2025). The process of curing epoxy–amine resins with a composition gradient in thick-walled cylindrical products. *Journal of Materials Science*, 60(11), 5267–5279. <https://doi.org/10.1007/s10853-025-10748-2>

Kheradpisheh, Meisam, Yas, Amir Hafez, & Hojjati, Mehdi. (2025). The effect of automated fiber placement process parameters on interlaminar shear strength of uncured prepreg bonded samples. *Journal of Composite Materials*, 59(12), 1477–1491.
<https://doi.org/10.1177/00219983241313280>

Kim, Y. J., Choi, S. H., Lee, S. J., & Jang, K.-S. (2021). Latent Curing, Chemorheological, Kinetic, and Thermal Behaviors of Epoxy Resin Matrix for Prepregs. *Industrial & Engineering Chemistry Research*, 60(17), 6153–6161. <https://doi.org/10.1021/acs.iecr.1c00576>

Klein, T., Pereira, A. C. M., Becker, C., Amico, S. C., Romanzini, D., & Bianchi, O. (2024). Effect of nano-silica and carbon nanotubes on the rheology and flammability behavior of epoxy. *Nano-Structures & Nano-Objects*, 39, 101260.
<https://doi.org/https://doi.org/10.1016/j.nanoso.2024.101260>

Kohlan, T. B., Atespare, A. E., Yildiz, M., Menceloglu, Y. Z., Unal, S., & Dizman, B. (2022). Synthesis and Structure–Property Relationship of Amphiphilic Poly(2-ethyl-co-2-(alkyl/aryl)-2-oxazoline) Copolymers. *ACS Omega*, 7(44), 40067–40077.
<https://doi.org/10.1021/acsomega.2c04809>

Kudo, K., Furutani, M., & Arimitsu, K. (2015). Imidazole Derivatives with an Intramolecular Hydrogen Bond as Thermal Latent Curing Agents for Thermosetting Resins. *ACS Macro Letters*, 4(10), 1085–1088. <https://doi.org/10.1021/acsmacrolett.5b00601>

Lammens, Nicolas, Kersemans, Mathias, Luyckx, Geert, Van Paepegem, Wim, & Degrieck, Joris. (2014). Improved accuracy in the determination of flexural rigidity of textile fabrics by the Peirce cantilever test (ASTM D1388). *Textile Research Journal*, 84(12), 1307–1314. <https://doi.org/10.1177/0040517514523182>

Lange, J., Altmann, N., Kelly, C. T., & Halley, P. J. (2000). Understanding vitrification during cure of epoxy resins using dynamic scanning calorimetry and rheological techniques. *Polymer*, 41(15), 5949–5955. [https://doi.org/https://doi.org/10.1016/S0032-3861\(99\)00758-2](https://doi.org/https://doi.org/10.1016/S0032-3861(99)00758-2)

Lee, J. H. (2021). Using Dihydrazides as Thermal Latent Curing Agents in Epoxy-Based Sealing Materials for Liquid Crystal Displays. *Polymers*, 13(1).
<https://doi.org/10.3390/polym13010109>

Li, C., Tan, J., Gu, J., Xue, Y., Qiao, L., & Zhang, Q. (2017). Facile synthesis of imidazole microcapsules via thiol-click chemistry and their application as thermally latent curing agent for epoxy resins. *Composites Science and Technology*, 142, 198–206. <https://doi.org/https://doi.org/10.1016/j.compscitech.2017.02.014>

Liu, X., Zhang, E., Liu, J., Qin, J., Wu, M., Yang, C., & Liang, L. (2023). Self-healing, reprocessable, degradable, thermadapt shape memory multifunctional polymers based on dynamic imine bonds and their application in nondestructively recyclable carbon fiber composites. *Chemical Engineering Journal*, 454, 139992. <https://doi.org/https://doi.org/10.1016/j.cej.2022.139992>

Lowry, M. S., O'Connell, E. M., Vincent, J. L., Goddard, R., White, T. A., Zheng, J. Q., Wong, R., & Bitler, S. P. (2008). *Cure evaluation of Intelimer ® latent curing agents for thermoset resin applications*.

Luís, J. (2014). *Effect of out-time aging in composite prepreg material Towards a testing methodology for material properties characterization*.

M R, S., Parameswaranpillai, J., Siengchin, S., & Thomas, S. (2022). *Handbook of Epoxy/Fiber Composites*. <https://doi.org/10.1007/978-981-19-3603-6>

Manivannan, M., & Rajendran, S. (2011). Investigation of inhibitive action of urea-Zn²⁺ system in the corrosion control of carbon steel in sea water. *International Journal of Engineering Science and Technology*, 3.

Mbotto Tonye, D., & Buet Gautier, K. (2021). Influence of the reinforcement on prepreg tack. *Polymer Composites*, 42(9), 4795–4803. <https://doi.org/https://doi.org/10.1002/pc.26188>

Michel, M., & Ferrier, E. (2020). Effect of curing temperature conditions on glass transition temperature values of epoxy polymer used for wet lay-up applications. *Construction and Building Materials*, 231, 117206. <https://doi.org/https://doi.org/10.1016/j.conbuildmat.2019.117206>

Mozaffari, S. M., & Beheshty, M. H. (2018). Thermally-Latent Curing Agents for Epoxy Resins: A Review. *Iranian Journal of Polymer Science and Technology*, 31(5), 409–426. <https://doi.org/10.22063/jipst.2019.1610>

Nassiet, V., Habas, J. P., Hassoune-Rhabour, B., Baziard, Y., & Petit, J. A. (2006). Correlation between viscoelastic behavior and cooling stresses in a cured epoxy resin system. *Journal of Applied Polymer Science*, 99, 679–690. <https://api.semanticscholar.org/CorpusID:136748532>

O'Brien, D., & Mather, P. (2001). Viscoelastic Properties of an Epoxy Resin during Cure. *Journal of Composite Materials*, 35, 883–904. <https://doi.org/10.1177/a037323>

Oishi, T., & Fujimoto, M. (1992). Synthesis and polymerization of N-[4-N'-(α -methylbenzyl)aminocarbonylphenyl]maleimide. *Journal of Polymer Science Part A: Polymer Chemistry*, 30(9), 1821–1830. <https://doi.org/https://doi.org/10.1002/pola.1992.080300905>

Oleszko-Torbus, N., Utrata-Wesołek, A., Bochenek, M., Lipowska-Kur, D., Dworak, A., & Wałach, W. (2020). Thermal and crystalline properties of poly(2-oxazoline)s. *Polymer Chemistry*, 11, 15–33.

Olson, L. D. (1994). *Curing epoxy resins using dicy, imidazole and acid*.

Ooi, S. K., Cook, W. D., Simon, G. P., & Such, C. H. (2000). DSC studies of the curing mechanisms and kinetics of DGEBA using imidazole curing agents. *Polymer*, 41(10), 3639–3649. [https://doi.org/https://doi.org/10.1016/S0032-3861\(99\)00600-X](https://doi.org/https://doi.org/10.1016/S0032-3861(99)00600-X)

Palmieri, F. L., Hudson, T. B., Smith, A. J., Cano, R. J., Kang, J. H., Lin, Y., Abbott, L. J., Clifford, B., Barnett, I. J., & Connell, J. W. (2022). Latent cure epoxy resins for reliable joints in secondary-bonded composite structures. *Composites Part B: Engineering*, 231, 109603. <https://doi.org/https://doi.org/10.1016/j.compositesb.2021.109603>

Pannone, M. C., & Macosko, C. W. (1987). Kinetics of isocyanate amine reactions. *Journal of Applied Polymer Science*, 34(7), 2409–2432. <https://doi.org/https://doi.org/10.1002/app.1987.070340707>

Parameswaranpillai, J., Pulikkalparambil, H., M R, S., & Siengchin, S. (2021). *Epoxy Composites: Fabrication, Characterization and Applications*.

Pearce, P. J., & Ennis, B. C. (1993). Aging and performance of structural film adhesives. IV. A modified epoxy with improved ambient temperature shelf life. *Journal of Applied Polymer Science*, 47(8), 1401–1409. <https://doi.org/https://doi.org/10.1002/app.1993.070470811>

Pouladvand, A. R., Mortezaei, M., Fattahi, H., & Amraei, I. A. (2020a). A novel custom-tailored epoxy prepreg formulation based on epoxy-amine dual-curable systems. *Composites Part A: Applied Science and Manufacturing*, 132, 105852. <https://doi.org/https://doi.org/10.1016/j.compositesa.2020.105852>

Pouladvand, A. R., Mortezaei, M., Fattahi, H., & Amraei, I. A. (2020b). A novel custom-tailored epoxy prepreg formulation based on epoxy-amine dual-curable systems. *Composites Part A: Applied Science and Manufacturing*, 132, 105852. <https://doi.org/https://doi.org/10.1016/j.compositesa.2020.105852>

Rahmathullah, A., Jeyarajasingam, A., Merritt, B., Vanlandingham, M., McKnight, S., & Palmese, G. (2009). Room Temperature Ionic Liquids as Thermally Latent Initiators for Polymerization of Epoxy Resins. *Macromolecules*, 42. <https://doi.org/10.1021/ma802669k>

Reuther, P., Dünnwald, P., Tabatabai, M., Schuh, C., Hartmann, L., & Ritter, H. (2022). Thermally Controlled Acceleration of Epoxy Resin Curing through Polymer-Bound Imidazole Derivatives with High Latency. *ACS Applied Polymer Materials*, 4(2), 1150–1158. <https://doi.org/10.1021/acsapm.1c01568>

Riccardi, C. C., Adabbo, H. E., & Williams, R. J. J. (1984). Curing reaction of epoxy resins with diamines. *Journal of Applied Polymer Science*, 29(8), 2481–2492. <https://doi.org/https://doi.org/10.1002/app.1984.070290805>

Robert P. Kretow. (1996). *The Evaluation of Various Substituted Ureas as Latent Accelerators for Dicyandiamide Cured Epoxy Resin Formulations*.

Rodošek, M., Mihelčič, M., Čolović, M., Šest, E., Šobak, M., Jerman, I., & Surca, A. K. (2020). Tailored Crosslinking Process and Protective Efficiency of Epoxy Coatings Containing Glycidyl-POSS. *Polymers*, 12(3). <https://doi.org/10.3390/polym12030591>

Rusnáková, S., Kalová, M., & Jonšta, Z. (2018). Overview of production of pre-preg, prototype and testing. *IOP Conference Series: Materials Science and Engineering*, 448(1), 012069. <https://doi.org/10.1088/1757-899X/448/1/012069>

Salamatgharamaleki, S., Atespare, A. E., Behroozi Kohlan, T., Yildiz, M., Menceloglu, Y. Z., Unal, S., & Dizman, B. (2025). Partially Hydrolyzed Poly(2-alkyl/aryl-2-oxazoline)s as Thermal Latent Curing Agents: Effect of Composition and Pendant Groups on Curing Behavior. *ACS Omega*, 10(7), 6753–6767. <https://doi.org/10.1021/acsomega.4c08659>

Schiller Arthur Maurice, Nawakowski Aleksandra Chrobok, & Wang Samuel Shan-Ning. (n.d.). *Substituted ureas as low temperature epoxy curing agents*.

Schmidt, C., Weber, P., Hocke, T., & Denkena, B. (2018). Influence of Prepreg Material Quality on Carbon Fiber Reinforced Plastic Laminates Processed by Automated Fiber Placement. *Procedia CIRP*, 67, 422–427. <https://doi.org/https://doi.org/10.1016/j.procir.2017.12.236>

Scott, J. M., Wells, G. M., & Phillips, D. C. (1980). Low temperature crack propagation in an epoxide resin. *Journal of Materials Science*, 15(6), 1436–1448. <https://doi.org/10.1007/BF00752123>

Shi, K., Shen, Y., Zhang, Y., & Wang, T. (2019a). A Modified Imidazole as a Novel Latent Curing Agent with Toughening Effect for Epoxy. *Engineered Science*, 5, 66–72. <https://doi.org/10.30919/es8d639>

Shi, K., Shen, Y., Zhang, Y., & Wang, T. (2019b). A Modified Imidazole as a Novel Latent Curing Agent with Toughening Effect for Epoxy. *Engineered Science*, 5, 66–72. <https://doi.org/10.30919/es8d639>

Sijbesma, R., Beijer, F., Brunsveld, L., Folmer, B., Hirschberg, J. H. K., Lange, R., Lowe, J., & Meijer, E. (1997). Reversible Polymers Formed from Self-Complementary Monomers Using

Quadruple Hydrogen Bonding. *Science (New York, N.Y.)*, 278, 1601–1604. <https://doi.org/10.1126/science.278.5343.1601>

Simmons, M., Caws, J., & Ellis, J. (2004). *ROOM TEMPERATURE STABLE EPOXY PREPREGS* (Patent US 6,787,237 B2). United States Patent.

Somarathne, Y. R., Herath, M., Epaarachchi, J., & Islam, M. M. (2024). Formulation of Epoxy Prepregs, Synthesization Parameters, and Resin Impregnation Approaches—A Comprehensive Review. *Polymers*, 16, 3326. <https://doi.org/10.3390/polym16233326>

Stoutland, O., HELGEN, L. O. N., & AGRE, C. L. (1959). Reactions of Diamines with Isocyanates and Isothiocyanates. *The Journal of Organic Chemistry*, 24(6), 818–820. <https://doi.org/10.1021/jo01088a022>

Tomuta, A. M., Ramis, X., Ferrando, F., & Serra, A. (2012). The use of dihydrazides as latent curing agents in diglycidyl ether of bisphenol A coatings. *Progress in Organic Coatings*, 74(1), 59–66. <https://doi.org/https://doi.org/10.1016/j.porgcoat.2011.10.004>

Ucar, C. A., & Dizman, B. (2024). Synthesis and Characterization of 1-(3-Aminopropyl)imidazole-Phenyl Isocyanate Adduct and Its Application as a Thermal Latent Curing Agent for Diglycidylether Bisphenol A Resin. *ACS Omega*, 9(33), 35579–35588. <https://doi.org/10.1021/acsomega.4c03300>

Uçar, C. A., & Dizman, B. (2025). Para-Toluenesulfonyl Isocyanate-Ethylenediamine Adduct as a Thermal Latent Curing Agent for Epoxy Resins. *Polymer Engineering & Science*, n/a(n/a). <https://doi.org/https://doi.org/10.1002/pen.27300>

Use of urea derivatives as accelerators for epoxy resins. (2010).

Vidil, T., Tournilhac, F., Musso, S., Robisson, A., & Leibler, L. (2016). Control of reactions and network structures of epoxy thermosets. *Progress in Polymer Science*, 62, 126–179. <https://doi.org/https://doi.org/10.1016/j.progpolymsci.2016.06.003>

Viegas, T. X., Bentley, M. D., Harris, J. M., Fang, Z., Yoon, K., Dizman, B., Weimer, R., Mero, A., Pasut, G., & Veronese, F. M. (2011). Polyoxazoline: Chemistry, Properties, and Applications in Drug Delivery. *Bioconjugate Chemistry*, 22(5), 976–986. <https://doi.org/10.1021/bc200049d>

Wang, J., Xu, Y. Z., Fu, Y. F., & Liu, X. D. (2016). Latent curing systems stabilized by reaction equilibrium in homogeneous mixtures of benzoxazine and amine. *Scientific Reports*, 6(1), 38584. <https://doi.org/10.1038/srep38584>

Wang, P., Chen, L., Xiao, H., & Zhan, T. (2020). Nitrogen/sulfur-containing DOPO based oligomer for highly efficient flame-retardant epoxy resin. *Polymer Degradation and Stability*, 171, 109023. <https://doi.org/https://doi.org/10.1016/j.polymdegradstab.2019.109023>

Wang, P., Xiao, H., Duan, C., Wen, B., & Li, Z. (2020). Sulfathiazole derivative with phosphaphhenanthrene group: Synthesis, characterization and its high flame-retardant activity on epoxy resin. *Polymer Degradation and Stability*, 173, 109078. <https://doi.org/https://doi.org/10.1016/j.polymdegradstab.2020.109078>

Wang, R.-M., Zheng, S.-R., & Zheng, Y.-P. (2011). 1 - Introduction to polymer matrix composites. In R.-M. Wang, S.-R. Zheng, & Y.-P. Zheng (Eds.), *Polymer Matrix Composites and Technology* (pp. 1–548). Woodhead Publishing. <https://doi.org/https://doi.org/10.1533/9780857092229.1>

Wang, Y., Mahapatra, S., Belnoue, J. P.-H., Ivanov, D. S., & Hallett, S. R. (2023). Understanding tack behaviour during prepreg-based composites' processing. *Composites Part A: Applied Science and Manufacturing*, 164, 107284. <https://doi.org/https://doi.org/10.1016/j.compositesa.2022.107284>

Weh, R., & de Klerk, A. (2017). Thermochemistry of Sulfones Relevant to Oxidative Desulfurization. *Energy & Fuels*, 31(6), 6607–6614. <https://doi.org/10.1021/acs.energyfuels.7b00585>

Wei, W., Sun, X., Ye, W., Zhang, B., Fei, X., Li, X., & Liu, X. (2020). Thermal latent curing agent for epoxy resins from neutralization of 2-methylimidazole with a phosphazene-containing polyfunctional carboxylic acid. *Polymers for Advanced Technologies*, 31. <https://doi.org/10.1002/pat.4884>

Xing, S., Yang, J., Huang, Y., Zheng, Q., & Zeng, J. (2015). Preparation and characterization of a novel microcapsule-type latent curing agent for epoxy resin. *Materials & Design*, 85, 661–670. <https://doi.org/https://doi.org/10.1016/j.matdes.2015.07.098>

Yang, B., Wei, Y., Liu, Y., & Qiu, Y. (2022). A thermal latent imidazole complex containing copper (II) as the curing agent for an epoxy-based glass fiber composite. *Textile Research Journal*, 92(11–12), 1867–1875. <https://doi.org/10.1177/00405175211069870>

Yang, X., Zhao, L., Li, Q., & Ma, L. (2020a). Preparation of Latent Curing Agent for Epoxy Resin by Encapsulation Technology. *IOP Conference Series: Materials Science and Engineering*, 746(1), 012021. <https://doi.org/10.1088/1757-899X/746/1/012021>

Yang, X., Zhao, L., Li, Q., & Ma, L. (2020b). Preparation of Latent Curing Agent for Epoxy Resin by Encapsulation Technology. *IOP Conference Series: Materials Science and Engineering*, 746, 012021. <https://doi.org/10.1088/1757-899X/746/1/012021>

Yao, J., Zhan, H., & Zou, Z. (2017a). Preparation and Curing Behaviour of Epoxy Based Film for Moderate Temperature Prepreg. *Polymers and Polymer Composites*, 25(8), 621–626. <https://doi.org/10.1177/096739111702500807>

Yao, J., Zhan, H., & Zou, Z. (2017b). Preparation and Curing Behaviour of Epoxy Based Film for Moderate Temperature Prepreg. *Polymers and Polymer Composites*, 25(8), 621–626. <https://doi.org/10.1177/096739111702500807>

Yee Low, H., & Ishida, H. (1999). Structural effects of phenols on the thermal and thermo-oxidative degradation of polybenzoxazines. *Polymer*, 40(15), 4365–4376. [https://doi.org/https://doi.org/10.1016/S0032-3861\(98\)00656-9](https://doi.org/https://doi.org/10.1016/S0032-3861(98)00656-9)

Yen, W.-P., Chen, K.-L., Yeh, M.-Y., Uramaru, N., Lin, H.-Y., & Wong, F. F. (2016). Investigation of soluble PEG-imidazoles as the thermal latency catalysts for epoxy-phenolic resins. *Journal of the Taiwan Institute of Chemical Engineers*, 59, 98–105. <https://doi.org/https://doi.org/10.1016/j.jtice.2015.08.007>

Yin, T., Rong, M. Z., Zhang, M. Q., & Yang, G. C. (2007). Self-healing epoxy composites – Preparation and effect of the healant consisting of microencapsulated epoxy and latent curing agent. *Composites Science and Technology*, 67(2), 201–212. <https://doi.org/https://doi.org/10.1016/j.compscitech.2006.07.028>

Ying, H., Zhang, Y., & Cheng, J. (2014). Dynamic urea bond for the design of reversible and self-healing polymers. *Nature Communications*, 5(1), 3218. <https://doi.org/10.1038/ncomms4218>

Yu, Z., Ma, S., Tang, Z., Liu, Y., Xu, X., Qiong, L., Zhang, K., Wang, B., & Wang, S. (2021). Amino acids as Latent Curing Agents and their Application in Fully Bio-based Epoxy Resins. *Green Chemistry*, 23. <https://doi.org/10.1039/D1GC02126E>

Yuan, Y. C., Rong, M. Z., Zhang, M. Q., Chen, J., Yang, G. C., & Li, X. M. (2008). Self-Healing Polymeric Materials Using Epoxy/Mercaptan as the Healant. *Macromolecules*, 41(14), 5197–5202. <https://doi.org/10.1021/ma800028d>

Zamani, S., van der Voort, S. H. E., Lange, J.-P., Kersten, S. R. A., & Ruiz, M. P. (2023). Polyurethane Recycling: Thermal Decomposition of 1,3-Diphenyl Urea to Isocyanates. *Polymers*, 15(11). <https://doi.org/10.3390/polym15112522>

Zhang, P., Ali Shah, S. A., Gao, F., Sun, H., Cui, Z., Cheng, J., & Zhang, J. (2019). Latent curing epoxy systems with reduced curing temperature and improved stability. *Thermochimica Acta*, 676, 130–138. <https://doi.org/https://doi.org/10.1016/j.tca.2019.03.022>

Zhang, S., Yang, P., Bai, Y., Zhou, T., Zhu, R., & Gu, Y. (2017). Polybenzoxazines: Thermal Responsiveness of Hydrogen Bonds and Application as Latent Curing Agents for Thermosetting Resins. *ACS Omega*, 2(4), 1529–1534. <https://doi.org/10.1021/acsomega.7b00075>

Zhang, X. (2011). Latent Curing Agent Modified Epoxy Sizing Agent for High Modulus Carbon Fiber. *The Open Materials Science Journal*, 5, 104–108. <https://doi.org/10.2174/1874088X01105010104>

Zhang, X., Wu, Y., Wei, J., Tong, J., & Yi, X. (2017). Curing kinetics and mechanical properties of bio-based composite using rosin-sourced anhydrides as curing agent for hot-melt prepreg. *Science China Technological Sciences*, 60(9), 1318–1331. <https://doi.org/10.1007/s11431-016-9029-y>

Zhang, Z. P., Rong, M. Z., & Zhang, M. Q. (2014). Room temperature self-healable epoxy elastomer with reversible alkoxyamines as crosslinkages. *Polymer*, 55(16), 3936–3943. <https://doi.org/https://doi.org/10.1016/j.polymer.2014.06.064>

Zhang, Z. P., Rong, M. Z., & Zhang, M. Q. (2018). Polymer engineering based on reversible covalent chemistry: A promising innovative pathway towards new materials and new functionalities. *Progress in Polymer Science*, 80, 39–93. <https://doi.org/https://doi.org/10.1016/j.progpolymsci.2018.03.002>

Zhao, L., Yang, X., Li, Q., & Ma, L. (2019). Latent curing agent DDM-PMMA microcapsule for epoxy resin. *Journal of Applied Polymer Science*, 136(28), 47757. <https://doi.org/https://doi.org/10.1002/app.47757>

Zhou, T., Gu, M., Jin, Y., & Wang, J. (2005). Mechanism and Kinetics of Epoxy-Imidazole Cure Studied with Two Kinetic Methods. *Polymer Journal*, 37(11), 833–840. <https://doi.org/10.1295/polymj.37.833>

APPENDIX A

Drapability measurements 10% Prepreg

Symbol	Property	Value	Measurements								
			Direction	warp 1	warp 2	warp 3	warp 4	weft 1	weft 2	weft 3	weft 4
G	Flexural rigidity	Duration (min)	30								
C	Bending length	Temperature (°C)	70	Alignment	mm	mm	mm	mm	mm	mm	mm
O	Overhang length	Unit	Result	top	50	53	52	55	51	59	51
W	Prepreg GSM	µj/m	889,02	back	58	50	55	57	60	50	50
CF GSM	245	mm	53,66	bottom top	55	52	57	57	55	52	52
		mm	107,31	bottom back	50	60	58	53	57	52	57
		g/m2	405	Average	53,25	53,75	55,5	55,5	55,75	53,25	52,5
Average	Warp	Weft		Std dev	3,42	3,77	2,29	1,66	3,27	3,42	2,69
				COV	6,42	7,01	4,13	2,99	5,86	6,42	5,13
				Total Average	53,66						
				Total Std dev	3,64						
				Total COV	6,78						

15 % Prepreg

Symbol	Property	Value	Measurements								
			Direction	warp 1	warp 2	warp 3	warp 4	weft 1	weft 2	weft 3	weft 4
G	Flexural rigidity	Duration (min)	30								
C	Bending length	Temperature (°C)	70	Alignment	mm	mm	mm	mm	mm	mm	mm
O	Overhang length	Unit	Result	top	53	40	44	48	59	55	56
W	Prepreg GSM	µj/m	886,22	back	56	50	46	57	58	52	54
CF GSM	245	mm	53,60	bottom top	40	48	51	56	54	55	54
		mm	107,20	bottom back	47	51	47	57	57	58	54
		g/m2	405	Average	49	47,25	47	54,5	57	55	54,5
Average	Warp	Weft		Std dev	6,124	4,323	2,55	3,775	1,871	2,121	0,866
				COV	12,5	9,149	5,424	6,926	3,282	3,857	1,589
				Total Average	53,6						
				Total Std dev	4,20						
				Total COV	7,84						

20 % Prepreg

Symbol	Property	Value	Measurements								
			Direction	warp 1	warp 2	warp 3	warp 4	weft 1	weft 2	weft 3	weft 4
G	Flexural rigidity	Duration (min)	30								
C	Bending length	Temperature (°C)	70	Alignment	mm	mm	mm	mm	mm	mm	mm
O	Overhang length	Unit	Result	top	61	62	56	52	58	47	55
W	Prepreg GSM	µj/m	912,52	back	54	60	53	52	51	53	48
CF GSM	245	mm	54,13	bottom top	55	63	57	53	56	44	56
		mm	108,25	bottom back	58	63	57	52	52	57	51
		g/m2	405	Average	57	62	55,75	52,25	54,25	50,25	52,5
Average	Warp	Weft		Std dev	2,74	1,22	1,64	0,43	2,86	5,07	3,20
				COV	4,80	1,98	2,94	0,83	5,27	10,09	6,10
				Total Average	54,13						
				Total Std dev	4,92						
				Total COV	9,08						

25 % Prepreg

Symbol	Property	Value	Measurements									
G	Flexural rigidity	Duration (min)	30	Direction	warp 1	warp 2	warp 3	warp 4	weft 1	weft 2	weft 3	weft 4
C	Bending length	Temperature (°C)	70	Alignment	mm	mm	mm	mm	mm	mm	mm	mm
O	Overhang length	Unit	Result	top	59	61	63	55	61	62	63	60
W	Prepreg GSM	µj/m	1268,51	back	61	59	59	57	60	63	61	58
CF GSM	245	mm	60,41	bottom top	63	60	61	57	61	61	59	61
		mm	120,81	bottom back	61	61	59	60	60	66	58	63
		g/m ²	405	Average	61	60,25	60,5	57,25	60,5	63	60,25	60,5
	Warp	Weft		Std dev	1,41	0,83	1,66	1,79	0,50	1,87	1,92	1,80
Average	59,75	61,25		COV	2,32	1,38	2,74	3,12	0,83	2,97	3,19	2,98
				Total Average	60,41							
				Total Std dev	2,13							
				Total COV	3,53							

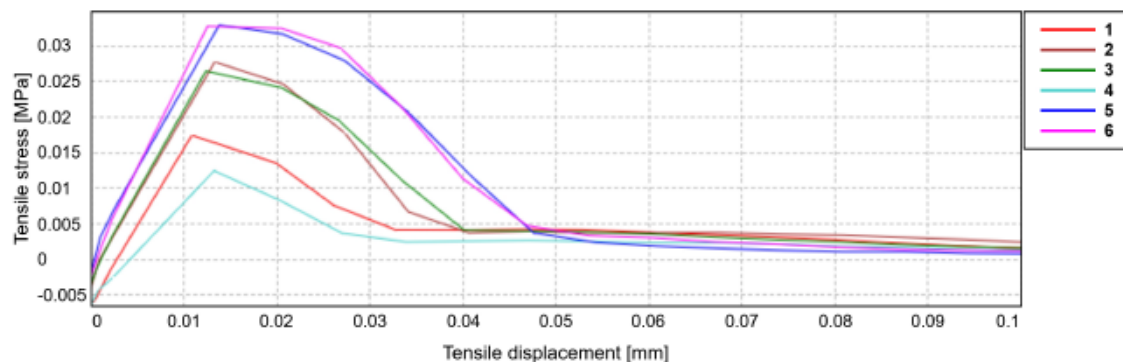
APPENDIX B

Tackiness measurements

	DoC (%)	Tackiness (N)	DoC (%)	Tackiness (N)	DoC (%)	Tackiness (N)	DoC (%)	Tackiness (N)
	10	69,4	15	86,34	20	100,8	25	64,58
	10	66,2	15	97,5	20	107,58	25	93,53
	10	82,37	15	78,65	20	104,84	25	88,4
	10	81,93	15	66,57	20	131,68	25	85,58
	10				20	114,73	25	113,16
	10				20	109,04	25	95
Average	74,98		82,27		111,45		90,042	
Std Dev	7,27		11,27		9,98		14,39	
COV	9,69		13,70		8,96		15,98	

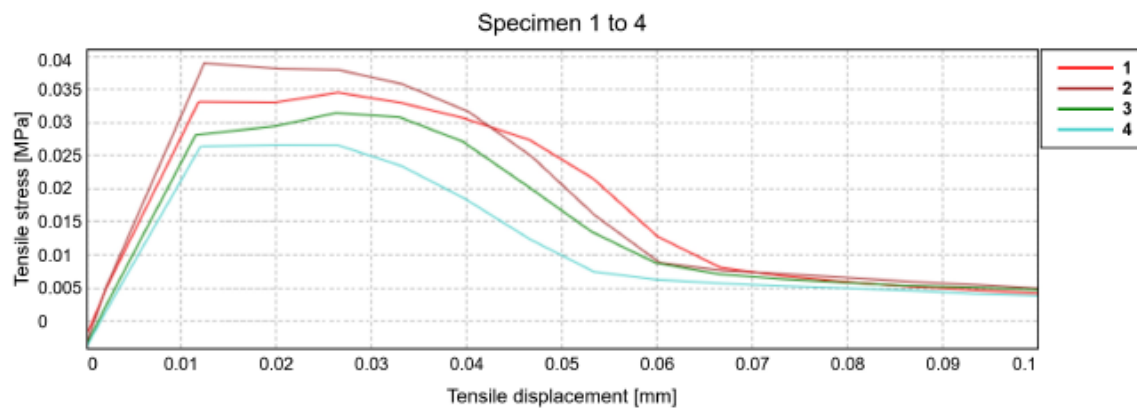
Test Metod	ASTMC297
Sample Name	2504-138_CAU - %10 prepreg
Rate 1	4.00 mm/min
Temperature C	23.1
Humudity %	49.8
Operator Name	Mehmet OLCAZ
LoadCell Calibration Date	09-2024
Cihaz No	C01-18 5 kN

Specimen 1 to 6



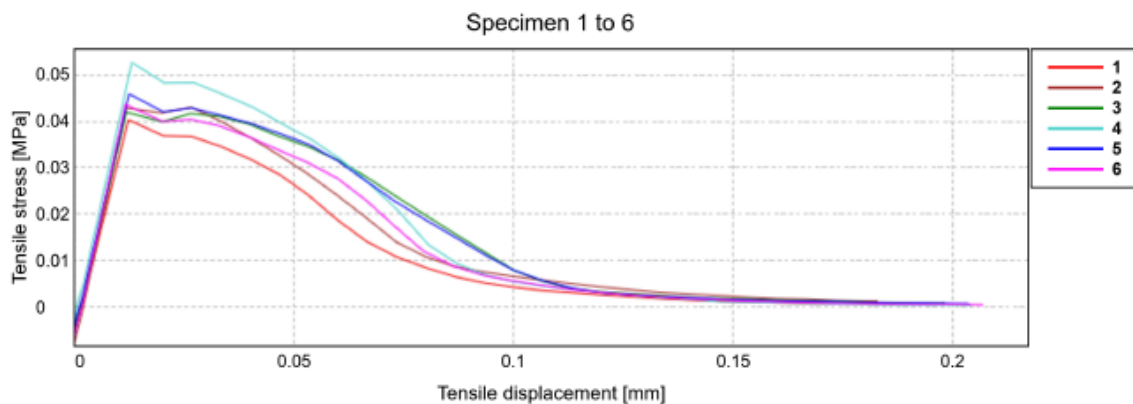
	Specimen label	Width [mm]	Length [mm]	Area [mm^2]	Tensile stress at Maximum Load [MPa]	Maximum Load [N]
1	1	50.00	50.00	2500.00	0.017	43.647
2	2	50.00	50.00	2500.00	0.028	69.392
3	3	50.00	50.00	2500.00	0.026	66.197
4	4	50.00	50.00	2500.00	0.012	31.170
5	5	50.00	50.00	2500.00	0.033	82.378
6	6	50.00	50.00	2500.00	0.033	81.933
Mean		50.00	50.00	2500.00	0.025	62.453
STDV		0.00	0.00	0.00	0.01	20.84
C.O.V		0.00	0.00	0.00	33.36	33.36

Test Method	ASTM C297
Sample Name	2504-138_CAU - %15 prepreg
Rate 1	4.00 mm/min
Temperature C	23.1
Humidity %	49.8
Operator Name	Mehmet OLCAZ
LoadCell Calibration Date	09-2024
Cihaz No	C01-18 5 kN



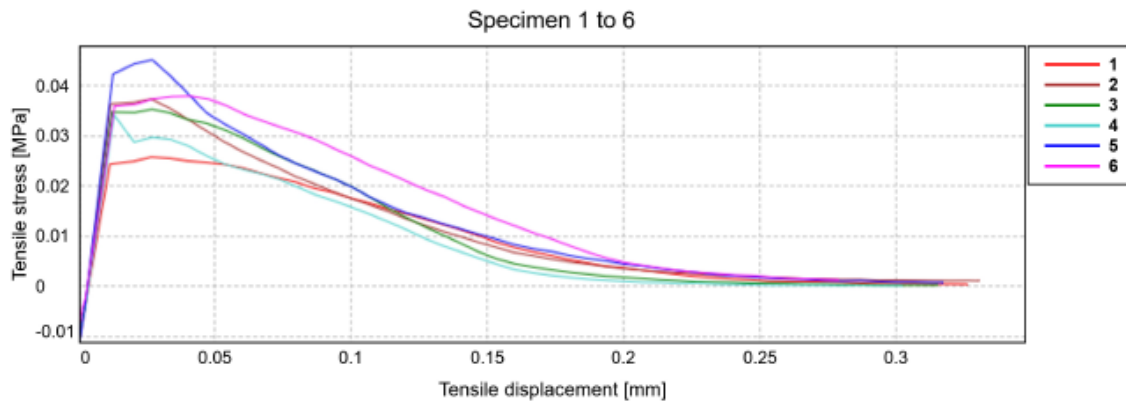
	Specimen label	Width [mm]	Length [mm]	Area [mm ²]	Tensile stress at Maximum Load [MPa]	Maximum Load [N]
1	1	50.00	50.00	2500.00	0.035	86.343
2	2	50.00	50.00	2500.00	0.039	97.495
3	3	50.00	50.00	2500.00	0.031	78.657
4	4	50.00	50.00	2500.00	0.027	66.573
Mean		50.00	50.00	2500.00	0.033	82.267
STDV		0.00	0.00	0.00	0.01	13.01
C.O.V		0.00	0.00	0.00	15.82	15.82

Test Metod	ASTMC297
Sample Name	2504-138_CAU - %20 prepreg
Rate 1	4.00 mm/min
Temperature C	23.3
Humudity %	49.9
Operator Name	Mehmet OLCAZ
LoadCell Calibration Date	09-2024
Cihaz No	C01-18 5 kN



	Specimen label	Width [mm]	Length [mm]	Area [mm ²]	Tensile stress at Maximum Load [MPa]	Maximum Load [N]
1	1	50.00	50.00	2500.00	0.040	100.796
2	2	50.00	50.00	2500.00	0.043	107.584
3	3	50.00	50.00	2500.00	0.042	104.845
4	4	50.00	50.00	2500.00	0.053	131.684
5	5	50.00	50.00	2500.00	0.046	114.736
6	6	50.00	50.00	2500.00	0.044	109.047
Mean		50.00	50.00	2500.00	0.045	111.449
STDV		0.00	0.00	0.00	0.00	10.94
C.O.V		0.00	0.00	0.00	9.81	9.81

Test Metod	ASTM C297
Sample Name	2504-138_CAU - %25 prepreg
Rate 1	4.00 mm/min
Temperature C	23.3
Humudity %	49.9
Operator Name	Mehmet OLCAZ
LoadCell Calibration Date	09-2024
Cihaz No	C01-18 5 kN



	Specimen label	Width [mm]	Length [mm]	Area [mm ²]	Tensile stress at Maximum Load [MPa]	Maximum Load [N]
1	1	50.00	50.00	2500.00	0.026	64.588
2	2	50.00	50.00	2500.00	0.037	93.532
3	3	50.00	50.00	2500.00	0.035	88.403
4	4	50.00	50.00	2500.00	0.034	85.585
5	5	50.00	50.00	2500.00	0.045	113.162
6	6	50.00	50.00	2500.00	0.038	95.006
Mean		50.00	50.00	2500.00	0.036	90.046
STDV		0.00	0.00	0.00	0.01	15.76
C.O.V		0.00	0.00	0.00	17.50	17.50